LIFT INCREASE OBTAINED WITH BOUNDARY LAYER SUCTION ON A 10% DOUBLE WEDGE AIRFOIL WITH A 20% CHORD LEADING AND TRAILING EDGE FLAPS

Thesis by

Harold William Davidson

In Partial Fulfillment of the Requirements

For the Degree of

Aeronautical Engineer

California Institute of Technology

Pasadena, California

1951

ACKOWLEDGEMENTS

The author wishes to express his thanks and appreciation to Dr. Clark B. Millikan under whose direction this investigation was conducted and to Dr. D.A. Morelli and Mr. R.W. Bell for their technical advice and helpful criticisms.

The author also wishes to thank the members of the GALCIT 10 ft. Wind Tunnel staff for their assistance on computing and plotting the data, and his fiance, Miss Elizabeth Friberg, for spending many evenings typing and re-typing the original manuscript.

ABSTRACT

In this investigation a study was made of the effects of boundary layer control on a 10% thick, double-wedge airfoil located between endplates. In particular, the study centered around a "high-lift" investigation in order to obtain an optimum configuration for the specific airfoil. The double-wedge airfoil was used since:1) it is a "high speed" airfoil, and 2) it has poor maximum lift and stalling characteristics.

The model used was equipped with a nose flap and a slotted trailing edge flap, both of 20% wing chord, and two suction slots, one aft of the nose flap (20% chord) and the other at the 70% wing chord. Five suction quantities were used on all possible configuration combinations. The maximum lift coefficient obtained was $C_{L_{max}} = 2.149$ at an angle of attack of 21° and a suction quantity equal to $C_Q = 0.0071$.* For this particular configuration, the approximate value of the horsepower required to supply the necessary suction quantity was determined. In addition to the force and moment tests, tuft studies of flow of the "optimum" configurations were made and reported.

---

* Configuration: Nose flap deflected 30°; trailing edge flap deflected 30°; slot A_1(forward slot)

TABLE OF CONTENTS

I. INTRODUCTION

As the speed of the airplane increases, the need for a thinner airfoil becomes greater. Thin, symmetrical airfoils, and especially double-wedge airfoils, have inherently unfavorable low speed characteristics such as a low maximum lift and a low angle of stall. In view of this, many methods have been employed to improve these characteristics.

The most logical method, and the one first used, was to employ a nose flap since the separation from the leading edge starts at a low angle of attack. This configuration in a double-wedge airfoil favorably changed the characteristics,[1] but the magnitude of the changes was not large enough to be considered adequate for practical purposes. The application of a trailing edge flap further increased the maximum lift, but it tended to counteract the increase in angle of stall obtained by the nose flap. Something else was needed to supplement the improvement due to the flaps.

For many years, the knowledge of boundary layer control and the advantages associated with it were known, but not until the advent of supersonic wings has it become exceedingly important. It is the purpose of this investigation to test a 10% thick double-wedge airfoil with nose flap and trailing edge flap under the influence of boundary layer suction. It is known by theory and by test that if the slow moving boundary layer is removed by suction or re-energized by blowing, separation can be delayed and a substantial lift increase obtained. Since for thin, symmetrical sections separation begins at the leading edge, a boundary layer slot was located at approximately the 20% wing chord, at the junction of

INTRODUCTION (cont'd)

the leading edge flap and the upper surface of the airfoil. Also with the airfoil at moderate angles of attack, an unfavorable pressure gradient occurs at the rear portion of the airfoil and moves forward steadily. In an attempt to re-establish a favorable pressure gradient over this aft portion, another boundary layer suction slot was located at the 70% wing chord, inclined 30° to the surface of the airfoil. As an added assistance a slotted trailing edge flap was used instead of a split or zap flap in the hope that this flap configuration would also improve the basic configuration.

The purpose of these investigations is to study the effect of boundary layer control on the characteristics of the basic double-wedge airfoil. Five suction quantities and two slot locations were tested with all possible configurations of the basic airfoil.

An attempt was made to determine the horsepower required to apply the boundary layer suction data obtained on the model to a full scale prototype airplane of the following dimensions:

Weight	= 10,000 lbs
Wing Area	= 440 ft^2
Aspect Ratio	= 5.5
MAC	= 9.5 ft
V	= 95.5 ft/sec
q	= 10.8 lb/ft^2
	= 0.002378 $slugs/ft^3$
$\frac{\text{chord length}}{\text{width of slot}}$	= 160

Full span slots

INTRODUCTION (cont'd)

The method followed was that suggested by Sir Handley Page. The results are presented herein on page 36.

As a result of these investigations an insight into future research was obtained. Suggestions along this line appear in the discussion of the test results.

II. DESCRIPTION OF TEST SET-UP

The model was tested in the closed throat Merrill Wind Tunnel of the Guggenheim Aeronautical Laboratory at the California Institute of Technology. The dimensions of the test section of this tunnel are 32" x 45". At the time of testing, the tunnel had three wire screens located just ahead of the contraction section primarily for the purpose of producing low turbulence flow.

The model tested was a 10% thick, double-wedge airfoil with a 20% chord nose flap and a 20% chord slotted trailing edge flap. To remove the boundary layer there were two slots, the front slot being located at the 20% wing chord or hinge line of the nose flap, and the rear slot being located at the 70% wing chord. The critical dimensions of the model are: wing chord = 8 inches; span = 24 inches; slot width = 0.05 inches. To approximate two-dimensional flow the model was installed between endplates of $6\frac{1}{2}$ inch radius. Attached to the outside of the endplates were the 3/4 inch I.D. brass air pipes which carried off the boundary layer to the outside of the tunnel and also acted as the attachment points for the model support system (See photos 1,2,and 6).

The double-wedge airfoil was set on the supporting struts, 15 3/4 inches from the leading edge of the tunnel working section. The air pipes were connected to the air suction system by 8 inch sections of rubber tubing. A spring of 1/16 inch wire was placed within each of these flexible tubes to prevent collapse by the suction. From here the suction system, consisting of 3/4 inch piping, from each side of the tunnel, went through a common gate valve to a 50 gallon drum located beneath the tunnel aft of the

DESCRIPTION OF TEST SET-UP (cont'd)

atmospheric slot (see figure 3). This drum acted as a "pressure reservoir" to prevent surging and maintain a constant suction pressure. The suction pressure was maintained by two Black and Decker Industrial Vacuum Cleaners whose characteristics are shown in figure 4. These were connected to the lower part of the reservoir (see photos 7 and 8) and the quantity of flow was regulated by the gate valve ahead of the inlet to the reservoir. The air flow was measured by setting a standard pitot tube in the outlet pipe of the cleaners.

For each test a certain total pressure (in inches of alcohol) was set on the "blowers", and maintained constant during the run. The model was then run through a sequence of angles of attack to determine the angle of stall. Once this was determined, the run was made, taking only lift data for 8 to 10 angles through the stall. In many cases, abrupt and severe buffeting prevented testing at any angles above the stall.

Throughout the investigation, except for the runs pertinent to the Reynolds number effect, the tunnel dynamic pressure was kept at $q = 20$ lb/ft^2. This value was chosen after an investigation of Reynolds number effects and a consideration of an optimum value for the maximum suction quantity coefficient.

For the tuft runs made at the end of the investigation, a window of plexiglas was located in the ceiling of the test section, through which pictures were taken using the normal lighting of the test section (two white flourescent tubes in upper corners of the test section).

DESCRIPTION OF TEST SET-UP (cont'd)

For those runs in which only slot Δ_1 was used, the rear slot was sealed by cellophane tape on the upper surface of the airfoil. When slot Δ_2 was used alone, slot Δ_1 was sealed with cellophane tape applied to the exterior side of the channel located inside of the model. This was done since the tape would otherwise tend to produce an early separation near the leading edge.

III. METHOD OF EXPERIMENTAL PRESENTATION

The data obtained in the investigation were reduced to dimensionless coefficient form and are presented as plotted points connected by suitably faired curves. Only lift component data were taken and in no instance were any corrections applied to the data.

Possible corrections applicable to the data could result from one or more of the following factors: 1. supporting struts, 2. wind tunnel walls, 3. tunnel flow inclinations, 4. tunnel flow irregularities. The supporting struts for the model were located outside of the endplates on the airflow pipes; therefore the presence of the struts should have a negligible effect on the lift data. A correction for the presence of the tunnel walls is not necessarily negligible, but due to the "two-dimensional" set-up of the model, the magnitude of such a correction is unknown. Tunnel flow inclination can also have an appreciable effect on the data by increasing or decreasing the apparent angle of attack*. The calibrations of the Merrill Wind Tunnel show a negligible flow inclination in the model test section. Possible factors under item 4 include variation of tunnel velocity across the working section, longitudinal pressure gradient in the working section, and turbulence level. The first two factors have been shown to exist by preliminary calibrations of the Merrill Wind Tunnel. Incomplete information on and understanding of the corrections led to their being neglected.

---

* $\alpha_g = 0^\circ$ was set by leveling the wing chord line inscribed on the endplates; $\alpha_g = 0^\circ$ is defined as the angle of attack at which $C_L = 0$ (for symmetrical airfoils).

METHOD OF EXPERIMENTAL PRESENTATION (cont'd)

From figure 8, it is seen that at $\alpha_g = 0^\circ$, the lift coefficient C_L, is not equal to zero but to 0.050. Since the model is symmetrical and there exists no flow inclination, the model was examined for possible errors. Upon investigation, the wing chord line was found to be inclined upward at an angle of 0.3° from the line inscribed on the endplates and taken to be the wing chord. It was also discovered that both the nose flap and the slotted trailing edge flap were warped downward (except at the ends) causing an effective camber in the airfoil. The effects of these conditions add up to a positive lift coefficient at $\alpha_g = 0^\circ$ of about the magnitude observed.

The data obtained are presented in five groups of plots:

1. Effects of Suction - shows increase of maximum lift as suction is increased
2. Effects of Slot Location - shows change of maximum lift for variation in slot location and combination
3. Flap Effectiveness - shows increase of maximum lift for increase in flap deflection
4. Variation of Maximum Lift with Flap Deflection - shows change in maximum lift with nose flap deflection for a given trailing edge flap deflection
5. Variation of Lift with Suction Quantity - shows change in lift at a given angle of attack as the suction quantity is increased (slot location as a parameter).

For groups 2,3, and 4, only the data for zero and maximum suction were used.

The tuft sketches (figures 73 to 81), appearing at the end of this

METHOD OF EXPERIMENTAL PRESENTATION (cont'd)

report were made using the tuft photographs as a guide. The solid-dotted lines indicate that the area to the rear of the dots has a turbulent boundary layer and the stall is imminent; the solid-dashed lines indicate that the flow has already separated from the airfoil in the area to the rear of the dashes. The photographs for only one run are included in the report to serve as an example and a check.

IV. DEFINITION OF CONFIGURATION SYMBOLS

S = Basic 10% double-wedge airfoil; span is 24 inches, chord is 8 inches; configuration includes circular endplates and air flow ducting from model through tunnel wall

F_N = 20% chord nose flap; deflection is 15° or 30° from wing chord plane (see figure 2)

F_S = 20% chord slotted trailing edge flap; deflection is 30° or 60° from the wing chord plane (see figure 2)

$\mathcal{A}_1$ = Boundary layer control slot located on wing upper surface at the junction of the nose flap and wing surface; width = 0.05 in.

$\mathcal{A}_2$ = Boundary layer control slot located on the wing upper surface at the 70% wing chord; slot is inclined 30° to the wing upper surface; width = 0.05 in.

V. DIMENSIONAL DATA

MODEL

Span = 24 inches

Chord = 8 inches

Wing Area = 1.33 ft^2

Slot Width = 0.05 inches = 0.0042 ft

Slot Area = 1.20 in^2 = 0.0083 ft^2

ENDPLATES

Circular, Diameter = 13 inches

Thickness = 0.125 inches

MATERIAL

Model - Brass

Endplates - 24ST Aluminum

BOUNDARY LAYER EQUIPMENT

Airflow ducting - 0.75 inch (internal diameter) pipe

Pressure Reservoir - 50 gallon drum

Feed Pumps - 2 Black and Decker commercial vacuum cleaners

VI. NOMENCLATURE

L = Total lift developed by airplane - lbs

W = Gross weight of airplane - lbs

C_L = Lift coefficient = $\frac{L}{\frac{1}{2}\rho V^2 S}$

C_D = Drag coefficient = $\frac{D}{\frac{1}{2}\rho V^2 S}$

V = Flight or free stream velocity - ft/sec

ρ = Density of air - slugs/ft^3

α_g = Geometrical angle of attack with reference to the wing chord plane

ψ = Angle of yaw

R = Reynolds number of flow

S = Wing area - ft^2

AR = Aspect ratio of wing

MAC = Mean aerodynamic chord - ft

Q = Quantity of air removed by boundary layer suction - ft^3/sec

C_Q = Quantity flow coefficient = $\frac{Q}{VS}$

δ_{F_N} = Deflection of nose flap in degrees as measured from the wing chord plane

δ_{F_S} = Deflection of slotted trailing edge flap in degrees as measured from the wing chord plane

$\Delta P = \Delta P_1 + \Delta P_2 + \Delta P_3$

ΔP_1 = Difference between the free stream static pressure and the static pressure at the 20% wing chord - lb/ft^2

ΔP_2 = Kinetic energy lost at exit - lb/ft^2

ΔP_3 = Internal pressure losses due to ducting - lb/ft^2

η = Efficiency of suction pumps

VII. INDEX OF RUNS

Run	Model Configuration	Test	q	φ	α_g	δ_{F_N}	δ_{F_S}	C_Q
1	S + $F_N F_S$ + $\Delta_1\Delta_2$	P_1	5	0	----	30°	60°	.0144
2	" + " + "		15			"	"	.0083
3	" + " + "		25			"	"	.0063
4	" + " + "		35			"	"	.0053
5	" + $\Delta_1\Delta_2$		5			0°	0°	.0148
6	" + "		15			"	"	.0085
7	" + "		25			"	"	.0066
8	" + "		35			"	"	.0054
9	"		20			"	"	
10	" + Δ_1		"			"	"	.0039
11	" + "		"			"	"	.0055
12	" + "		"			"	"	.0063
13	" + "		"			"	"	.0071
14	" + $\Delta_1\Delta_2$		"			"	"	"
15	" + "		"			"	"	.0063
16	" + "		"			"	"	.0055
17	" + "		"			"	"	.0039
18	" + F_N		"			15°	0°	0
19	" + " + $\Delta_1\Delta_2$		"			"	"	.0039
20	" + " + "		"			"	"	.0055
21	" + " + "		"			"	"	.0063
22	" + " + "		"			"	"	.0071
23	" + " + Δ_1		"			"	"	"
24	" + " + "		"			"	"	.0063
25	" + " + "		"			"	"	.0055
26	" + " + "		"			"	"	.0039
27	" + "	▼	"	▼	▼	30°	"	0

INDEX OF RUNS (Cont'd)

Run	Model Configuration	Test	q	ψ	αg	δ_{F_N}	δ_{F_S}	C_Q
28	S + F_N + Δ_1	P_1	20	0	——	30°	0°	.0039
29	" + " + "		"			"	"	.0055
30	" + " + "		"			"	"	.0063
31	" + " + "		"			"	"	.0070
32	" + " + $\Delta_1\Delta_2$		"			"	"	"
33	" + " + "		"			"	"	.0063
34	" + " + "		"			"	"	.0055
35	" + " + "		"			"	"	.0039
36	" + F_NF_S		"			"	30°	0
37	" + " + $\Delta_1\Delta_2$		"			"	"	.0039
38	" + " + "		"			"	"	.0055
39	" + " + "		"			"	"	.0063
40	" + " + "		"			"	"	.0070
41	" + " + Δ_1		"			"	"	.0071
42	" + " + "		"			"	"	.0063
43	" + " + "		"			"	"	.0055
44	" + " + "		"			"	"	.0039
45	" + "		"			"	60°	0
46	" + " + Δ_1		"			"	"	.0039
47	" + " + "		"			"	"	.0055
48	" + " + "		"			"	"	.0063
49	" + " + "		"			"	"	.0071
50	" + " + $\Delta_1\Delta_2$		"			"	"	"
51	" + " + "		"			"	"	.0063
52	" + " + "		"			"	"	.0055
53	" + " + "		"			"	"	.0039
54	" + "	↓	"	↓	↓	15°	"	0

INDEX OF RUNS (Cont'd)

Run	Model Configuration	Test	q	ψ	α_g	δ_{F_N}	δ_{F_S}	C_Q
55	S + $F_N F_S$ + $\Delta_1\Delta_2$	P_1	20	0	---	15°	60°	.0039
56	" + " + "		"			"	"	.0055
57	" + " + "		"			"	"	.0063
58	" + " + "		"			"	"	.0071
59	" + " + Δ_1		"			"	"	"
60	" + " + "		"			"	"	.0063
61	" + " + "		"			"	"	.0055
62	" + " + "		"			"	"	.0039
63	" + "		"			"	30°	0
64	" + " + Δ_1		"			"	"	.0039
65	" + " + "		"			"	"	.0055
66	" + " + "		"			"	"	.0063
67	" + " + "		"			"	"	.0071
68	" + " + $\Delta_1\Delta_2$		"			"	"	"
69	" + " + "		"			"	"	.0063
70	" + " + "		"			"	"	.0055
71	" + " + "		"			"	"	.0039
72	" + F_S		"			0°	"	0
73	" + " + $\Delta_1\Delta_2$		"			"	"	.0039
74	" + " + "		"			"	"	.0055
75	" + " + "		"			"	"	.0063
76	" + " + "		"			"	"	.0071
77	" + " + Δ_1		"			"	"	"
78	" + " + "		"			"	"	.0063
79	" + " + "		"			"	"	.0055
80	" + " + "		"			"	"	.0039
81	" + "	↓	"	↓	↓	"	60°	0

INDEX OF RUNS (Cont'd)

Run	Model Configuration	Test	q	ψ	α_g	δ_{F_N}	δ_{F_S}	C_Q
82	S + F_S + Δ_1	P_1	20	0	---	0°	60°	.0039
83	" + " + "					"	"	.0055
84	" + " + "					"	"	.0063
85	" + " + "					"	"	.0071
86	" + " + $\Delta_1\Delta_2$					"	"	"
87	" + " + "					"	"	.0063
88	" + " + "					"	"	.0055
89	" + " + "					"	"	.0039
90	" + " + Δ_2					"	"	"
91	" + " + "					"	"	.0055
92	" + " + "					"	"	.0063
93	" + " + "					"	"	.0071
94	" + " + "					"	30°	"
95	" + " + "					"	"	.0063
96	" + " + "					"	"	.0055
97	" + " + "					"	"	.0039
98	" + F_NF_S + Δ_2					15°	"	"
99	" + " + "					"	"	.0055
100	" + " + "					"	"	.0063
101	" + " + "					"	"	.0071
102	" + " + "					"	60°	"
103	" + " + "					"	"	.0063
104	" + " + "					"	"	.0055
105	" + " + "					"	"	.0039
106	" + " + "					30°	"	"
107	" + " + "					"	"	.0055
108	" + " + "	↓	↓	↓	↓	"	"	.0063

INDEX OF RUNS (Cont'd)

Run	Model Configuration	Test	q	ψ	α_g	δ_{F_N}	δ_{F_S}	C_Q
109	S + $F_N F_S$ + Δ_2	P_1	20	0	---	30°	60°	.0071
110	" + " + "	"	"			"	30°	"
111	" + " + "	"	"			"	"	.0063
112	" + " + "	"	"			"	"	.0055
113	" + " + "	"	"			"	"	.0039
114	" + F_N + Δ_2	"	"			"	0°	"
115	" + " + "	"	"			"	"	.0055
116	" + " + "	"	"			"	"	.0063
117	" + " + "	"	"			"	"	.0071
118	" + " + "	"	"			15°	"	"
119	" + " + "	"	"			"	"	.0063
120	" + " + "	"	"			"	"	.0055
121	" + " + "	"	"			"	"	.0039
122	" + Δ_2	"	"			0°	"	"
123	" + "	"	"			"	"	.0055
124	" + "	"	"			"	"	.0063
125	" + "	"	"			"	"	.0071
126	" + "	Tuft Pict.	"			"	"	"
127	" + $F_N F_S$ + Δ_2	Tuft Pict.	"			30°	60°	"
128	" + " + $\Delta_1 \Delta_2$	Tuft Pict.	"			"	"	"
129	" + " + Δ_1	Tuft Pict.	"			"	30°	"
130	" + Δ_1	Tuft Pict.	"			0°	0°	"
131	" + $\Delta_1 \Delta_2$	Tuft Pict.	"	↓	↓	"	"	"

INDEX OF RUNS (Cont'd)

Run	Model Configuration	Test	q	ψ	g	δ_{F_N}	δ_{F_S}	C_Q
132	S	Tuft Pict.	20	0	---	0°	0°	0
133	"	P_2	5			"	"	
134	"	"	10			"	"	
135	"	"	15			"	"	
136	"	"	20			"	"	
137	"	"	30			"	"	
138	"+$F_N F_S$	Tuft Pict.	20			30°	30°	
139	"+ "	"	"			"	60°	

VIII. INDEX OF FIGURES

I GENERAL

II EXPERIMENTAL RESULTS

A. MISCELLANEOUS

B. EFFECTS OF SUCTION

INDEX OF FIGURES (cont'd)

INDEX OF FIGURES (cont'd)

Page

INDEX OF FIGURES (cont'd)

INDEX OF FIGURES (cont'd)

INDEX OF FIGURES (cont'd)

Page

F. LIFT VARIATION WITH SUCTION QUANTITY

G. TUFT SKETCHES

INDEX OF FIGURES (cont'd)

IX. DISCUSSION

The experimental results appear in figures 4 through 81, while tables of $C_{L_{max}}$ and $\Delta C_{L_{max}}$ for each configuration appear on pages 34 and 35 respectively.

Since the Reynolds number effects show only a small variation in maximum lift coefficient (figures 5 to 7), Reynolds number changes have been neglected throughout this report. The value of the tunnel dynamic pressure, q, used was selected after consideration of both the Reynolds number and the suction quantity. The intentions were to be able to investigate a range of C_Q values and yet keep the maximum value within a reasonable limit*.

Increasing the suction quantity for all configurations increases the maximum lift except for a few instances with slot δ_2. From the results presented in figures 8 to 34, it is apparent that the forward slot is more effective in increasing the maximum lift than either slot δ_2 or the slot combination $\delta_1\delta_2$**. The lift increment obtained by increasing the suction quantity is also greater for slot δ_1 than for the other slot configurations, but decreases with increasing suction quantity***. The greatest gains in lift on the basic airfoil arise from deflecting the nose flap, e.g., $C_L = 0.250$ for a

---

* It should be emphasized that when slot configuration $\delta_1\delta_2$ was used, the suction quantity removed at each slot was less than for the single slot δ_1 or δ_2 configuration. Since the static pressure at slot δ_1 is less than that at slot δ_2, it is apparent that the suction quantity removed from each slot was not equal; a greater amount would be removed through slot δ_2 due to the lower pressure head. Therefore the effectiveness of slot δ_1 is decreased.

** The application of this wing to an actual full scale airplane was kept in mind throughout this investigation so that the horsepower required and available for the boundary layer suction was kept as low as possible.

*** This effect is shown later in a section of cross plots (figures 64 to 72).

DISCUSSION (cont'd)

15° deflection. Deflecting the nose flap also greatly changes the angle of stall of the airfoil. Changing the suction quantity was found to have a minor effect on the stall angle. The angle of stall is also influenced to some extent by the deflection of the slotted trailing edge flap. In particular for the case where the nose flap is deflected with the slotted flap, the angle of stall actually decreases. The maximum angle of stall obtained was 23° for the SF_N, $\delta F_N = 30^{\circ}$, $C_Q \neq 0$ configuration. For the maximum lift configuration as well as most of the high lift configurations the stall was sudden and was usually accompanied by severe buffeting. In several instances, the lift obtained with suction applied on slot Δ_2 was actually lower than the maximum lift of the basic airfoil without suction. As this condition disappeared as the suction quantity was increased, it is apparent that the lower suction quantities were insufficient to re-establish the flow over the rear of the airfoil.

Figures 35 to 43 present the effects of slot location for each basic configuration for a $C_Q = 0.0071$. In each case the location of the slot aft of the nose flap (slot Δ_1) proved superior to a slot located on the 70% wing chord (slot Δ_2). It also appears that the slot combination $\Delta_1\Delta_2$ is superior to the slot Δ_2. However the figures demonstrate that slot Δ_2 is better than no slot at all. Slot Δ_1 gives maximum lift coefficient increments of from 0.1 for the "flaps up" configuration to 0.55 for the SF_NF_S, $\delta_{F_N} = \delta_{F_S} = 30^{\circ}$ configuration.

Figures 44 to 59 present the flap effectiveness for the nose flap, slotted trailing edge flap, and their combinations for $C_Q = 0.0071$ and various slot configurations. The nose flap results indicate:

DISCUSSION (cont'd)

1. the greater the nose flap deflection, the greater the lift
2. slot Δ_1 increases the lift increments obtained for a given flap deflection more than either slot Δ_2 or slot $\Delta_1\Delta_2$
3. the angle of stall increases with nose flap deflection but remains relatively constant as the slot location varies

The slotted flap results indicate:

1. there is an optimum slotted flap deflection, after which the maximum lift decreases for increasing flap deflection*
2. slot Δ_1 increases the lift obtained for a given flap deflection more than either slot Δ_2 or slot $\Delta_1\Delta_2$
3. the angle of stall decreases for a slotted flap deflection

The slotted flap effectiveness, for $\delta_{F_N} = 15^\circ$, indicates the same conditions as does the previous case where $\delta_{F_N} = 0^\circ$. For the slotted flap effectiveness where the nose flap is deflected 30°, the characteristics of the nose flap influence the slotted flap such that:

1. for $C_Q = 0$, the lift obtained with the slotted flap at 60° is greater than the lift obtained with the flap at 30°
2. slot Δ_1 increases the lift obtained for a given flap deflection more than either slot Δ_1 or slot $\Delta_1\Delta_2$

* This effect is clearly shown in figures 60 to 63

DISCUSSION (cont'd)

3. the angle of stall decreases for slot Δ_1 and slot $\Delta_1\Delta_2$, and increases for slot Δ_2

Figures 60 to 63 show the variation of the maximum lift coefficient with flap deflection for the maximum suction quantity (C_Q = 0.0071) and for the various slot configurations. For the basic airfoil with no suction, figure 60 indicates that the most profitable configuration is $\delta_{F_N} = 30^\circ$, $\delta_{F_S} = 60^\circ$. From the curves it is apparent that more lift could have been obtained by deflecting the nose flap past 30°. For the slot Δ_1 configuration, figure 61, the optimum configuration was $\delta_{F_N} = \delta_{F_S} = 30^\circ$. The plot also indicates that:

1. a higher lift could be obtained by deflecting the nose flap to a greater angle
2. there exists an optimum slotted flap deflection past which the lift decreases with increasing flap deflection

These same results are apparent in the slot $\Delta_1\Delta_2$ configuration, figure 63, however on figure 62, slot Δ_2 , the optimum configuration again becomes $\delta_{F_N} = 30^\circ$, $\delta_{F_S} = 60^\circ$ as in the "suction off" condition. Future investigations with the airfoil should center around increasing the nose flap angle and slotted flap angle past 30° in increments to determine this optimum flap configuration and obtain a greater maximum lift.

In the last group of figures (figures 64 to 72), the variation of the lift with suction quantity (slot configuration as parameter) for angles below the stall angle are presented for each model configuration.

DISCUSSION (cont'd)

The general result that these plots indicate is that by increasing the suction quantity above the maximum used, the lift increase obtained would be small and undoubtedly insufficient to warrant the increase in the horsepower for the suction. Thus future study with this particular airfoil should center around flap deflections and possibly suction distribution, but not suction quantity.

On page 36, the horsepower required to operate this boundary layer control on a full scale airplane is estimated. The formula used is $hp = \frac{Q(\Delta P)}{550\,\eta}$, where ΔP is the sum of the losses and pressure head chargeable to the suction pump. Some of the values have been assumed due insufficient data while others have been obtained from references (see particularly reference 12). The value obtained was $\frac{54.6}{\eta}$, a value considered reasonable and not too demanding upon an airplane power plant.

The final group of figures present the results of the tuft investigations conducted on the optimum model configurations. The main indications are that flow separation begins at the leading edge and progresses rearward. Suction and flap deflection only tend to delay the leading edge separation to higher angles of attack.

X. SUMMARY OF RESULTS

This thesis presents results of an investigation of boundary layer suction as a means of increasing the maximum lift coefficient of a double-wedge supersonic airfoil operating at low subsonic speeds.

The model used was a 10% thick, double-wedge airfoil located between endplates with spanwise suction slots at the 20% and 70% wing chord. Both a 20% chord nose flap and a 20% chord slotted trailing edge flap were incorporated on the model. Boundary layer suction was applied to the forward slot, to the rear slot, and to both simultaneously, for all possible model configurations. The greatest increase in lift was obtained with both flaps deflected 30° and with maximum suction ($C_Q = 0.0071$) applied to the forward slot only ($C_{L_{max}} = 2.149$). In all cases the greatest increments in lift were obtained with the nose flap and front slot combinations. For the slotted trailing edge flap, there appeared to be an optimum deflection (between 30° and 60°) past which the lift would decrease. The rear slot in most instances proved to be much less effective in increasing the lift, than the front slot.

XI. REFERENCES

1. Rose, Leonard M. and Altman, John M.,"Low Speed Experimental Investigation of a Thin, Faired, Double-Wedge Airfoil Section With Nose and Trailing Edge Flaps," NACA T.N. 1934

2. Rose, Leonard M., and Altman, John M.,"Low Speed Investigation of the Stalling of a Thin, Faired, Double-Wedge Airfoil with Nose Flap," NACA T.N. 2172

3. Page, Sir F. Handley,"Slower and Safer Flying," Journal of the Royal Aeronautical Society, December 1950

4. Kruger, W."Calculations and Experimental Investigations on the Feed-Power Requirements of Airplanes with Boundary Layer Control," NACA T.M. 1167, September 1947

5. Horton, E.A., Racisz, S.F., Paradiso, N.J.,"Investigations of Boundary Layer Control to Improve the Lift and Drag Characteristics of the NACA 65_2-415 Airfoil Section with Double Slotted and Plain Flaps," NACA T.N. 2149, August 1950

6. Fage, A., and Sargent, R.F.,"Design of Suction Slots,"R&M 2127, February 1944

7. Smith, A.M.O.,"A Preliminary Study of the Problem of Boundary Layer Control," Thesis, California Institute of Technology, June 1938

8. Goldstein, "Low Drag and Suction Airfoils," Journal of the Institute of Aeronautical Sciences, April 1948

9. Schrenk, "Reasearch on Boundary Layer Control at Gottingen Institute of Aeronautics," CGD - 149, January 1946

10. Pfenninger,W.,"Investigations on Reductions of Friction on Wings, in Particular by Means of Boundary Layer Suction," NACA T.M. 1181, August 1947

REFERENCES (cont'd)

11. Tetervin, N.,"A Review of Boundary Layer Literature," NACA T.N. 1384, July 1947

12. Wallace, R.E.,"Low-Speed Investigation of a Double Wedge Airfoil With Leading-Edge Slat," Thesis, California Institute of Technology, June 1951

XII. TABLE I

SUMMARY OF TEST RESULTS IN TERMS OF $C_{L_{max}}$

Config.	Flap Deflection	$C_Q=0$	Slot #1				Slot #2				Slot #1&2			
			$C_Q=$ .0039	$C_Q=$ .0055	$C_Q=$ .0063	$C_Q=$ .0071	$C_Q=$ .0039	$C_Q=$ .0055	$C_Q=$ .0063	$C_Q=$ .0071	$C_Q=$ .0039	$C_Q=$ .0055	$C_Q=$ .0063	$C_Q=$ .0071
SF_N	$\delta_{F_N}=0°$	.740 9°	.794 9°	.825 10°	.845 10°	.870 10°	.780 9°	.800 9°	.805 9°	.815 9°	.772 9°	.805 9°	.821 9°	.832 9°
	$\delta_{F_N}=15°$	.999 14°	1.106 14°	1.142 15°	1.162 15°	1.170 15°	1.076 14°	1.094 14°	1.104 14°	1.112 14°	1.062 14°	1.092 14°	1.107 14°	1.117 14°
	$\delta_{F_N}=30°$	1.138 17°	1.421 22°	1.514 23°	1.560 23°	1.563 23°	1.113 17°	1.149 17°	1.164 17°	1.182 17°	1.204 24°	1.303 23°	1.366 23°	1.415 22°
SF_S	$\delta_{F_S}=0°$	.740 9°	.794 9°	.825 10°	.845 10°	.870 10°	.780 9°	.800 9°	.805 9°	.815 9°	.772 9°	.805 9°	.821 9°	.832 9°
	$\delta_{F_S}=30°$	1.475 6°	1.570 7°	1.595 7°	1.595 7°	1.615 8°	1.424 7°	1.448 7°	1.466 7°	1.481 7°	1.529 7°	1.568 7°	1.582 7°	1.595 7°
	$\delta_{F_S}=60°$	1.415 6°	1.486 7°	1.522 7°	1.536 7°	1.555 8°	1.425 7°	1.441 7°	1.456 7°	1.460 7°	1.476 6°	1.501 7°	1.512 7°	1.528 7°
SF_NF_S $\delta_{F_N}=15°$	$\delta_{F_S}=0°$	.999 14°	1.106 14°	1.142 15°	1.162 15°	1.170 15°	1.076 14°	1.094 14°	1.104 14°	1.112 14°	1.062 14°	1.092 14°	1.107 14°	1.117 14°
	$\delta_{F_S}=30°$	1.675 12°	1.747 13°	1.802 13°	1.826 13°	1.845 13°	1.655 12°	1.672 12°	1.684 12°	1.690 12°	1.718 12°	1.774 12°	1.781 12°	1.795 12°
	$\delta_{F_S}=60°$	1.575 11°	1.694 12°	1.725 13°	1.744 13°	1.765 13°	1.622 12°	1.647 12°	1.655 12°	1.665 12°	1.645 12°	1.684 12°	1.701 12°	1.715 12°
SF_NS_S $\delta_{F_N}=30°$	$\delta_{F_S}=0°$	1.138 17°	1.421 22°	1.514 23°	1.560 23°	1.563 23°	1.113 17°	1.149 17°	1.164 17°	1.182 17°	1.204 24°	1.303 23°	1.366 23°	1.415 22°
	$\delta_{F_S}=30°$	1.603 14°	2.025 20°	2.096 21°	2.135 21°	2.149 21°	1.713 20°	1.773 19°	1.894 19°	1.830 18°	1.762 16°	1.951 19°	2.015 19°	2.033 19°
	$\delta_{F_S}=60°$	1.810 20°	1.988 19°	2.055 20°	2.086 20°	2.100 20°	1.844 19°	1.871 19°	1.889 19°	1.895 19°	1.864 19°	1.953 19°	1.982 19°	1.995 19°

Note: Upper number in each box represents $C_{L_{MAX}}$
Lower " " " " " angle of attack (α_g) at which $C_{L_{MAX}}$ occurred.

XIII. TABLE II

SUMMARY OF TEST RESULTS IN TERMS OF $\Delta C_{L_{max}}$

Config.	Flap Deflection	$C_Q=0$	Slot Δ_1			Slot Δ_2			Slot $\Delta_1\Delta_2$		
			$C_Q=$ .0039	$C_Q=$ .0055	$C_Q=$ .0063	$C_Q=$ .0071	$C_Q=$ .0039	$C_Q=$ .0055	$C_Q=$ .0063	$C_Q=$ .0071	$C_Q=$ .0039	$C_Q=$ .0055	$C_Q=$ .0063	$C_Q=$ .0071
SF_N	$\delta_{F_N}=0°$	.740 9°	.054 0°	.085 1°	.105 1°	.130 1°	.040 0°	.060 1°	.065 1°	.075 1°	.032 1°	.065 1°	.081 1°	.092 1°
	$\delta_{F_N}=15°$	.999 14°	.107 0°	.143 1°	.163 1°	.171 1°	.077 0°	.095 0°	.105 0°	.113 0°	.063 0°	.093 0°	.108 0°	.118 0°
	$\delta_{F_N}=30°$	1.138 17°	.283 5°	.376 6°	.422 6°	.425 6°	-.025 0°	.011 0°	.026 0°	.044 0°	.066 7°	.165 6°	.228 6°	.277 6°
SF_S	$\delta_{F_S}=0°$	.740 9°	.054 0°	.085 1°	.105 1°	.130 1°	.040 0°	.060 1°	.065 1°	.075 1°	.032 1°	.065 1°	.081 1°	.092 1°
	$\delta_{F_S}=30°$	1.475 6°	.095 1°	.120 1°	.120 1°	.140 2°	-.051 1°	-.027 1°	-.009 1°	.006 1°	.054 1°	.093 1°	.107 1°	.120 1°
	$\delta_{F_S}=60°$	1.415 6°	.071 1°	.107 1°	.121 1°	.140 2°	.010 1°	.026 1°	.041 1°	.045 1°	.061 0°	.086 1°	.097 1°	.113 1°
SF_NF_S $\delta_{F_N}=15°$	$\delta_{F_S}=0°$	.999 14°	.107 0°	.143 1°	.163 1°	.171 1°	.077 0°	.095 0°	.105 0°	.113 0°	.063 0°	.093 0°	.108 0°	.118 0°
	$\delta_{F_S}=30°$	1.675 12°	.072 1°	.127 1°	.151 1°	.170 1°	-.020 0°	-.003 0°	.009 0°	.015 0°	.043 0°	.099 0°	.106 0°	.120 0°
	$\delta_{F_S}=60°$	1.575 11°	.119 1°	.150 1°	.169 1°	.190 1°	.047 0°	.072 0°	.080 0°	.090 0°	.070 0°	.109 0°	.126 0°	.140 0°
SF_NS_S $\delta_{F_N}=30°$	$\delta_{F_S}=0°$	1.138 17°	.283 5°	.376 6°	.422 6°	.425 6°	-.025 0°	.011 0°	.026 0°	.044 0°	.066 7°	.165 6°	.228 6°	.277 6°
	$\delta_{F_S}=30°$	1.603 14°	.422 6°	.493 7°	.532 7°	.546 7°	.110 6°	.170 5°	.291 5°	.227 4°	.159 2°	.348 5°	.412 5°	.430 5°
	$\delta_{F_S}=60°$	1.810 20°	.178 -1°	.245 0°	.276 0°	.290 0°	.034 -1°	.061 -1°	.079 -1°	.085 -1°	.054 -1°	.143 -1°	.172 -1°	.185 -1°

Note: Upper number in each box represents increase of $C_{L_{max}}$ above $C_Q=0$ configuration

Lower number in each box represents increase of angle of attack above $C_Q=0$ configuration

XIV. HORSEPOWER COMPUTATIONS[1]

$$hp = \frac{Q(\Delta P)}{550\eta}, \text{ where } \Delta P = \Delta P_1 + \Delta P_2 + \Delta P_3$$

Assume the following dimensional data of a full scale airplane:

W = Weight = 10,000 lbs
S = Wing Area = 440 ft^2 $\quad C_{L_{max}} = 2.100$
MAC = 9.5 ft
AR = Aspect Ratio = 5.5 ft $\quad C_Q = 0.0071$

$$\rho = 0.002378 \text{ slugs/ft}^3$$

For level flight: $L = W = \frac{1}{2}\rho V^2 C_L S$

$$\text{or } V = \left[\frac{2W}{\rho C_L S}\right]^{\frac{1}{2}} = \left[\frac{20{,}000}{.002378 \times 2.1 \times 440}\right]^{\frac{1}{2}} = 95.5 \text{ ft/sec}$$

$$Q = C_Q V S = 0.0071 \times 95.5 \times 440 = 298 \text{ ft}^3/\text{sec}$$

ΔP_1 = p(free stream) - p (20% wing chord)* = 1.50 x q

= 1.50 x 40 = 60 lb/ft^2

$\Delta P_2 = \frac{\rho}{2} V^2$ (Assuming boundary layer air leaves with free stream velocity) $= \frac{\rho}{2}(95.5)^2 = 10.84$ lb/ft^2

$\Delta P_3 = 30$ lb/ft^2 **

$$\Delta P = \Delta P_1 + \Delta P_2 + \Delta P_3 = 60 + 10.84 + 30 = 100.84$$

$$hp = \frac{298\ (100.84)}{550\ \eta} = \frac{54.6}{\eta}$$

---

* The value of the static pressure at the 20% wing chord was obtained from Reference 12

** This value is assumen and is relatively high, however, it allows a "dirty" air duct configuration that might be necessary in a military airplane

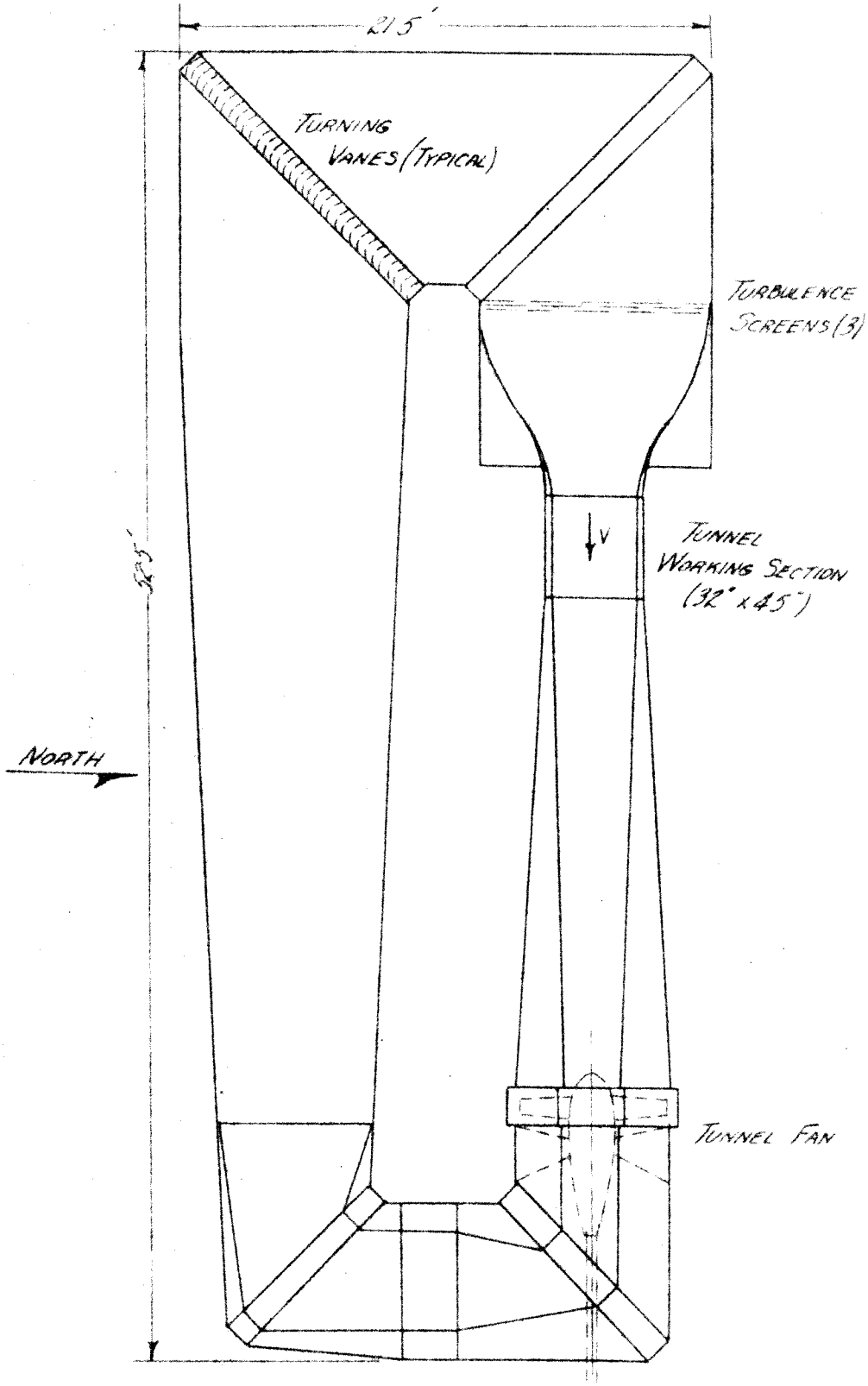

PLANVIEW OF THE MERRILL WIND TUNNEL

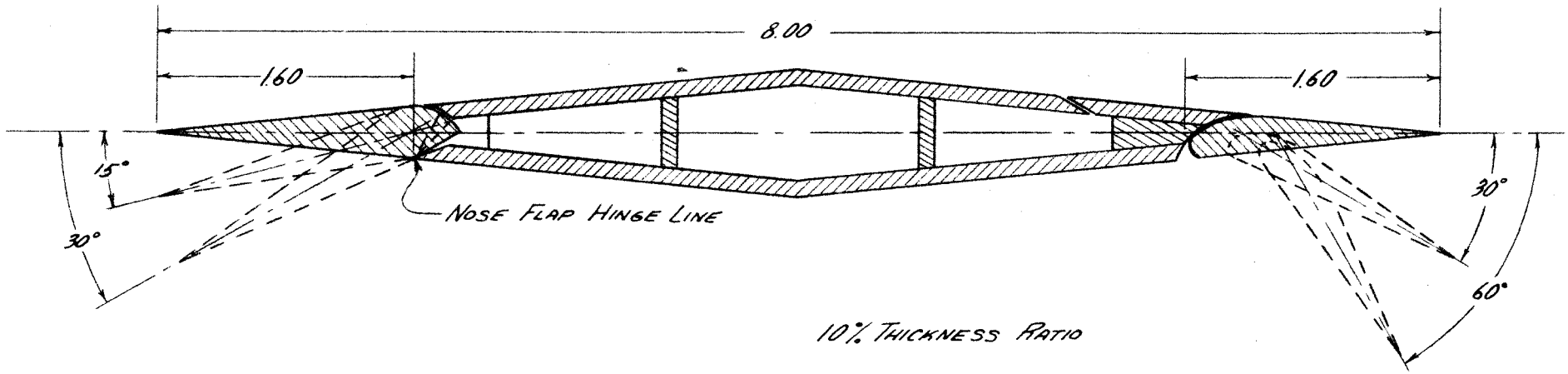

SKETCH SHOWING AIRFOIL CROSS-SECTION

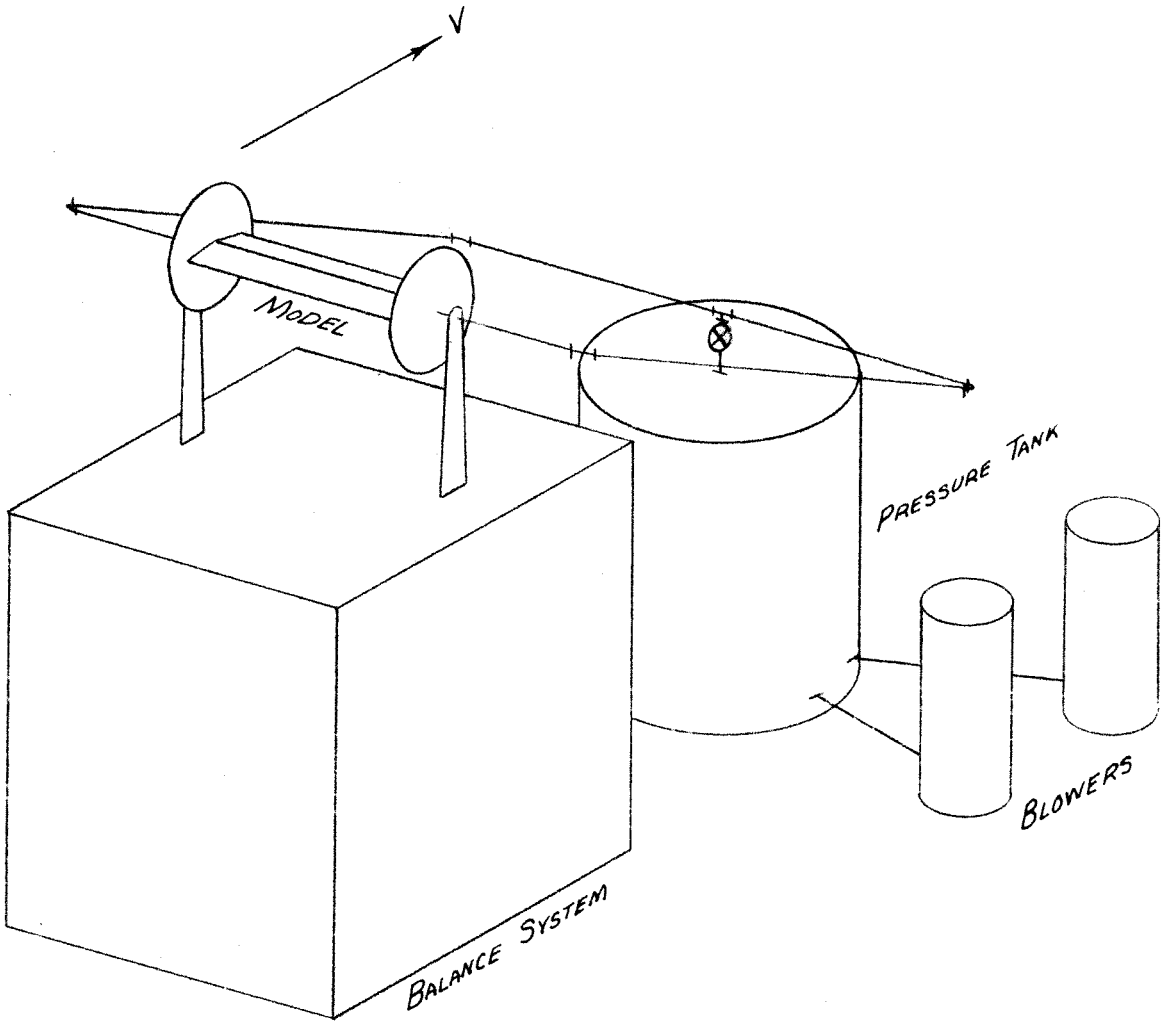

DIAGRAMMATIC SKETCH
OF MODEL AND EQUIPMENT SET-UP

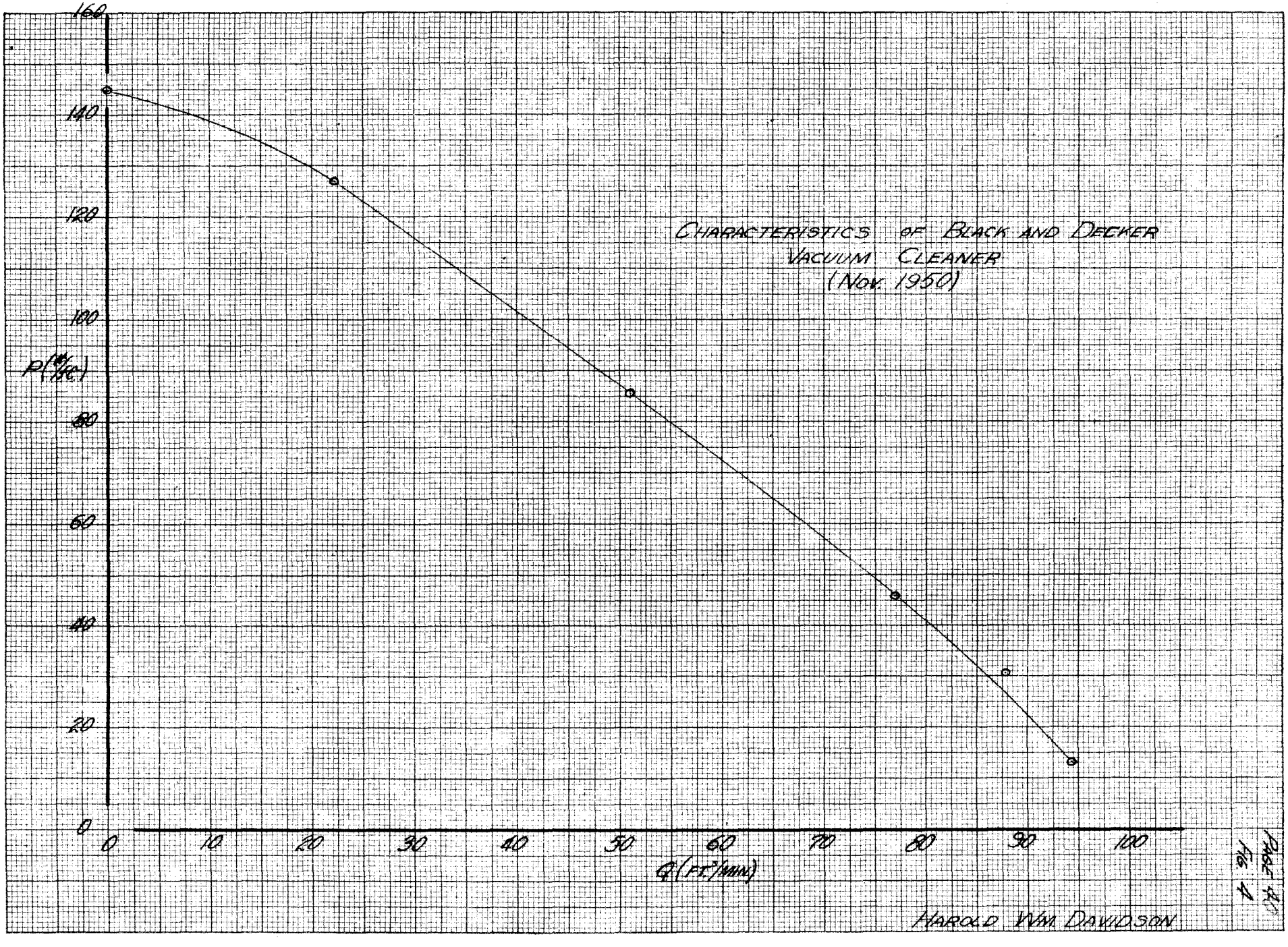
CHARACTERISTICS OF BLACK AND DECKER
VACUUM CLEANER
(Nov. 1950)
P(in H2O)
160
140
120
100
80
60
40
20
0
0
10
20
30
40
50
60
70
80
90
100
Q(FT³/MIN)
HAROLD WM DAWSON

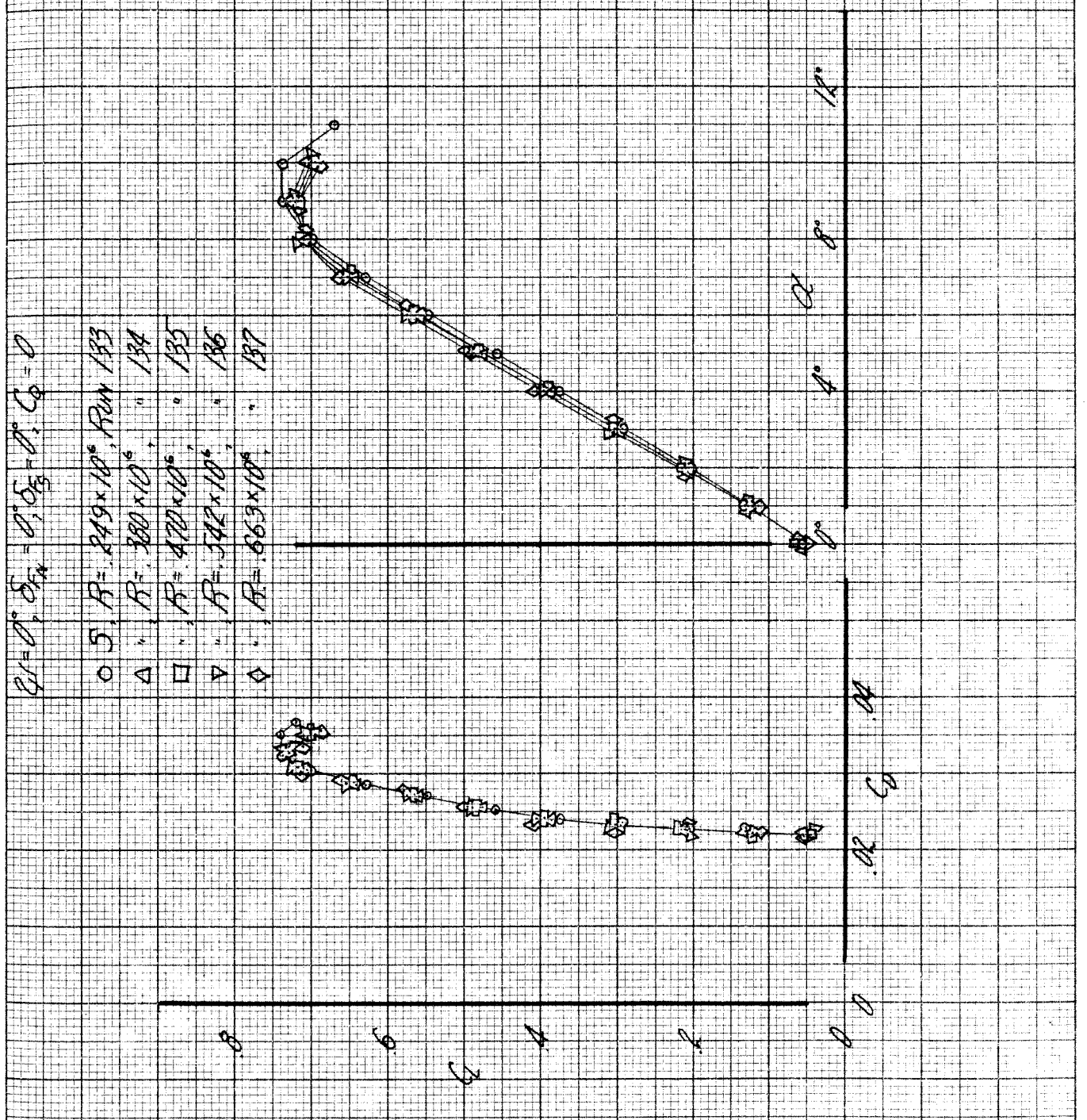

EFFECT OF REYNOLDS NUMBER
ON THE FLAPS UP CONFIGURATION
NO SUCTION

$\varphi = 0°, \delta_{F_N} = 0°, \delta_{F_S} = 0°$

○ $S + \Delta_1 \Delta_2$, $R = .249 \times 10^6$, $C_Q = .0148$, RUN 5
△ " + " , $R = .470 \times 10^6$, $C_Q = .0085$, " 6
□ " + " , $R = .605 \times 10^6$, $C_Q = .0066$, " 7
▽ " + " , $R = .716 \times 10^6$, $C_Q = .0054$, " 8

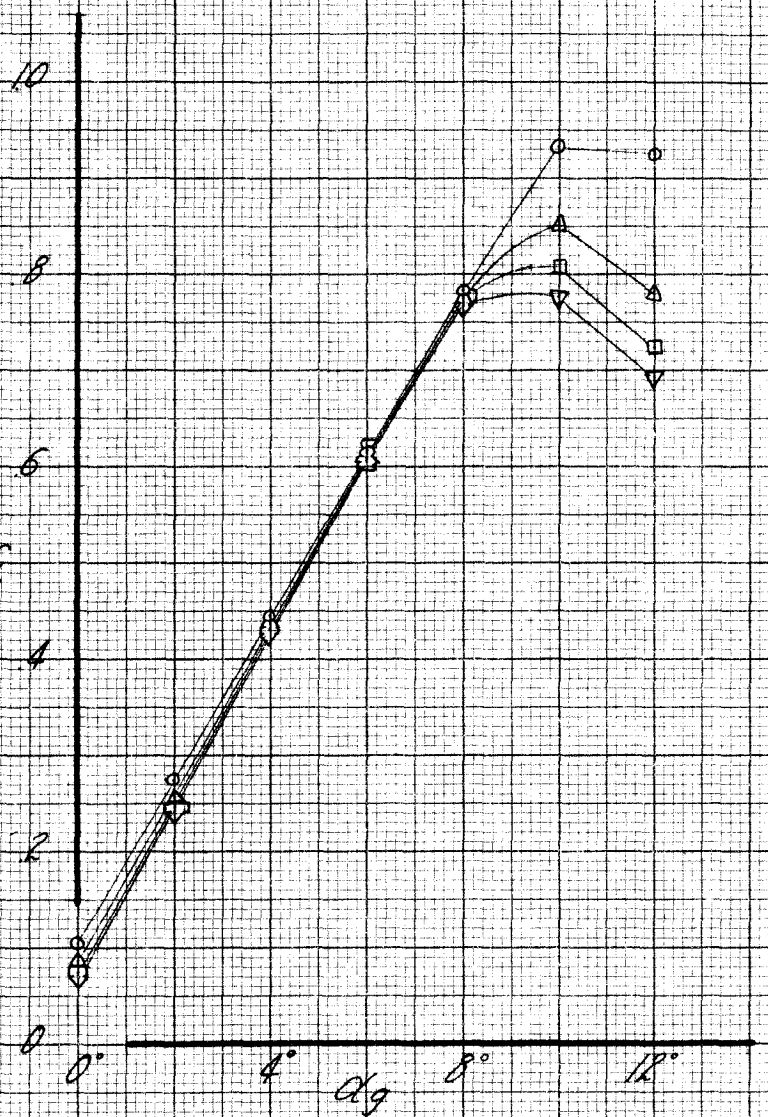

EFFECTS OF REYNOLDS NUMBER ON THE
"FLAPS UP" CONFIGURATION
FULL SUCTION, $(\Delta_1 \Delta_2)$

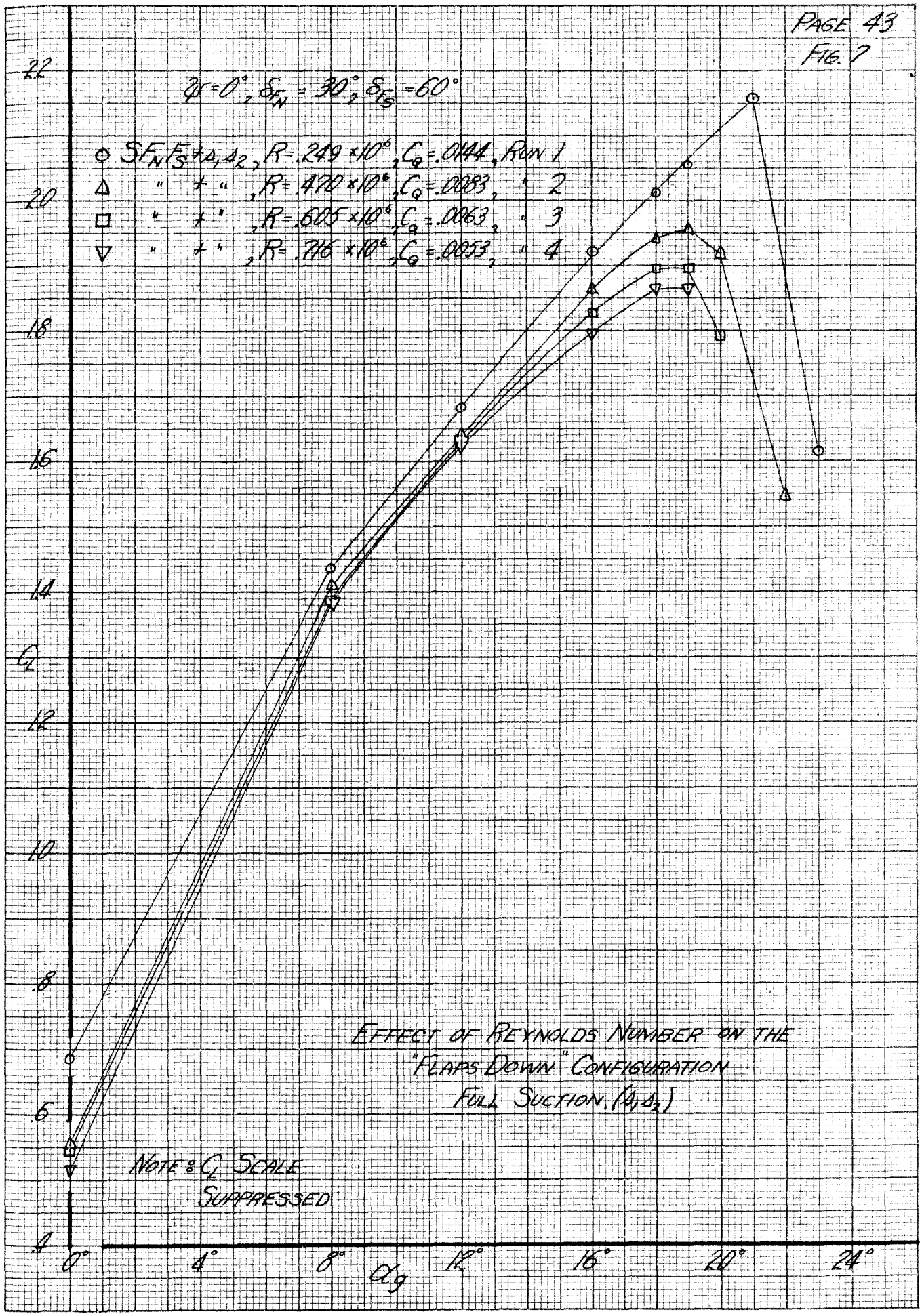
$\alpha_T = 0°, \delta_N = 30°, \delta_S = 60°$
○ $S/F_N/F_S + A_1 A_2$, $R = .249 \times 10^6$, $C_Q = .0144$, Run 1
△ " + " , $R = .470 \times 10^6$, $C_Q = .0083$, " 2
□ " + " , $R = .605 \times 10^6$, $C_Q = .0063$, " 3
▽ " + " , $R = .716 \times 10^6$, $C_Q = .0053$, " 4
22
20
18
16
14
12
10
8
6
4
C_L
0°
4°
8°
12°
16°
20°
24°
α_g
EFFECT OF REYNOLDS NUMBER ON THE "FLAPS DOWN" CONFIGURATION FULL SUCTION. ($A_1 A_2$)
NOTE: C_L SCALE SUPPRESSED

$q = 20 LB/FT^2$, $\alpha = 0°$, $\delta_{F_N} = 0°$, $\delta_{F_S} = 0°$

○	S	$C_Q = 0$	RUN 9
△	" + Δ_1	$C_Q = .0039$	" 10
□	" + "	$C_Q = .0055$	" 11
▽	" + "	$C_Q = .0063$	" 12
◇	" + "	$C_Q = .0071$	" 13

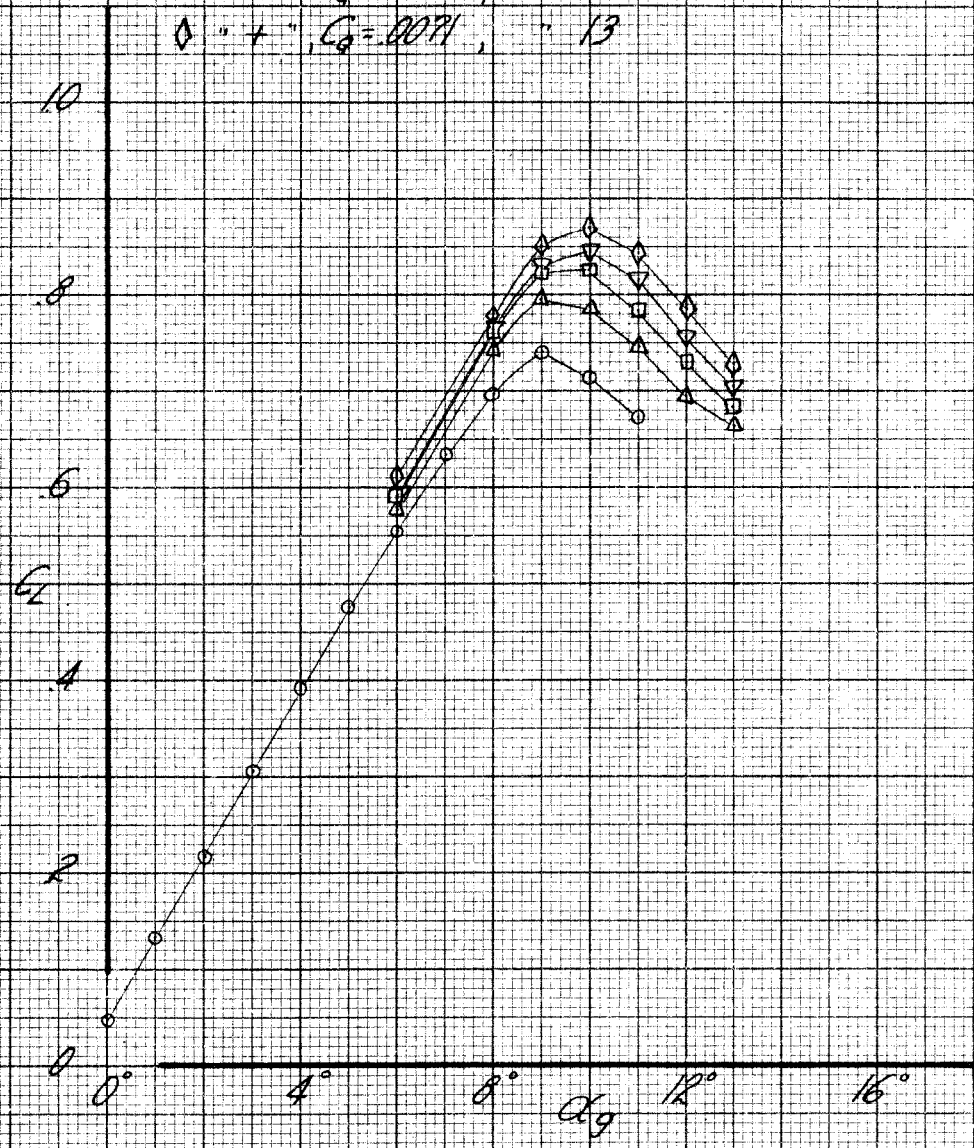

EFFECT OF SUCTION
ON THE "FLAPS UP" CONFIGURATION
SLOT Δ_1

$q = 20$ LB/FT.^{2}, $\alpha_s = 0°$, $\delta_{f_N} = 0°$, $\delta_{f_S} = 0°$

○	S	$C_Q = 0$	RUN 9
△	" + Δ_2	$C_Q = .0039$	" 122
□	" + "	$C_Q = .0055$	" 123
▽	" + "	$C_Q = .0063$	" 124
◇	" + "	$C_Q = .0071$	" 125

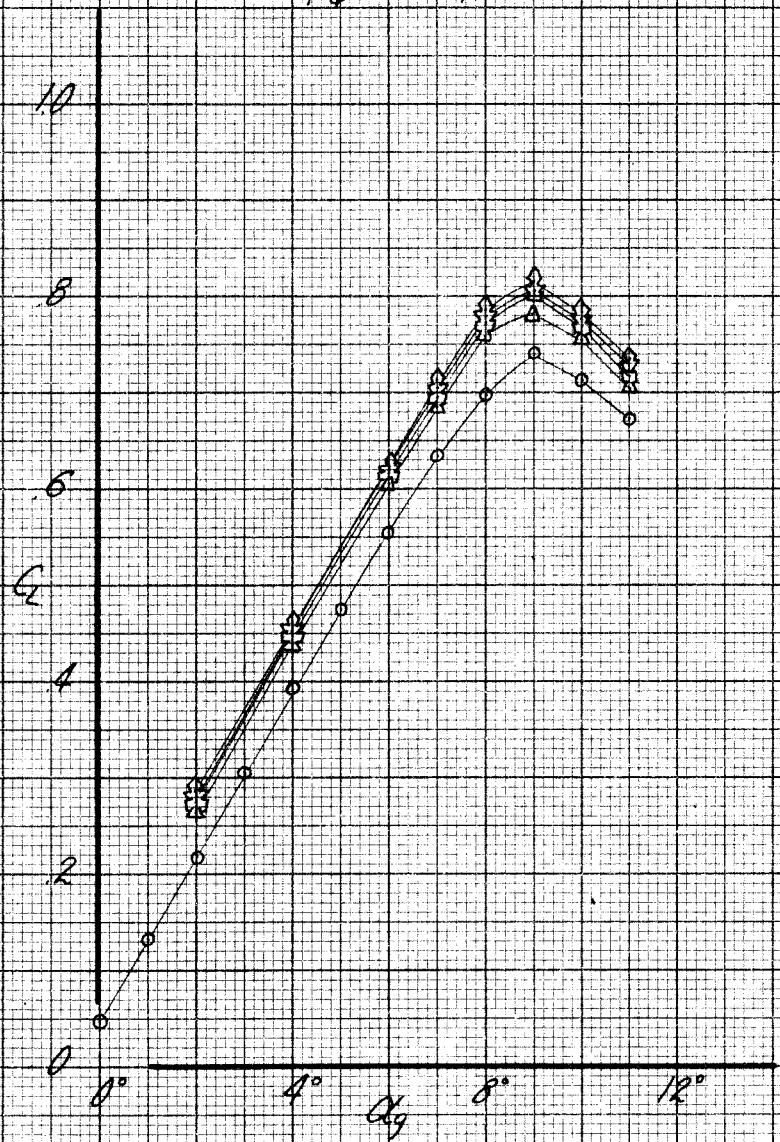

EFFECT OF SUCTION
ON THE "FLAPS UP" CONFIGURATION
SLOT S_2

$q = 20 LB/FT.^2$, $\alpha = 0°$, $\delta_{FN} = 0°$, $\delta_{FS} = 0°$

○	S	$C_Q = 0$	RUN 9
△	" + $S_1 S_2$	$C_Q = .0039$	" 17
□	" + "	$C_Q = .0055$	" 16
▽	" + "	$C_Q = .0063$	" 15
◇	" + "	$C_Q = .0071$	" 14

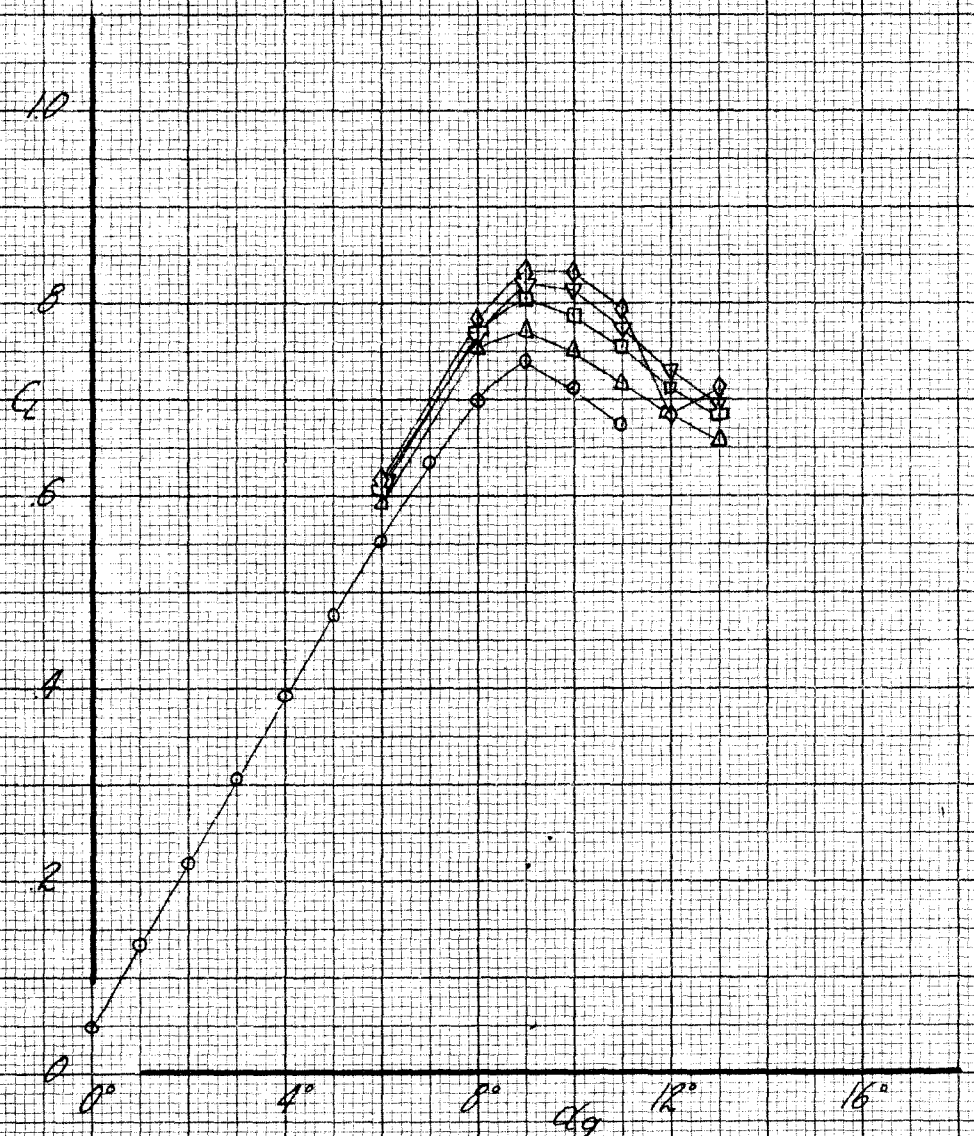

EFFECT OF SUCTION
ON THE "FLAPS UP" CONFIGURATION
SLOTS $S_1 S_2$

$q = 20$ LB/FT.^{2}, $\alpha_r = 0°$, $\delta_{FN} = 15°$, $\delta_F = 0°$

○	SF_N	$C_Q = 0$	RUN 18
△	" A_1	$C_Q = .0039$	" 26
□	" "	$C_Q = .0055$	" 25
▽	" "	$C_Q = .0063$	" 24
◇	" "	$C_Q = .0077$	" 23

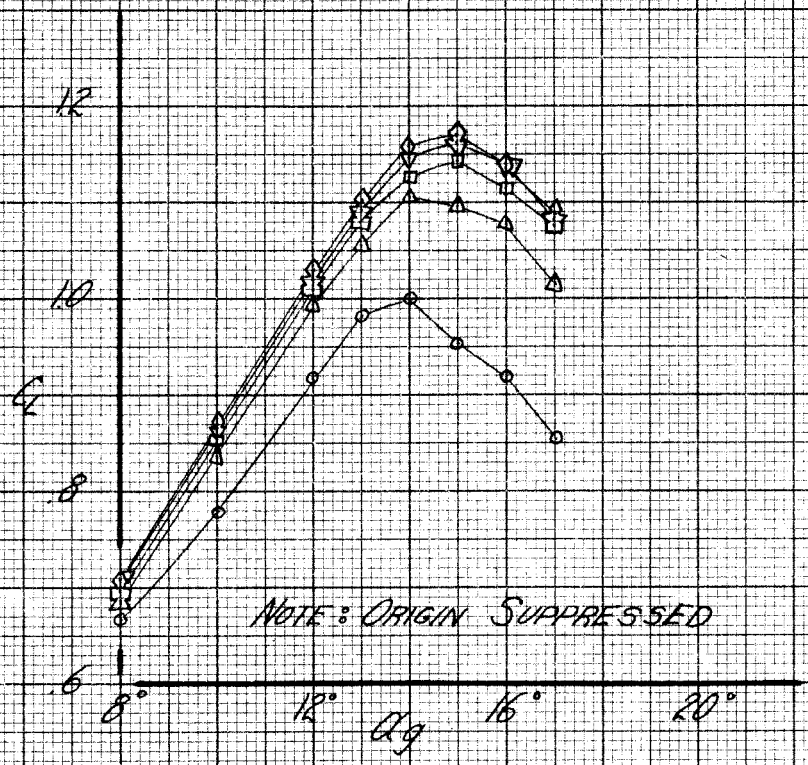

EFFECT OF SUCTION
NOSE FLAP DEFLECTED 15°
SLOT A_1

$q = 20 LB/FT^2$, $\alpha_T = 0°$, $\delta_{F_N} = 15°$, $\delta_{F_S} = 0°$

○	SF_N	$C_Q = 0$	RUN 18
△	"	$\times\ S_2$, $C_Q = .0039$	" 121
□	"	" , $C_Q = .0055$	" 120
▽	"	" , $C_Q = .0063$	" 119
◇	"	" , $C_Q = .0071$	" 118

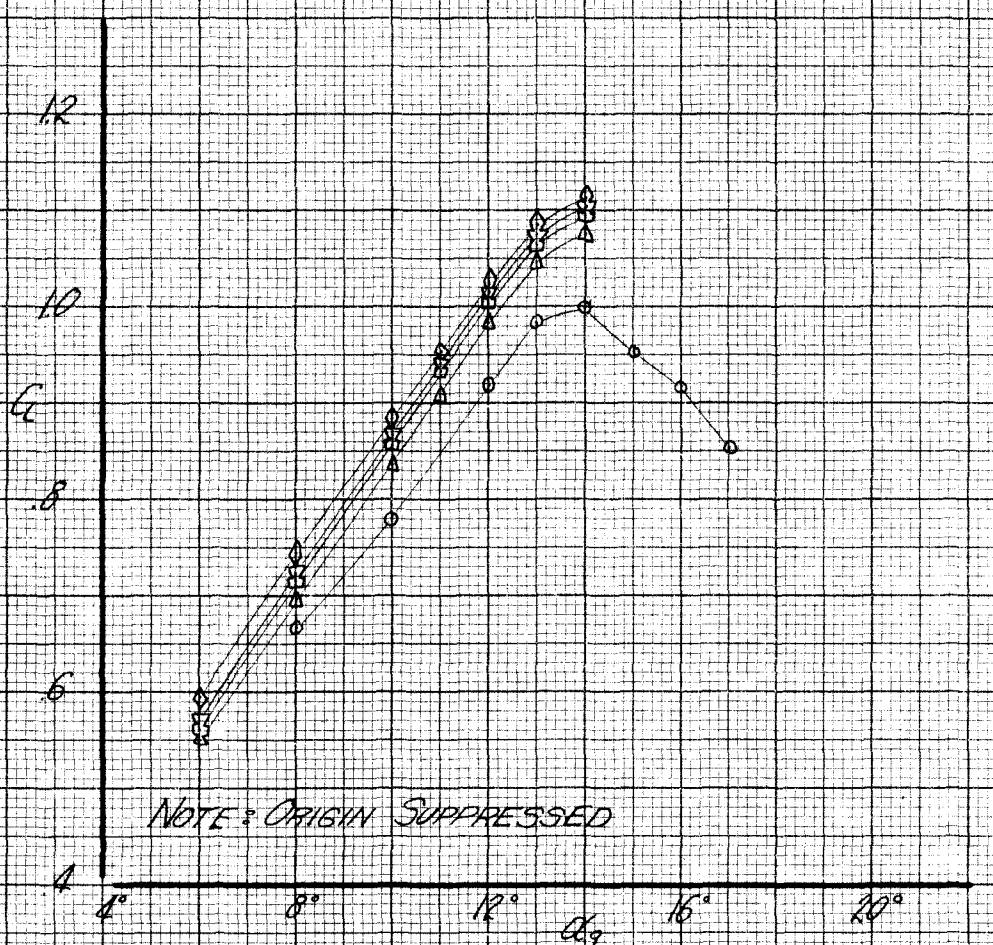

EFFECT OF SUCTION
NOSE FLAP DEFLECTED 15°
SLOT S_2

FIG. 13

$q = 20$ LB/FT.^{2}, $\alpha = 0°$, $\delta_{FN} = 15°$, $\delta_{FS} = 0°$

○ SF_N, $C_Q = 0$, RUN 18
△ " + $S_1 S_2$, $C_Q = .0039$, " 19
□ " + " , $C_Q = .0055$, " 20
▽ " + " , $C_Q = .0063$, " 21
◇ " + " , $C_Q = .0071$, " 22

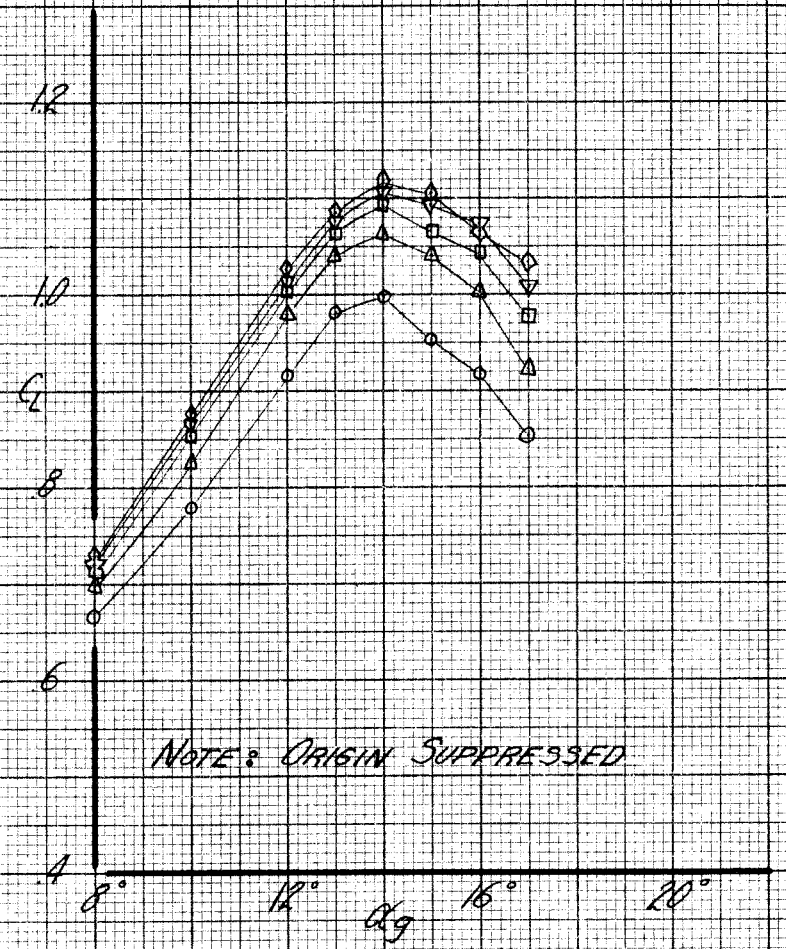

NOTE: ORIGIN SUPPRESSED

EFFECT OF SUCTION
NOSE FLAP DEFLECTED 15°
SLOTS $S_1 S_2$

FIG 14

$q = 20$ LB/FT.^{2}, $\gamma_s = 0°$, $\delta_{F_N} = 30°$, $\delta_{F_S} = 0°$

○	SF_N	$C_Q = 0$	RUN 27
△	" + A_1	$C_Q = .0039$	" 28
□	" + "	$C_Q = .0055$	" 29
▽	" + "	$C_Q = .0063$	" 30
◇	" + "	$C_Q = .0070$	" 31

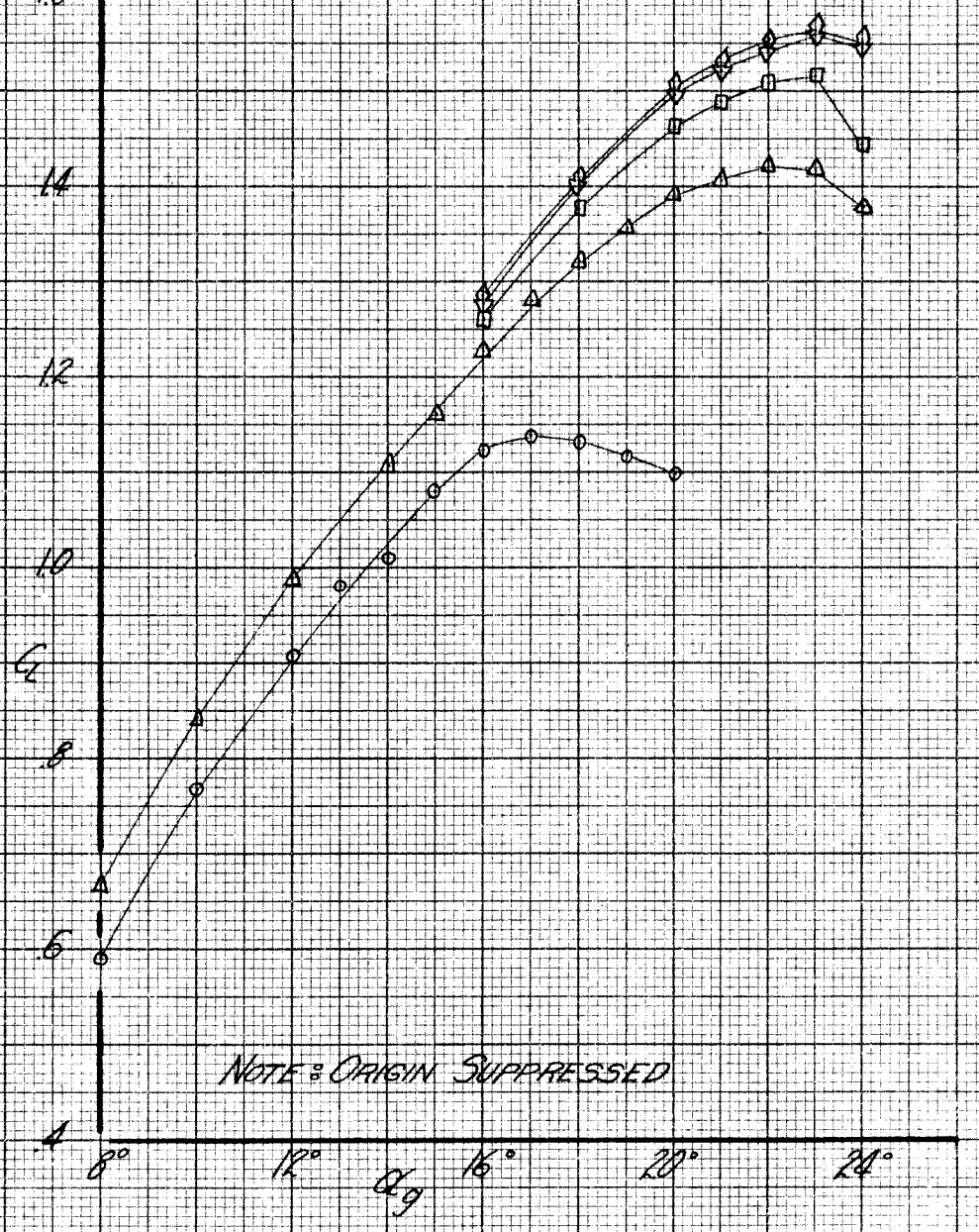

EFFECT OF SUCTION
NOSE FLAP DEFLECTED 30°
SLOT A_1

$q = 20$ LB/FT.^{2}, $\alpha = 0°$, $\delta_{F_N} = 30°$, $\delta_{F_S} = 0°$

○	SF_N	$C_Q = 0$	RUN 27
△	" + A_2	$C_Q = .0039$	" 114
□	" + "	$C_Q = .0055$	" 115
▽	" + "	$C_Q = .0063$	" 116
◇	" + "	$C_Q = .0071$	" 117

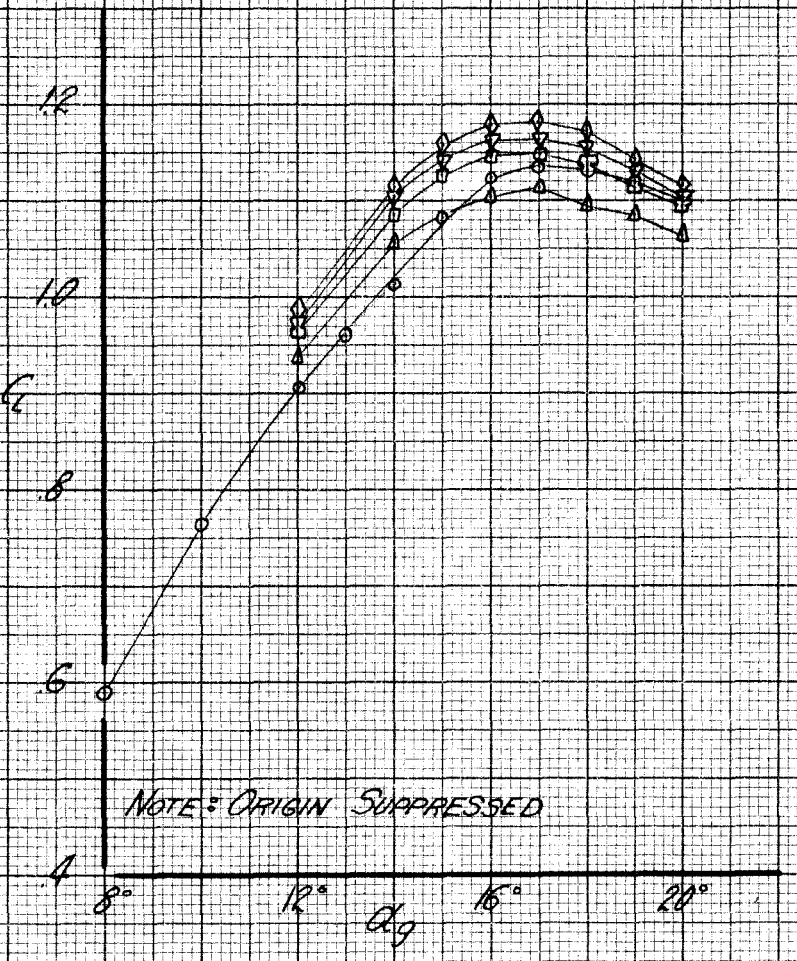

EFFECT OF SUCTION
NOSE FLAP DEFLECTED 30°
SLOT A_2

FIG. 16

$q = 20$ LB/FT.^{2}, $\alpha = 0°$, $\delta_{FN} = 30°$, $\delta_S = 0°$

○	SF_N		$C_Q = 0$	RUN 27
△	"	+ S_1, S_2	$C_Q = .0039$	" 35
□	"	+ "	$C_Q = .0055$	" 34
▽	"	+ "	$C_Q = .0063$	" 33
◇	"	+ "	$C_Q = .0070$	" 32

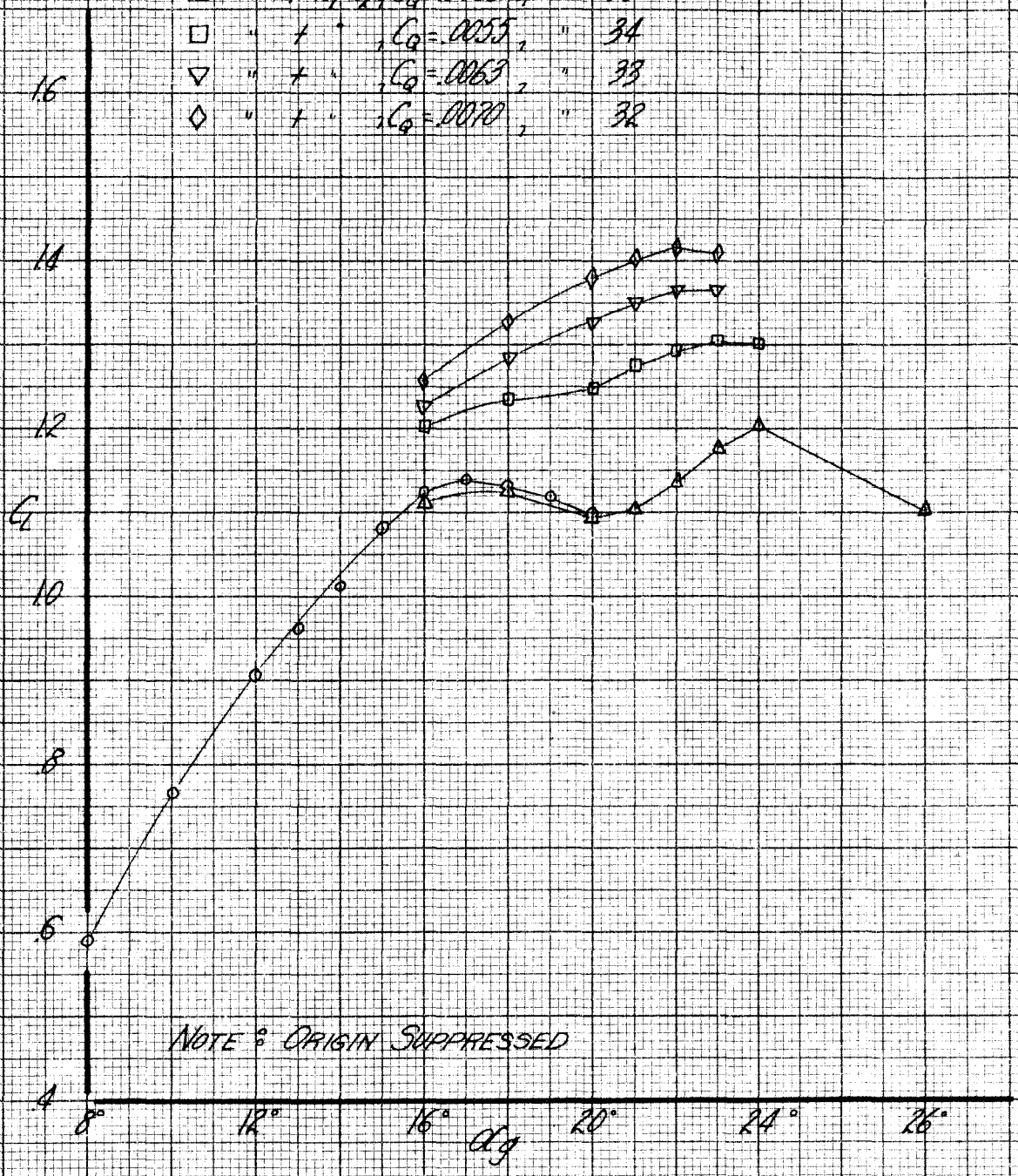

NOTE ° ORIGIN SUPPRESSED

EFFECT OF SUCTION
NOSE FLAP DEFLECTED 30°
SLOTS S_1, S_2

$q = 20$ LB/FT.^{2}; $i_t = 0°$, $\delta_{F_N} = 0°$, $\delta_{F_S} = 30°$

○	SF_S	$C_Q = 0$	RUN 82
△	" + Δ_1	$C_Q = .0039$	" 80
□	" +	$C_Q = .0055$	" 79
▽	" +	$C_Q = .0063$	" 78
◇	" +	$C_Q = .0071$	" 77

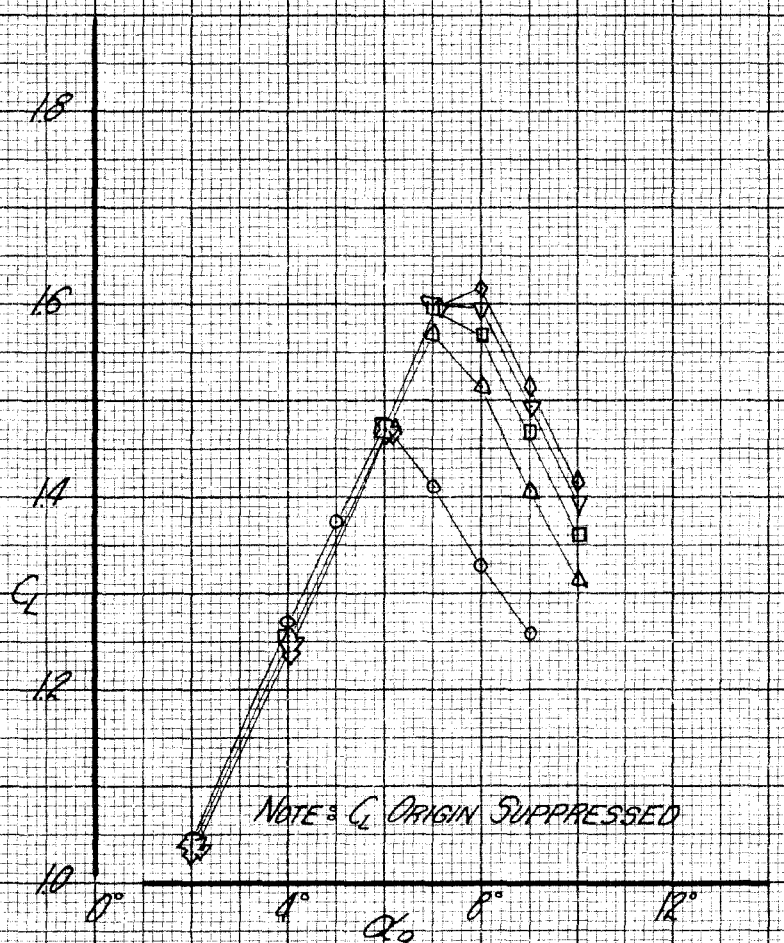

EFFECT OF SUCTION
SLOTTED FLAP DEFLECTED 30°
SLOTS Δ_1

$q = 20.4$ LB/FT.^{2}, $\psi = 0°$, $\delta_N = 0°$, $\delta_S = 30°$

○	SF_S	, $C_Q = 0$	, RUN	72
△	" + Δ_2	, $C_Q = .0039$	, "	97
□	" + "	, $C_Q = .0055$	, "	96
▽	" + "	, $C_Q = .0063$	, "	95
◇	" + "	, $C_Q = .0077$	, "	94

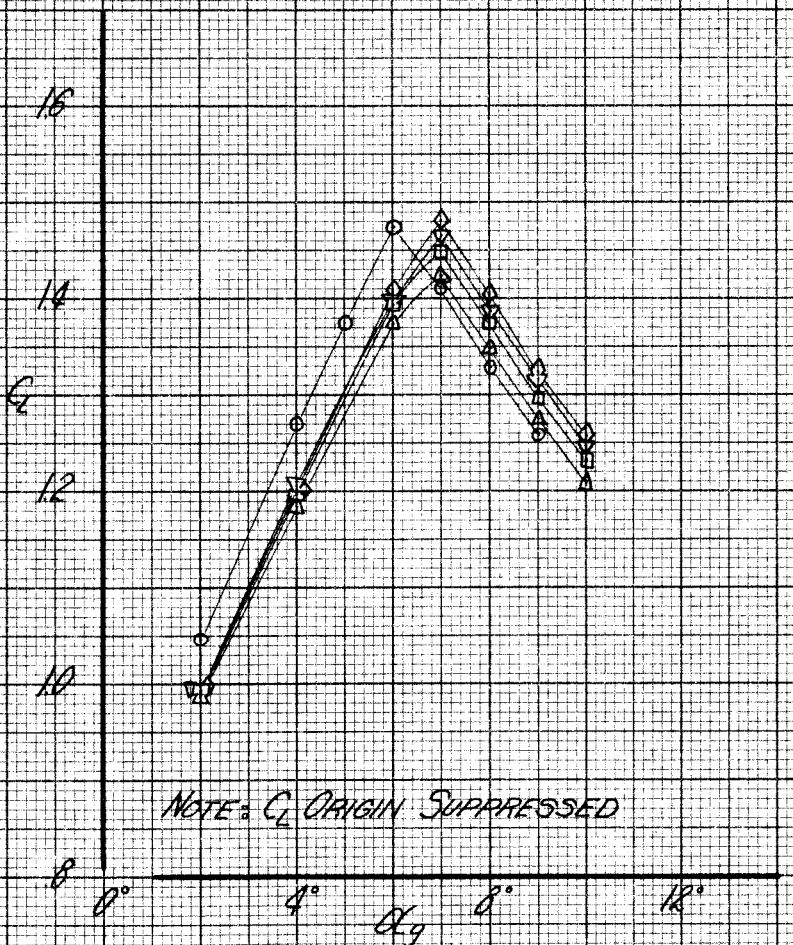

NOTE: C_L ORIGIN SUPPRESSED

EFFECT OF SUCTION
SLOTTED FLAP DEFLECTED 30°
SLOT Δ_2

$q = 20$ LB/FT.^{2}; $\gamma = 0°$, $\delta_{F_N} = 0°$, $\delta_{F_S} = 30°$

○	SF_S	, $C_Q = 0$,	RUN	72
△	" + $A_1 A_2$,	$C_Q = .0039$,	"	73
□	" +	, $C_Q = .0055$,	"	74
▽	" +	, $C_Q = .0063$,	"	75
◇	" +	, $C_Q = .0071$,	"	76

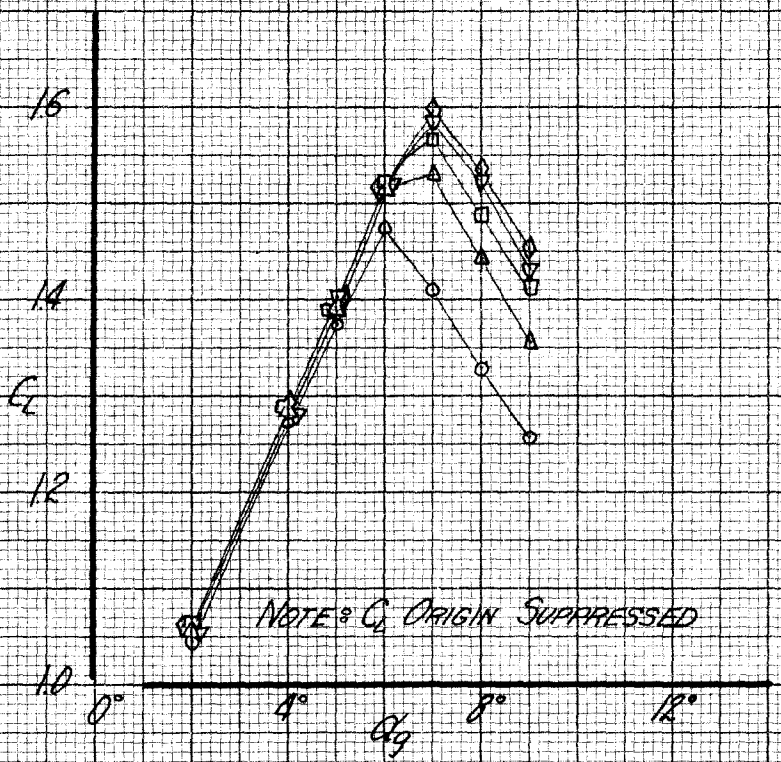

EFFECTS OF SUCTION
SLOTTED FLAP DEFLECTED 30°
SLOTS $A_1 A_2$

$q = 20$ LB/FT., $\alpha_i = 0°$, $\delta_{F_N} = 0°$, $\delta_{F_S} = 60°$

○	SA_S	$C_Q = 0$	RUN 81
△	" + S_{A_1}	$C_Q = .0039$	" 82
□	" + "	$C_Q = .0055$	" 83
▽	" + "	$C_Q = .0063$	" 84
◇	" + "	$C_Q = .0071$	" 85

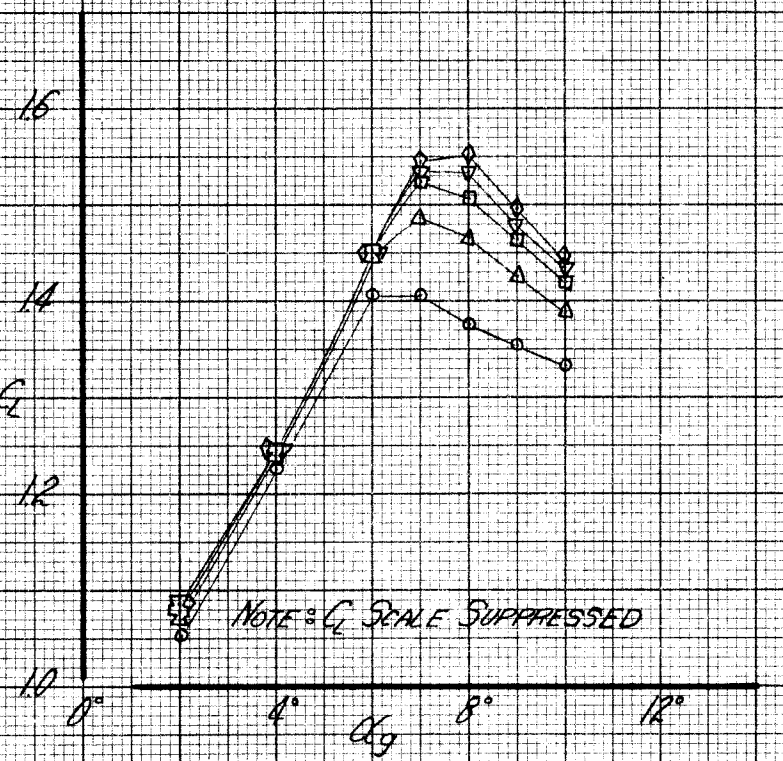

EFFECT OF SUCTION
SLOTTED FLAP DEFLECTED 60°
SLOT S_1

$q = 20 LB/FT^2$, $\alpha = 0°$, $\delta_{F_N} = 0°$, $\delta_{F_S} = 60°$

○	S_{F_S}	$C_Q = 0$	RUN 81
△	" + Δ_2	$C_Q = .0039$	" 90
□	" + "	$C_Q = .0055$	" 91
▽	" + "	$C_Q = .0063$	" 92
◇	" + "	$C_Q = .0071$	" 93

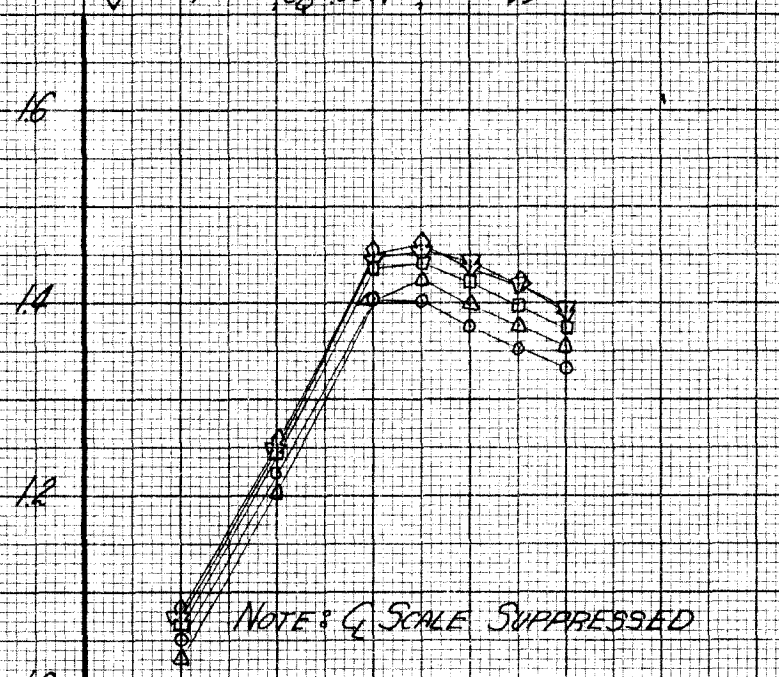

EFFECTS OF SUCTION
SLOTTED FLAP DEFLECTED 60°
SLOT 4_L

$q = 20.6$ lb/ft.^{2}, $\psi = 0°$, $\delta_{FN} = 0°$, $\delta_{FS} = 60°$

○	SF_S	, $C_Q = 0$	,	RUN 81
△	" + S_1 S_2	, $C_Q = .0039$	,	" 89
□	" + "	, $C_Q = .0055$	,	" 88
▽	" + "	, $C_Q = .0063$	,	" 87
◇	" + "	, $C_Q = .0077$	,	" 86

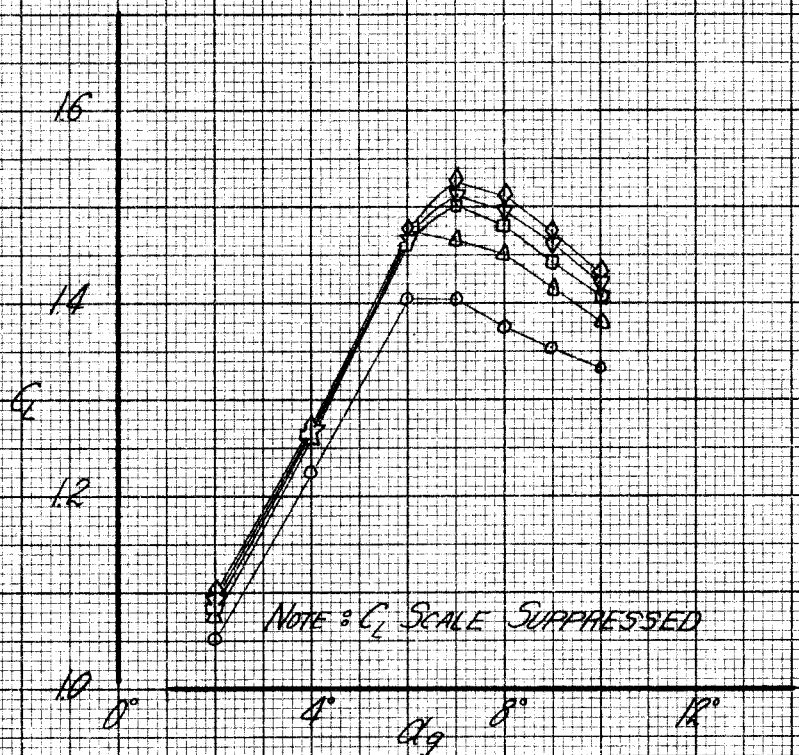

EFFECTS OF SUCTION
SLOTTED FLAP DEFLECTED 60°
SLOTS S_1 S_2

$q = 20$ LB/FT.^{2}, $\alpha_t = 0°$, $\delta_{F_N} = 15°$, $\delta_{F_S} = 30°$

○ $SF_N F_S$, $C_Q = 0$, RUN 63
△ " $+ A_1$, $C_Q = .0039$, " 64
□ " " , $C_Q = .0055$, " 65
▽ " " , $C_Q = .0063$, " 66
◇ " " , $C_Q = .0071$, " 67

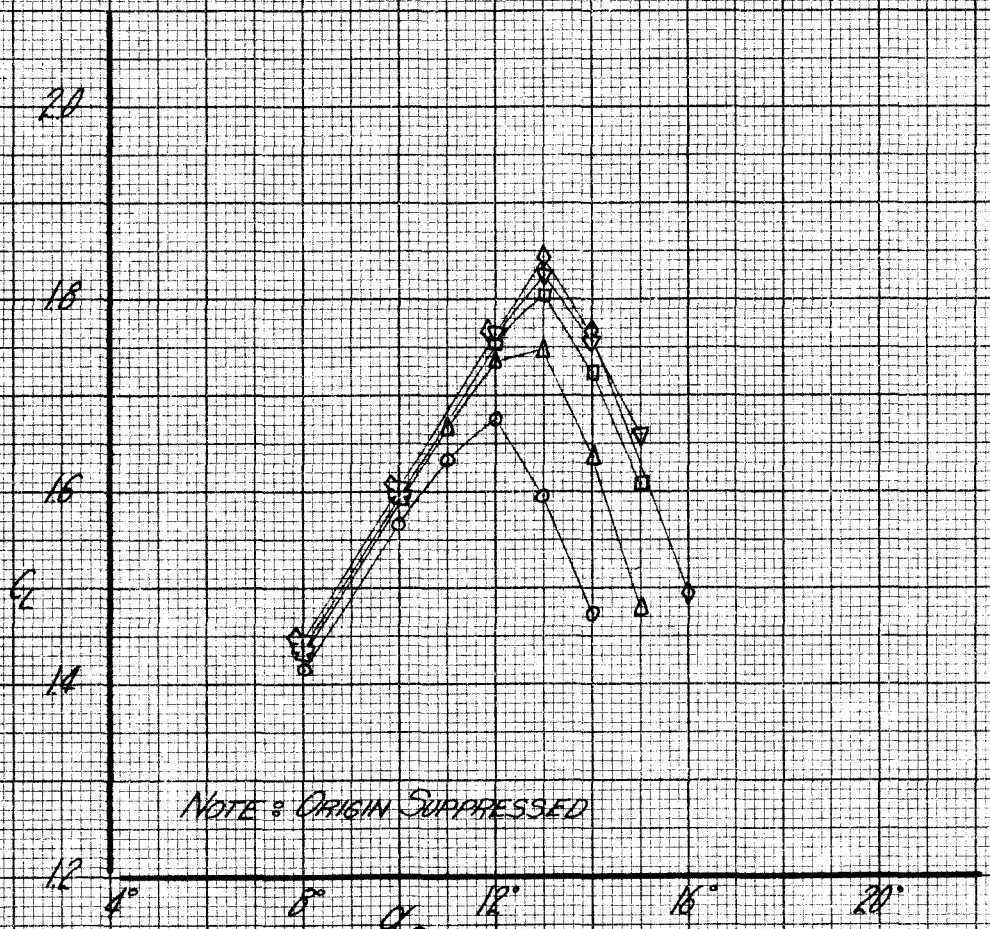

EFFECTS OF SUCTION
NOSE FLAP DEFLECTED 15°
SLOTTED " " 30°
SLOTS A_1

$q = 20 LB/FT^2$, $\alpha_f = 0°$, $\delta_{F_N} = 15°$, $\delta_{F_S} = 30°$

○	$SF_N F_S$	$C_Q = 0$	RUN 63
△	"	$+ \Delta_2$, $C_Q = .0039$	" 98
□	"	" , $C_Q = .0055$	" 99
▽	"	" , $C_Q = .0063$	" 100
◇	"	" , $C_Q = .0071$	" 101

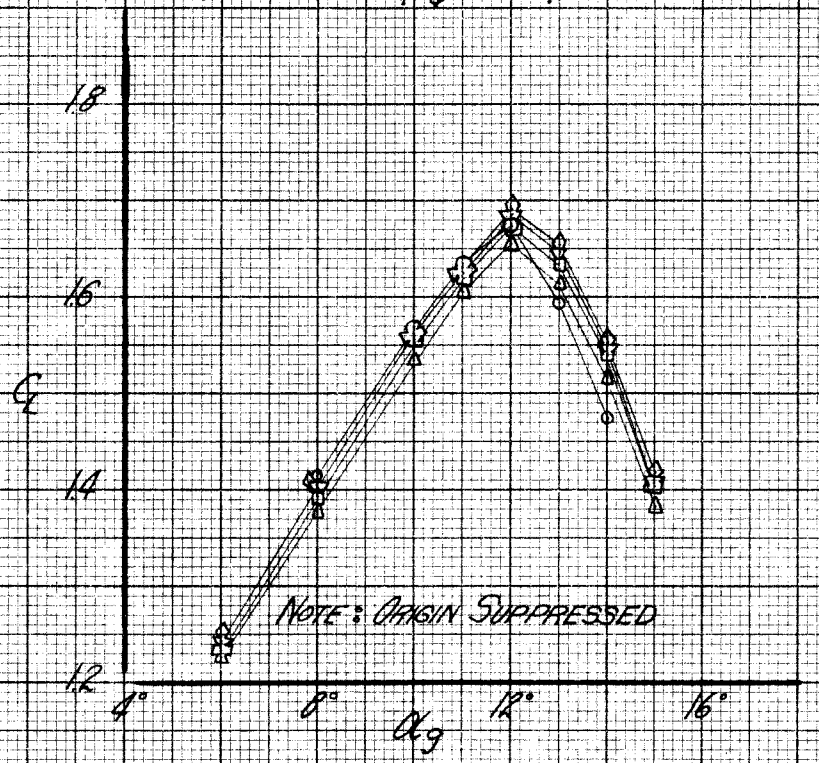

EFFECT OF SUCTION
NOSE FLAP DEFLECTED 15°
SLOTTED " " 30°
SLOT Δ_2

FIG. 25

$q = 20$ LB/FT², $\alpha = 0°$, $\delta_{F_N} = 15°$, $\delta_{F_S} = 30°$

○	SF_NF_S	$C_Q = 0$	RUN 63
△	" + $S_1 S_2$	$C_Q = .0039$	" 71
□	" + "	$C_Q = .0055$	" 70
▽	" + "	$C_Q = .0063$	" 69
◇	" + "	$C_Q = .0071$	" 68

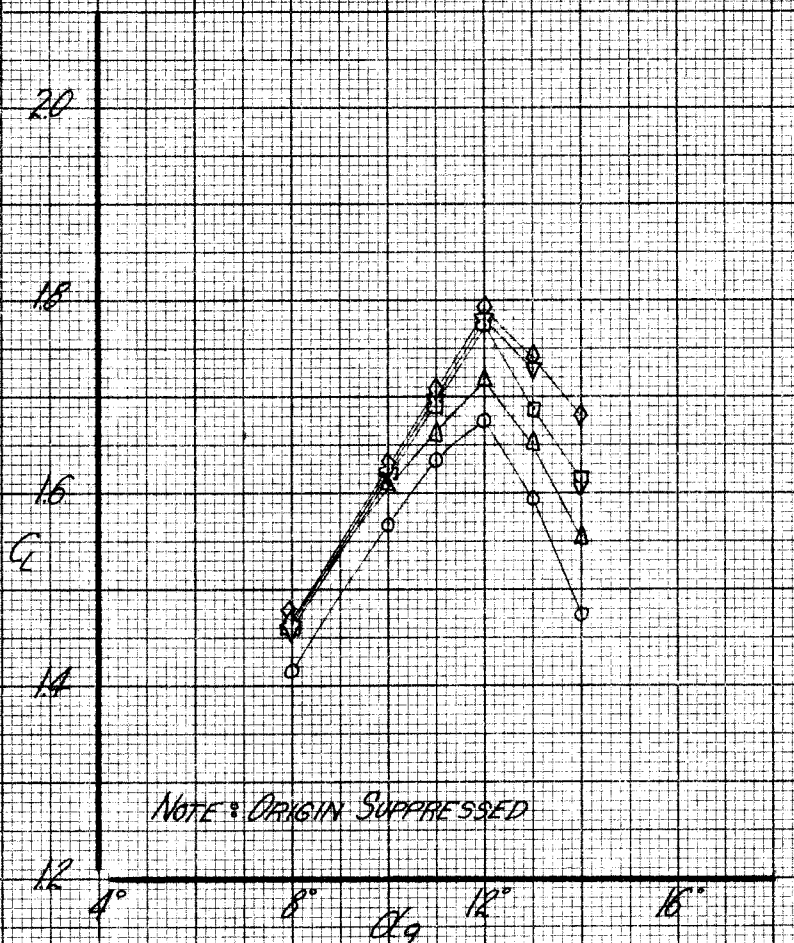

EFFECTS OF SUCTION
NOSE FLAP DEFLECTED 15°
SLOTTED " " 30°
SLOTS S_1, S_2

$q = 20$ LB/FT., $\alpha_t = 0°$, $\delta_{FN} = 15°$, $\delta_F = 60°$

○	SFNLE	, $C_Q = 0$	, RUN	54
△	"	+ A_1 , $C_Q = .0039$	, "	62
□	"	+ " , $C_Q = .0055$	, "	61
▽	"	+ " , $C_Q = .0063$	, "	60
◇	"	+ " , $C_Q = .0071$	, "	59

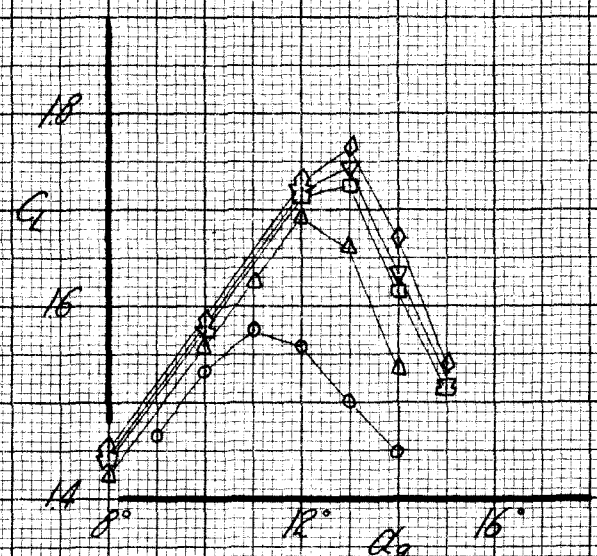

NOTE: ORIGIN SUPPRESSED

EFFECT OF SUCTION
NOSE FLAP DEFLECTED 15°
SLOTTED " " 60°
SLOT A_1

$q = 20$ LB/FT^2, $\alpha = 0°$, $\delta_{F_N} = 15°$, $\delta_{F_S} = 60°$

○	SF_NF_S	$C_Q = 0$	RUN 54
△	"	Δ_z, $C_Q = .0039$	" 105
□	"	" , $C_Q = .0053$	" 104
▽	"	" , $C_Q = .0063$	" 103
◇	"	" , $C_Q = .0071$	" 102

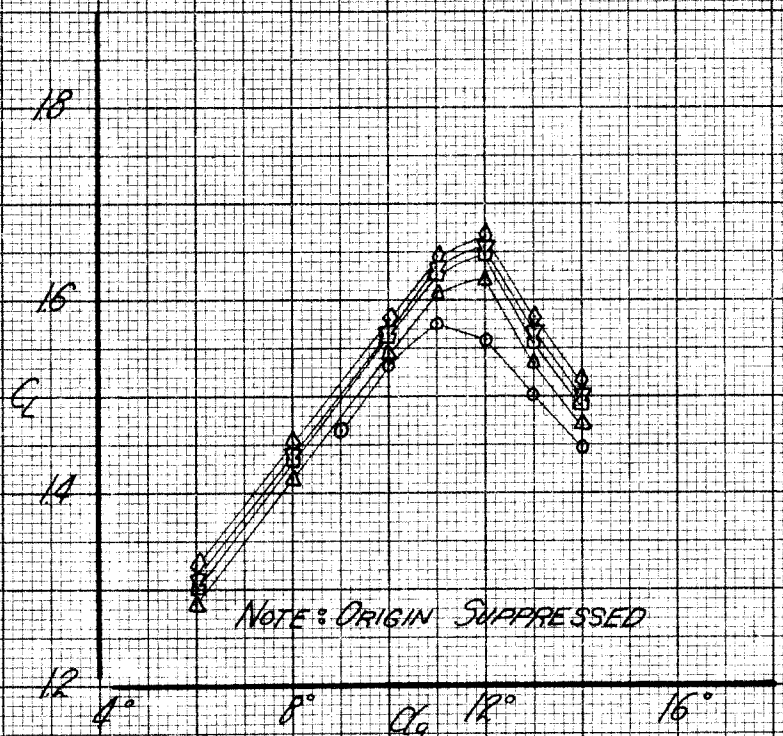

EFFECTS OF SUCTION
NOSE FLAP DEFLECTED 15°
SLOTTED " " 60°
SLOT Δ_z

$q = 20 LB/FT^2$, $\delta_S = 0°$, $\delta_{F_N} = 15°$, $\delta_{F_S} = 60°$

○	$SF_N F_S$	, $C_Q = 0$	, RUN	54
△	" + $A_1 A_2$	, $C_Q = .0039$	, "	55
□	" + "	, $C_Q = .0055$	, "	56
▽	" + "	, $C_Q = .0063$	, "	57
◇	" + "	, $C_Q = .0071$	, "	58

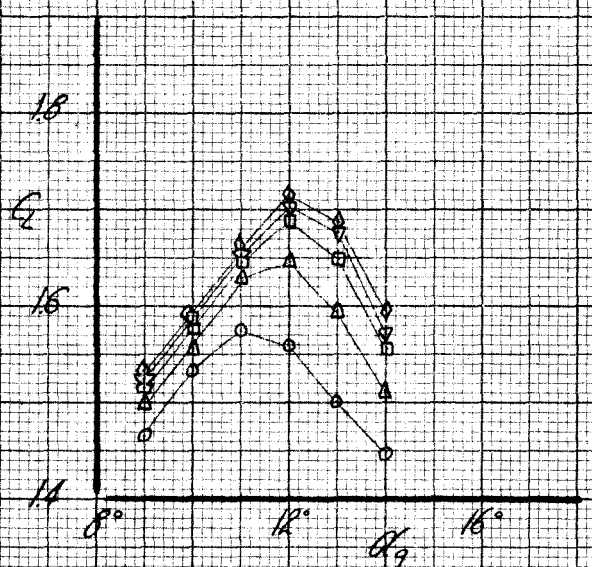

NOTE: ORIGIN SUPPRESSED

EFFECTS OF SUCTION
NOSE FLAP DEFLECTED 15°
SLOTTED " " 60°
SLOTS $A_1 A_2$

$q = 20$ LB/FT.^{2}, $\alpha = 0°$, $\delta_{FN} = 30°$, $\delta_{FS} = 30°$

○ $SF_N F_S$, $C_Q = 0$, RUN 36
△ " + A_1, $C_Q = .0039$, " 44
□ " + " , $C_Q = .0055$, " 43
▽ " + " , $C_Q = .0063$, " 42
◇ " + " , $C_Q = .0077$, " 41

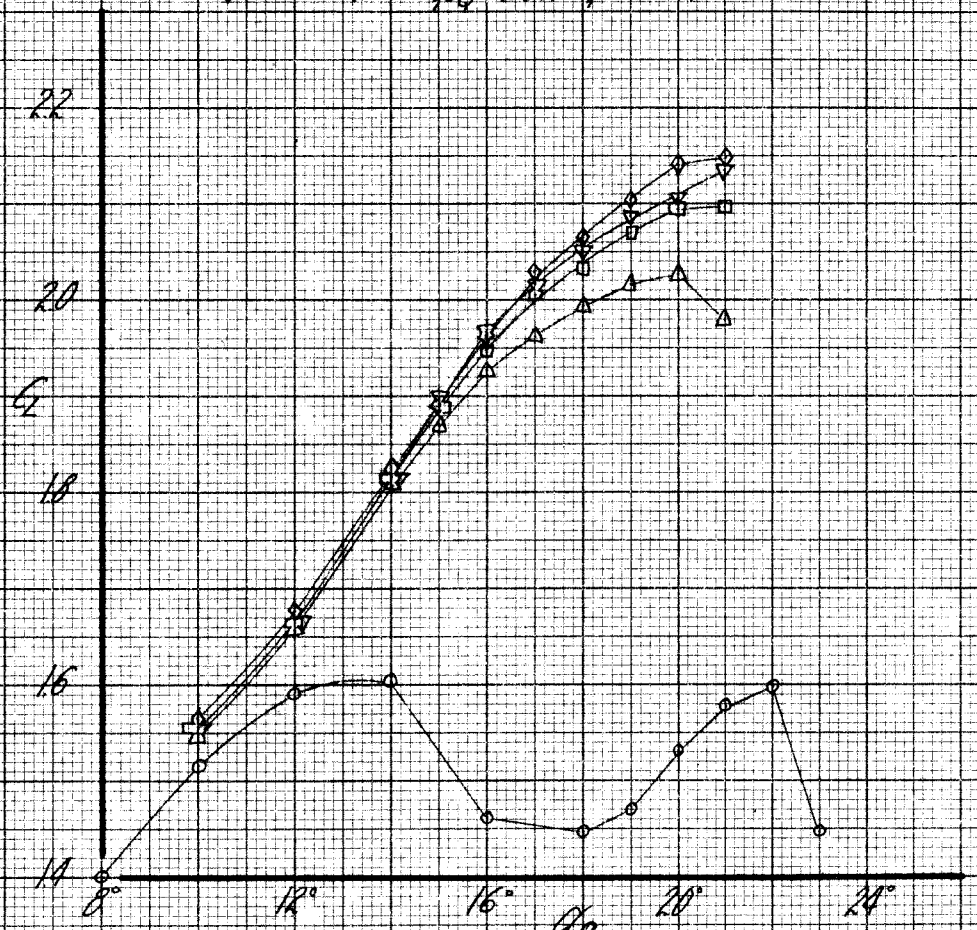

NOTE: ORIGIN SUPPRESSED

EFFECTS OF SUCTION
NOSE FLAP DEFLECTED 30°
SLOTTED " " 30°
SLOT A_1

$q = 20$ LB/FT.^{2}, $\beta_s = 0°$, $\delta_{F_N} = 30°$, $\delta_{F_S} = 30°$

○	SYMBOLS	$C_\phi = 0$	RUN 36
△	"	Δ_2, $C_\phi = .0039$	" 113
□	"	" $C_\phi = .0055$	" 112
▽	"	" $C_\phi = .0063$	" 111
◇	"	" $C_\phi = .0071$	" 110

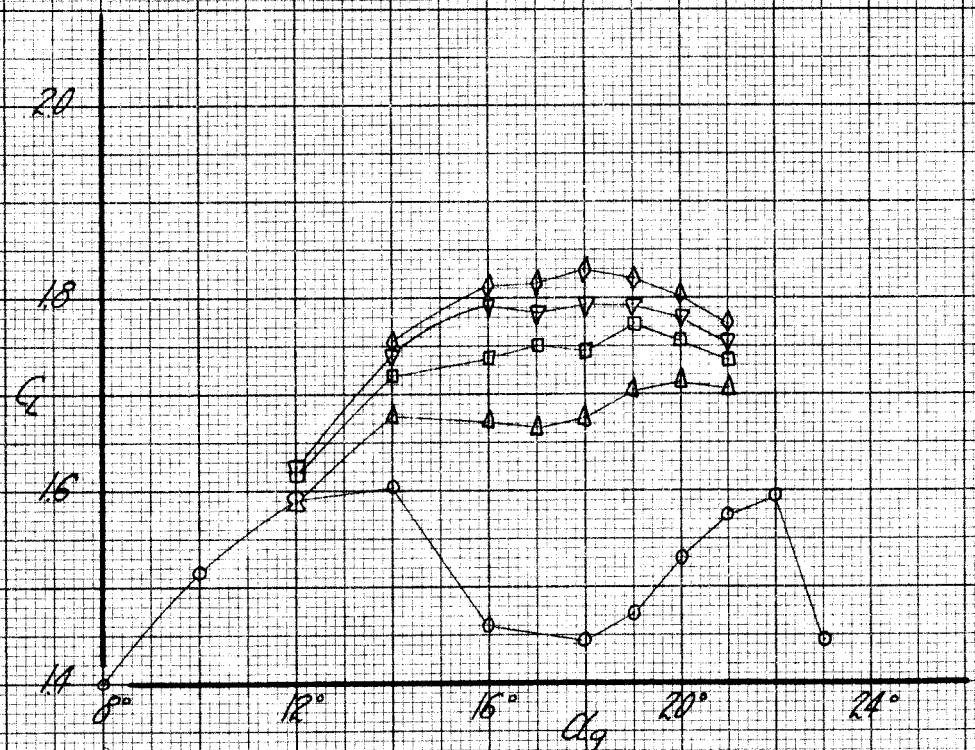

NOTE: ORIGIN SUPPRESSED

EFFECTS OF SUCTION
NOSE FLAP DEFLECTED 30°
SLOTTED " " 30°
SLOT Δ_2

$q = 20$ LB/FT^2; $i = 0°$; $\delta_{FN} = 30°$; $\delta_S = 30°$

○	SF_NF_S	, $C_Q = 0$	, RUN	36
△	"	+ $A_1 A_2$, $C_Q = .0039$	, "	37
□	"	+ " , $C_Q = .0055$	, "	38
▽	"	+ " , $C_Q = .0063$	, "	39
◇	"	+ " , $C_Q = .0070$	, "	40

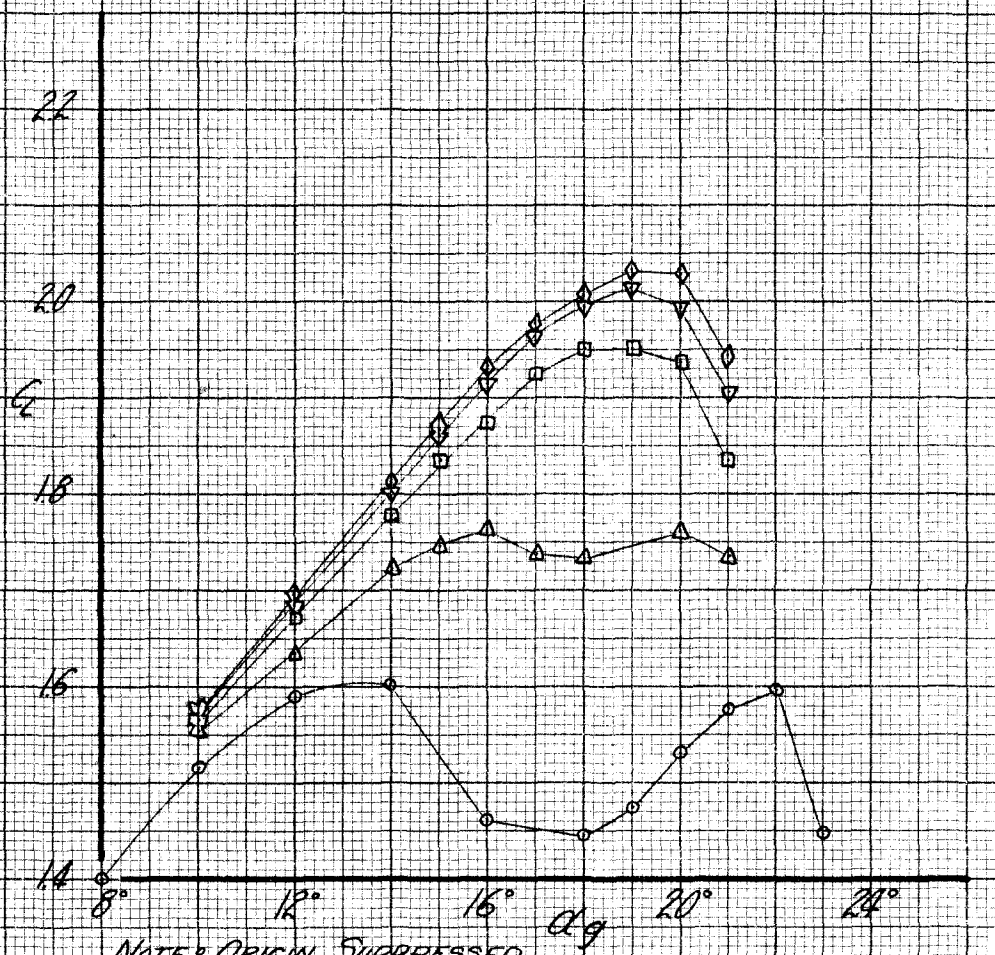

NOTE: ORIGIN SUPPRESSED

EFFECT OF SUCTION
NOSE FLAP DEFLECTED 30°
SLOTTED " " 30°
SLOTS A_1, A_2

$q = 20$ LB/FT^2, $\alpha_s = 0°$, $\delta_{F_N} = 30°$, $\delta_{F_S} = 60°$

○	SF_NF_S	$C_Q = 0$	RUN 45
△	" + Δ_1	$C_Q = .0039$	" 46
□	" +	$C_Q = .0055$	" 47
▽	" +	$C_Q = .0063$	" 48
◇	" +	$C_Q = .0071$	" 49

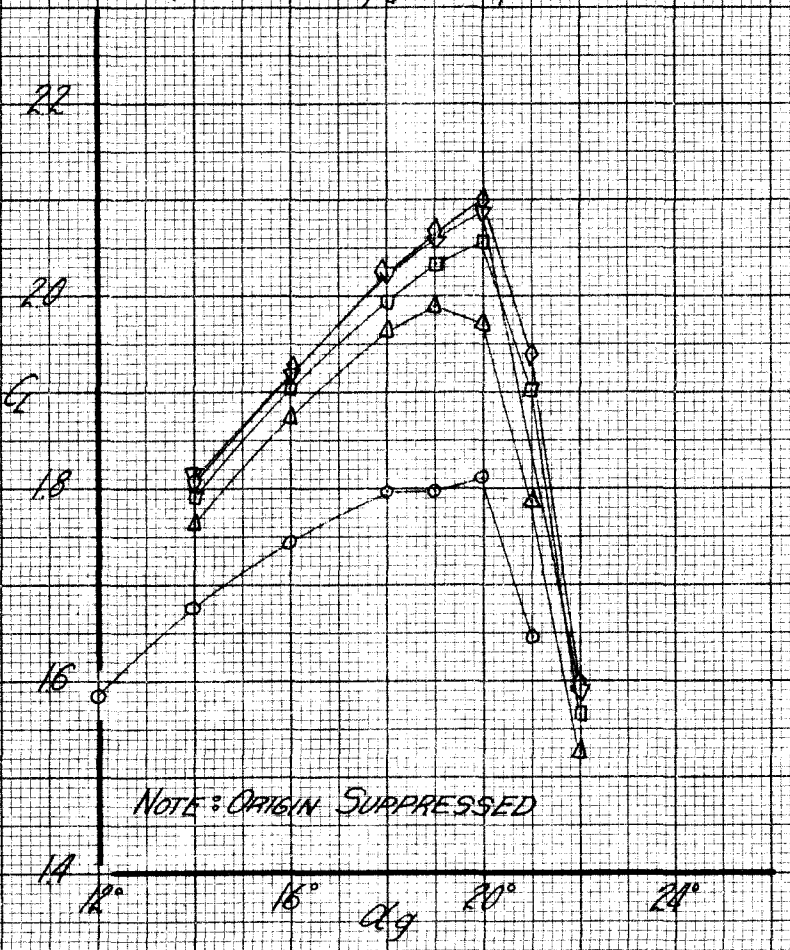

EFFECT OF SUCTION
NOSE FLAP DEFLECTED 30°
SLOTTED " " 60°
SLOTS Δ_1

$q = 20 LB/FT^2$, $\alpha_t = 0°$, $\delta_{F_N} = 30°$, $\delta_{F_S} = 60°$

○	$S_{F_N F_S}$	$C_Q = 0$	RUN 45
△	" + Δ_2	$C_Q = .0039$	" 106
□	" + "	$C_Q = .0055$	" 107
▽	" + "	$C_Q = .0063$	" 108
◇	" + "	$C_Q = .0081$	" 109

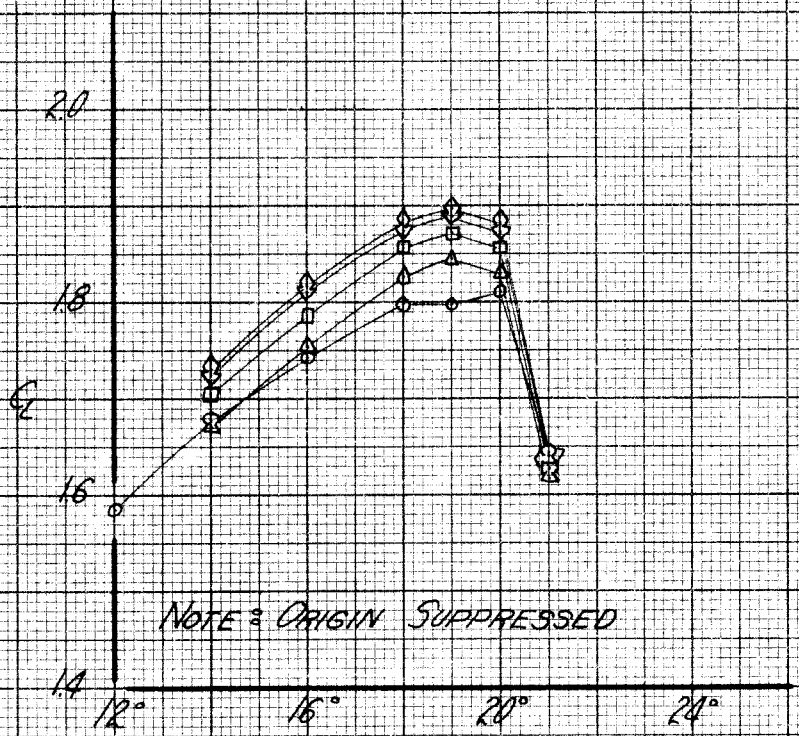

EFFECTS OF SUCTION
NOSE FLAP DEFLECTED 30°
SLOTTED " " 60°
SLOT Δ_2

$q = 20$ LB/FT^2, $\beta = 0°$, $\delta_{F_N} = 30°$, $\delta_{F_S} = 60°$

○	$SF_N F_S$	$C_Q = 0$	RUN 45
△	" + $S_1 S_2$	$C_Q = .0039$	" 53
□	" + "	$C_Q = .0055$	" 52
▽	" + "	$C_Q = .0063$	" 51
◇	" + "	$C_Q = .0071$	" 50

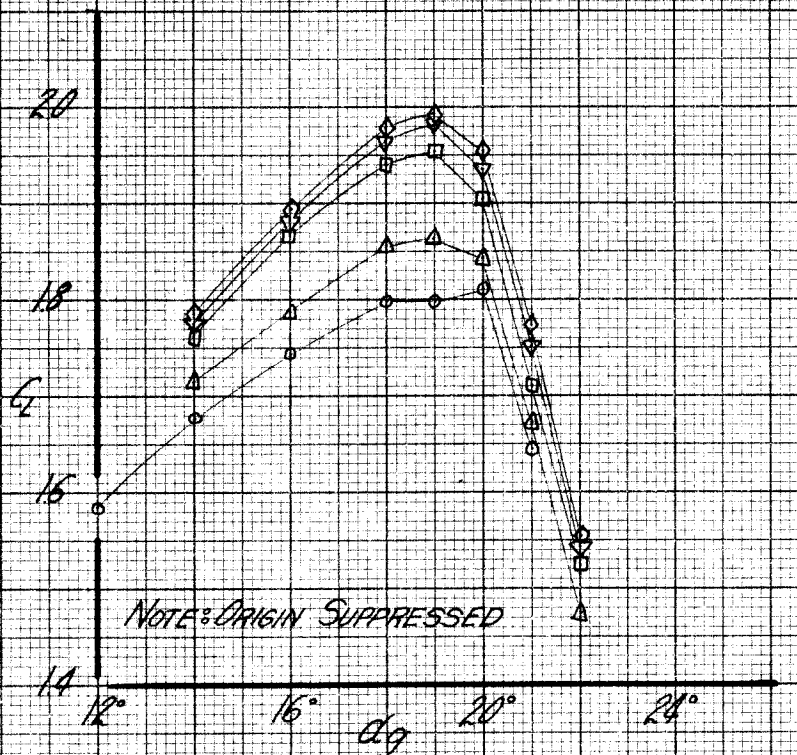

EFFECTS OF SUCTION
NOSE FLAP DEFLECTED 30°
SLOTTED " " 60°
SLOTS $S_1 S_2$

$q = 20$ LB/FT.; $\delta_f = 0°$, $\delta_{FN} = 0°$, $\delta_{FS} = 0°$

○ S , $C_Q = 0$, RUN 9
△ " $+\Delta_1$, $C_Q = .0071$, " 13
□ " $+\Delta_2$, " , " 125
▽ " $+\Delta_1, \Delta_2$ " , " 14

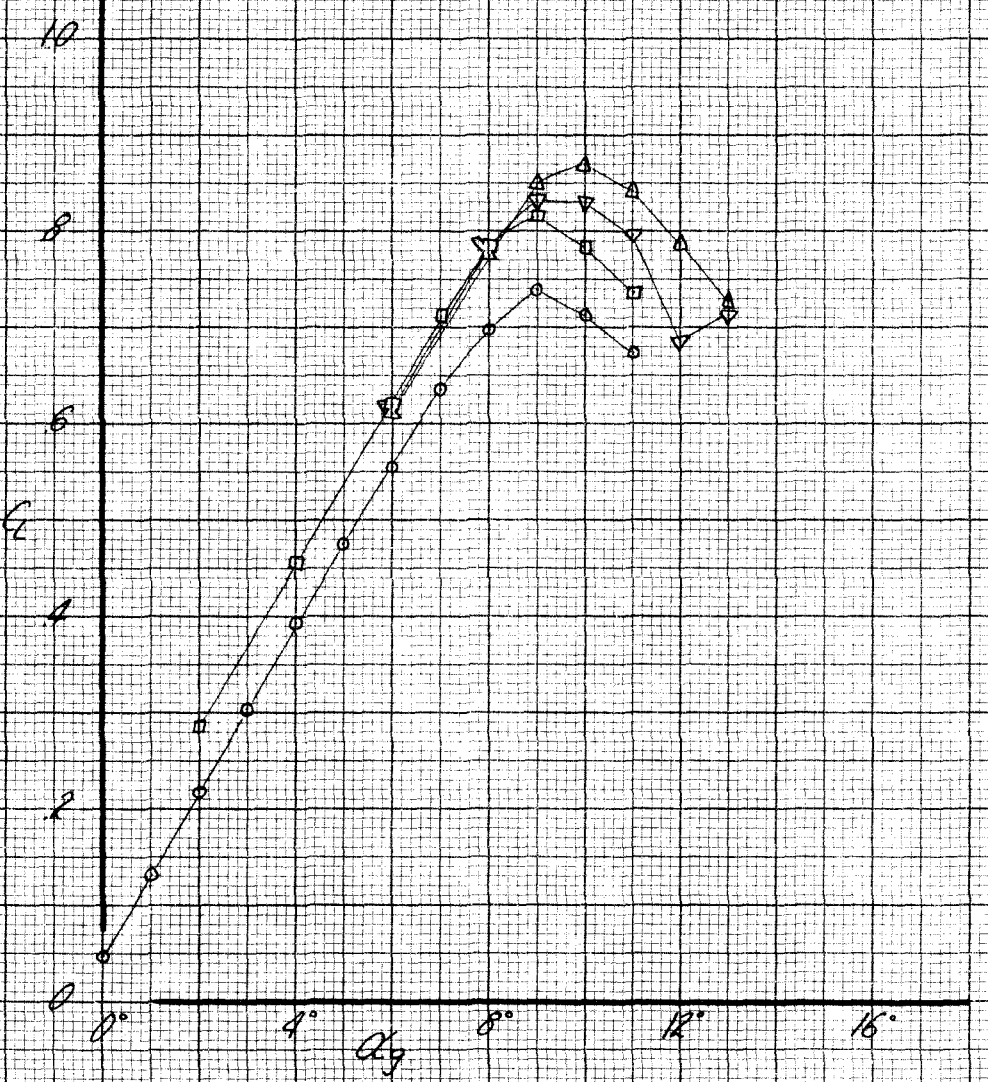

EFFECT OF SLOT LOCATION
"FLAPS UP" CONFIGURATION
$C_Q = .0071$

$q = 20$ LB/FT^2, $\gamma_s = 0°$, $\delta_{F_N} = 15°$, $\delta_{F_S} = 0°$

○ SF_N, $C_Q = 0$, Run 18
△ " + Δ_1, $C_Q = .0071$, " 23
□ " + Δ_2, " " 18
▽ " + $\Delta_1 \Delta_2$, " " 22

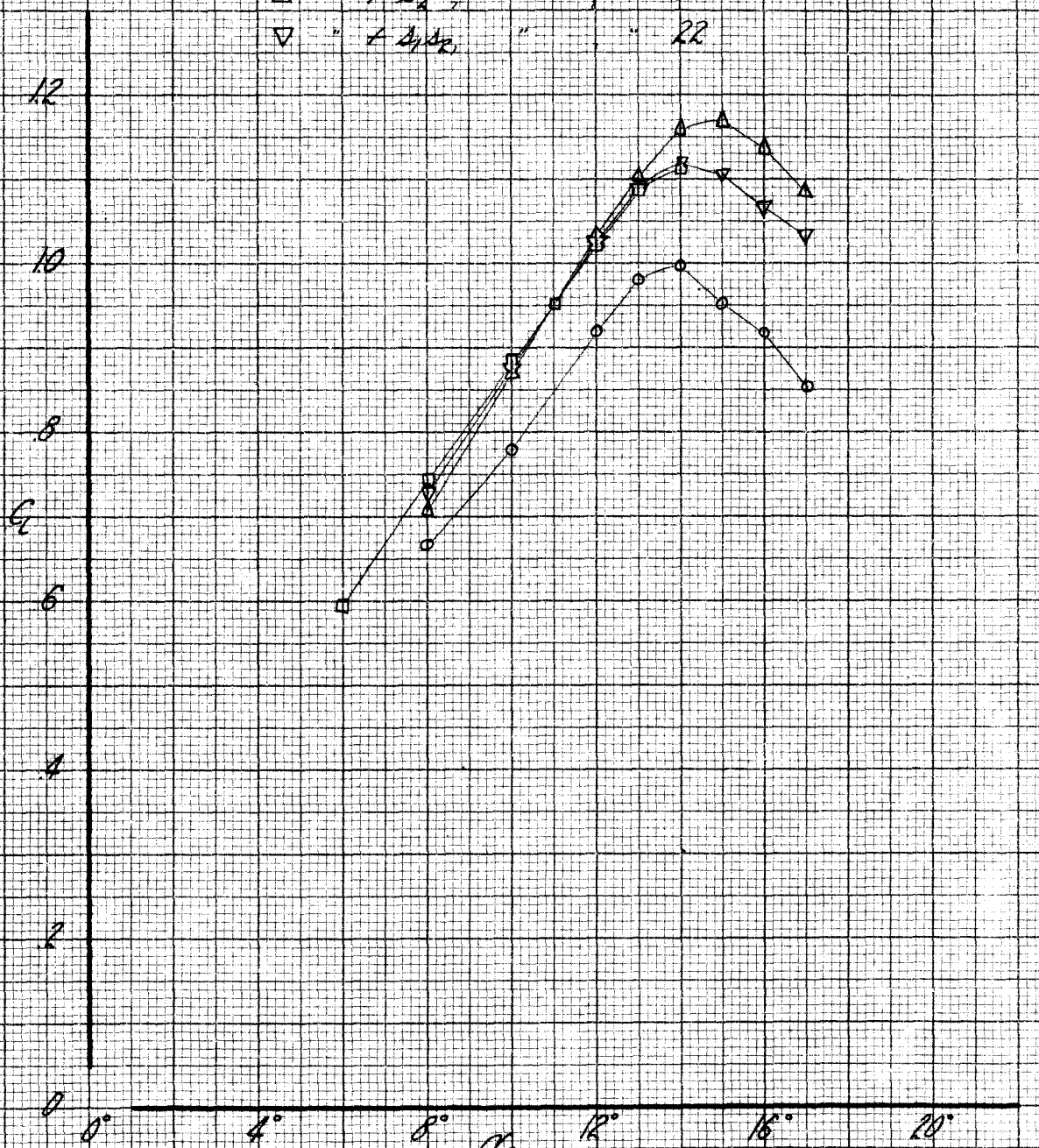

EFFECT OF SLOT LOCATION
NOSE FLAP DEFLECTED 15°
$C_Q = .0071$

$q = 20$ LB/FT.^{2}, $\alpha_s = 0°$, $\delta_{F_N} = 30°$, $\delta_{F_S} = 0°$

○ SF_N, $C_Q = 0$, RUN 27
△ " $\wedge\Delta_1$, $C_Q = .0071$, " 31
□ " $\wedge\Delta_2$, " " 117
▽ " $\wedge\Delta_1\Delta_2$, " " 32

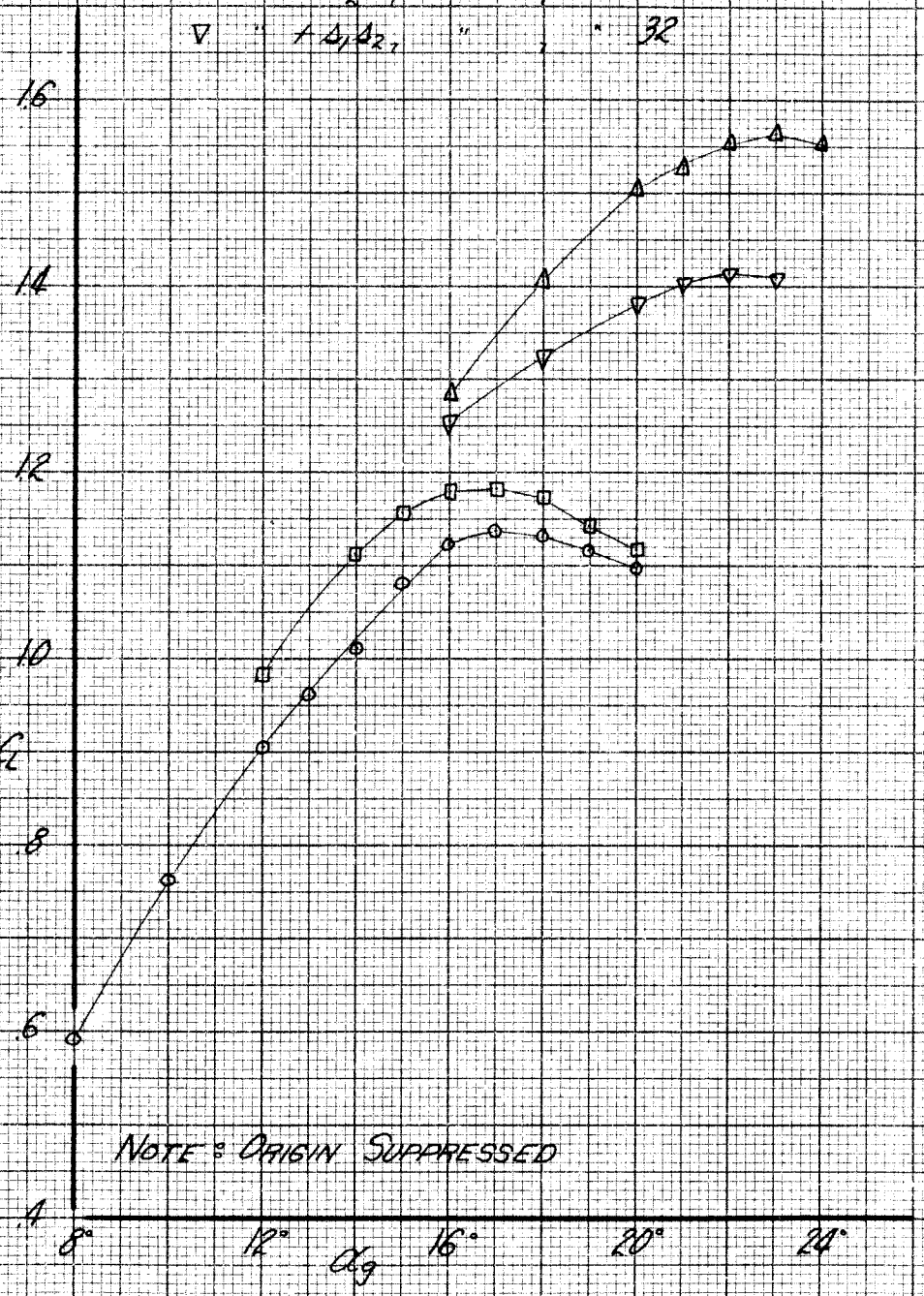

NOTE: ORIGIN SUPPRESSED

EFFECTS OF SLOT LOCATION
NOSE FLAP DEFLECTED 30°
$C_Q = .0071$

$q = 20$ LB/FT^2, $i_t = 0°$, $\delta_{F_4} = 0°$, $\delta_{F_5} = 30°$

○	SF_5	, $C_Q = 0$	, RUN	72
△	"	$+\Delta_1$, $C_Q = .0071$	"	77
□	"	$+\Delta_2$, "	"	94
▽	"	$+\Delta_1\Delta_2$, "	"	76

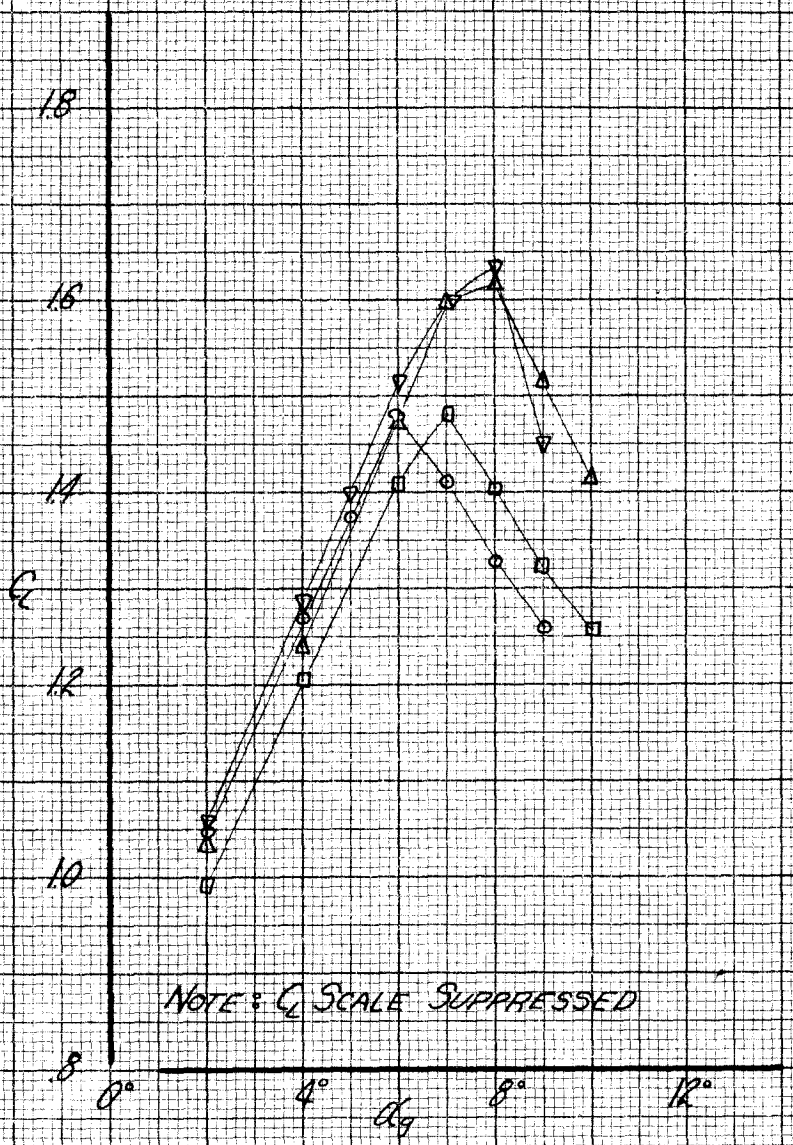

NOTE: C_L SCALE SUPPRESSED

EFFECT OF SLOT LOCATION
SLOTTED FLAP DEFLECTED 30°

$C_Q = .0071$

$q = 20 LB/FT^2$, $\delta_f = 0°$, $\delta_{FN} = 0°$, $\delta_{FS} = 60°$

○ SF_S, $C_Q = 0$, RUN 81
△ " × Δ_1, $C_Q = .0071$, " 85
□ " × Δ_2, " " , " 93
▽ " × $\Delta_1\Delta_2$, " " , " 86

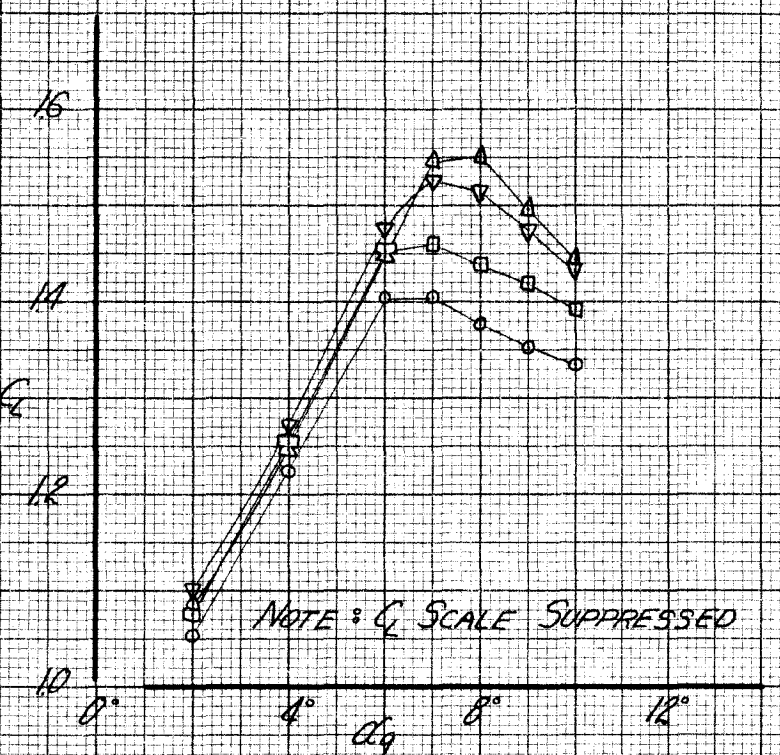

EFFECT OF SLOT LOCATION
SLOTTED FLAP DEFLECTED 60°
$C_Q = .0071$

$q = 20$ LB/FT^2, $i_t = 0°$, $\delta_{FN} = 15°$, $\delta_{FS} = 30°$

○ $\delta_{FN} F_S$, $C_Q = 0$, RUN 63
△ " + Δ_1, $C_Q = .0071$, " 67
□ " + Δ_2, " " " 101
▽ " + $\Delta_1 \Delta_2$, " " " 68

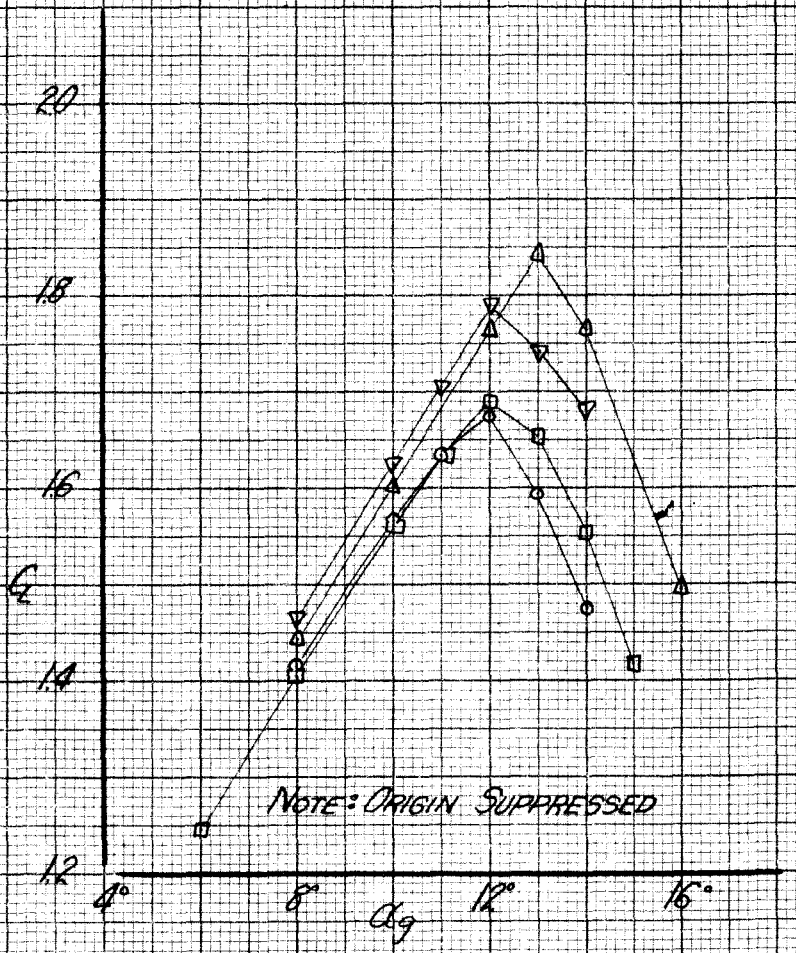

EFFECT OF SLOT LOCATION
NOSE FLAP DEFLECTED 15°
SLOTTED " " 30°
$C_Q = .0071$

$q = 20$ LB/FT.^{2}, $\alpha_t = 0°$, $\delta_{F_N} = 15°$, $\delta_{F_S} = 60°$

○ $SF_N F_S$, $C_Q = 0$, RUN 54
△ " $+\Delta_1$, $C_Q = .0071$, " 59
□ " $+\Delta_2$, " , " 102
▽ " $+\Delta_1\Delta_2$, " , " 58

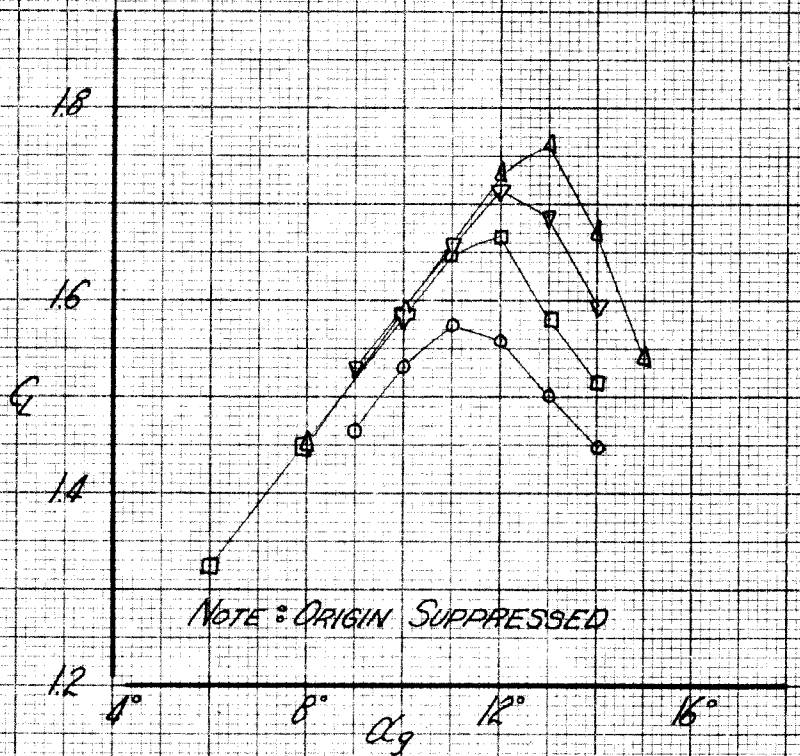

EFFECT OF SLOT LOCATION
NOSE FLAP DEFLECTED 15°
SLOTTED " " 60°
$C_Q = .0071$

$q = 20$ LB/FT.^{2}, $\alpha_f = 0°$, $\delta_{f_N} = 30°$, $\delta_{f_S} = 30°$

○ $SF_N F_S$, $C_\phi = 0$, RUN 36
△ " + δ_1, $C_\phi = .0071$, " 41
□ " + δ_2, " " 110
▽ " + $\delta_1 \delta_2$, " " 40

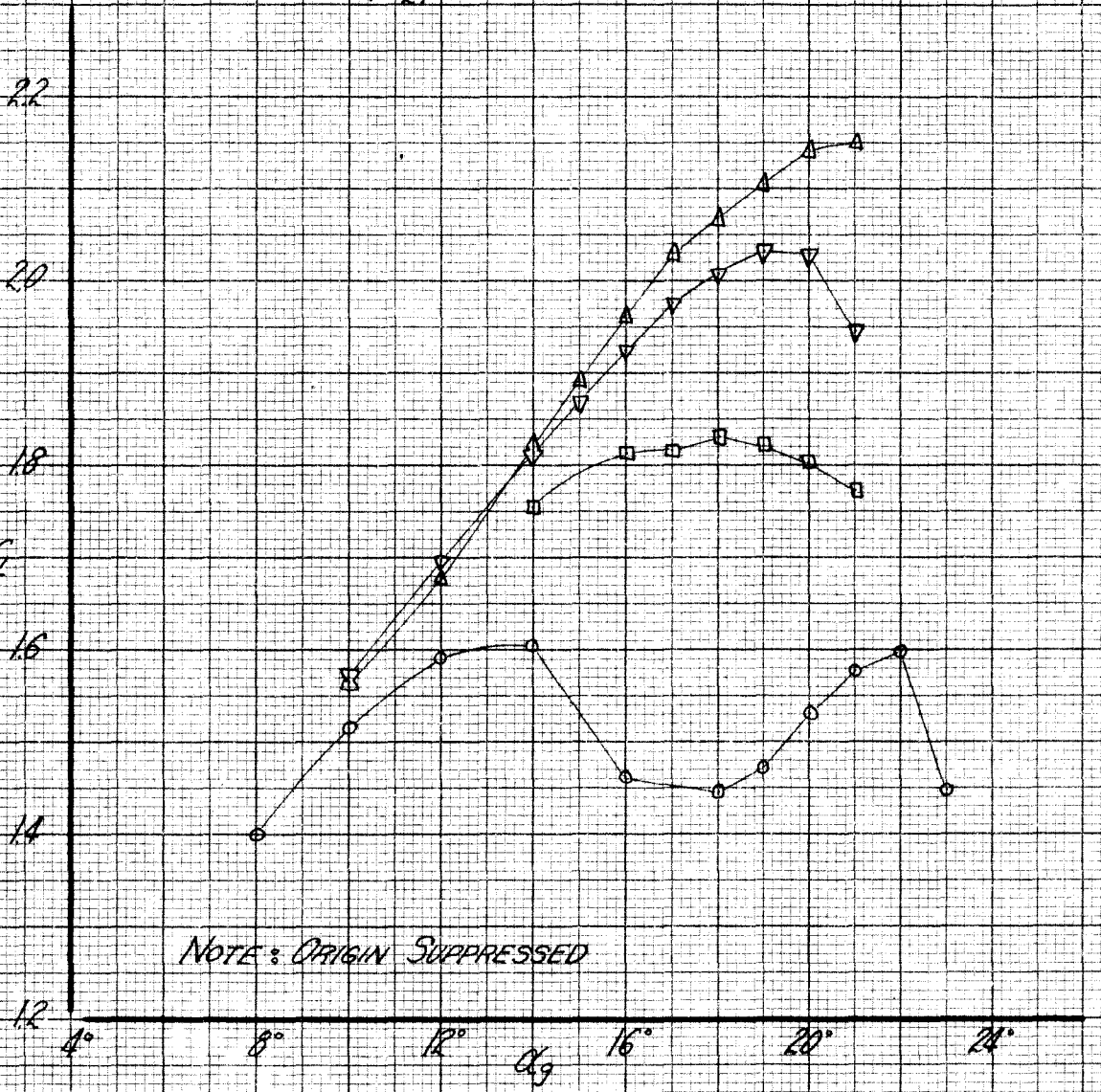

NOTE: ORIGIN SUPPRESSED

EFFECT OF SLOT LOCATION
NOSE FLAP DEFLECTED 30°
SLOTTED " " 30°
$C_\phi = .0071$

$q = 20$ LB/FT^2, $\beta = 0°$, $\delta_{F_N} = 30°$, $\delta_{F_S} = 60°$

○ SF_NF_S, $C_Q = 0$, RUN 45
△ " $+\Delta_1$, $C_Q = .0021$, " 49
□ " $+\Delta_2$, " " " 109
▽ " $+\Delta_1\Delta_2$, " " " 50

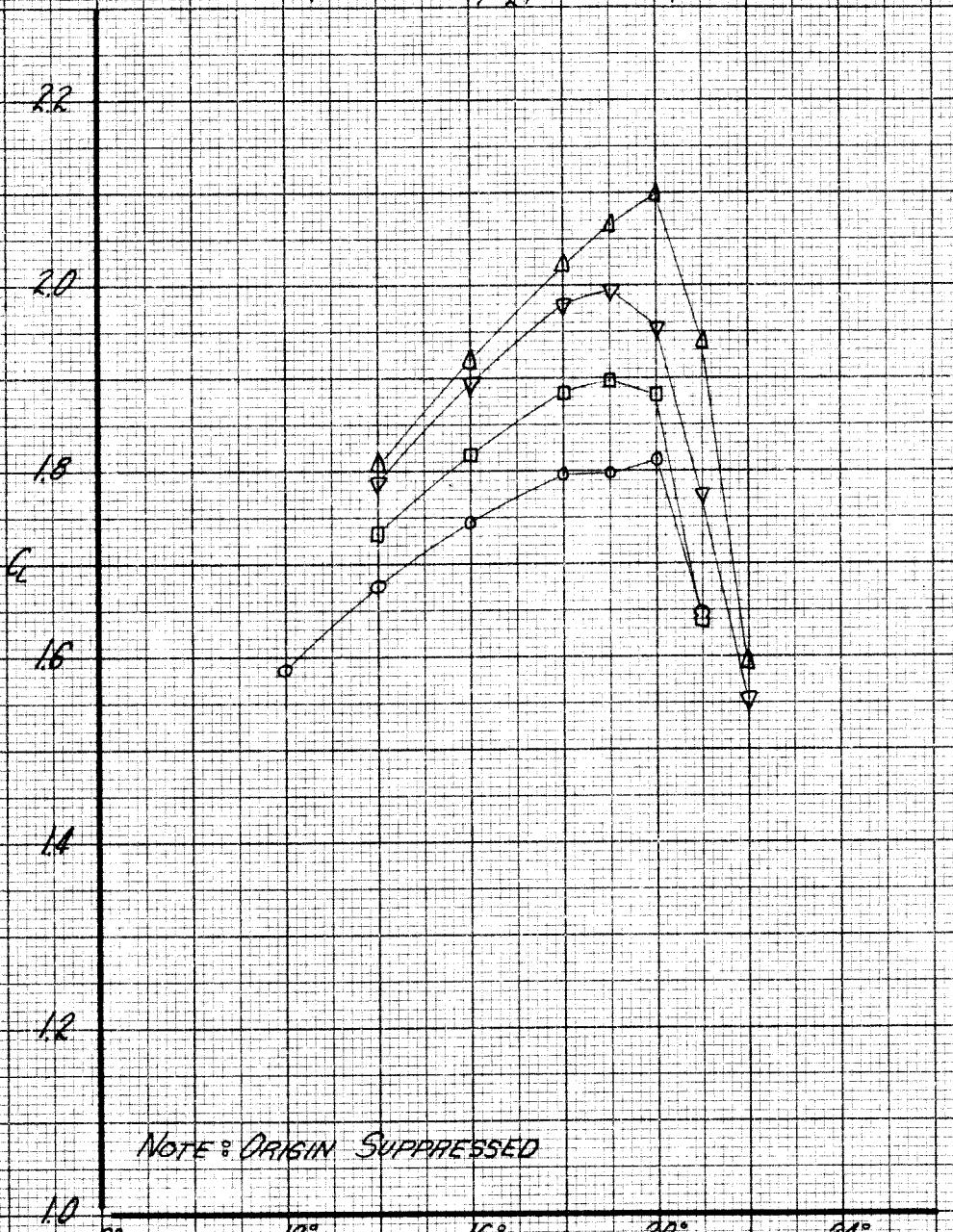

NOTE: ORIGIN SUPPRESSED

EFFECT OF SLOT LOCATION
NOSE FLAP DEFLECTED 30°
SLOTTED " " 60°
$C_Q = .0021$

FIG. 44

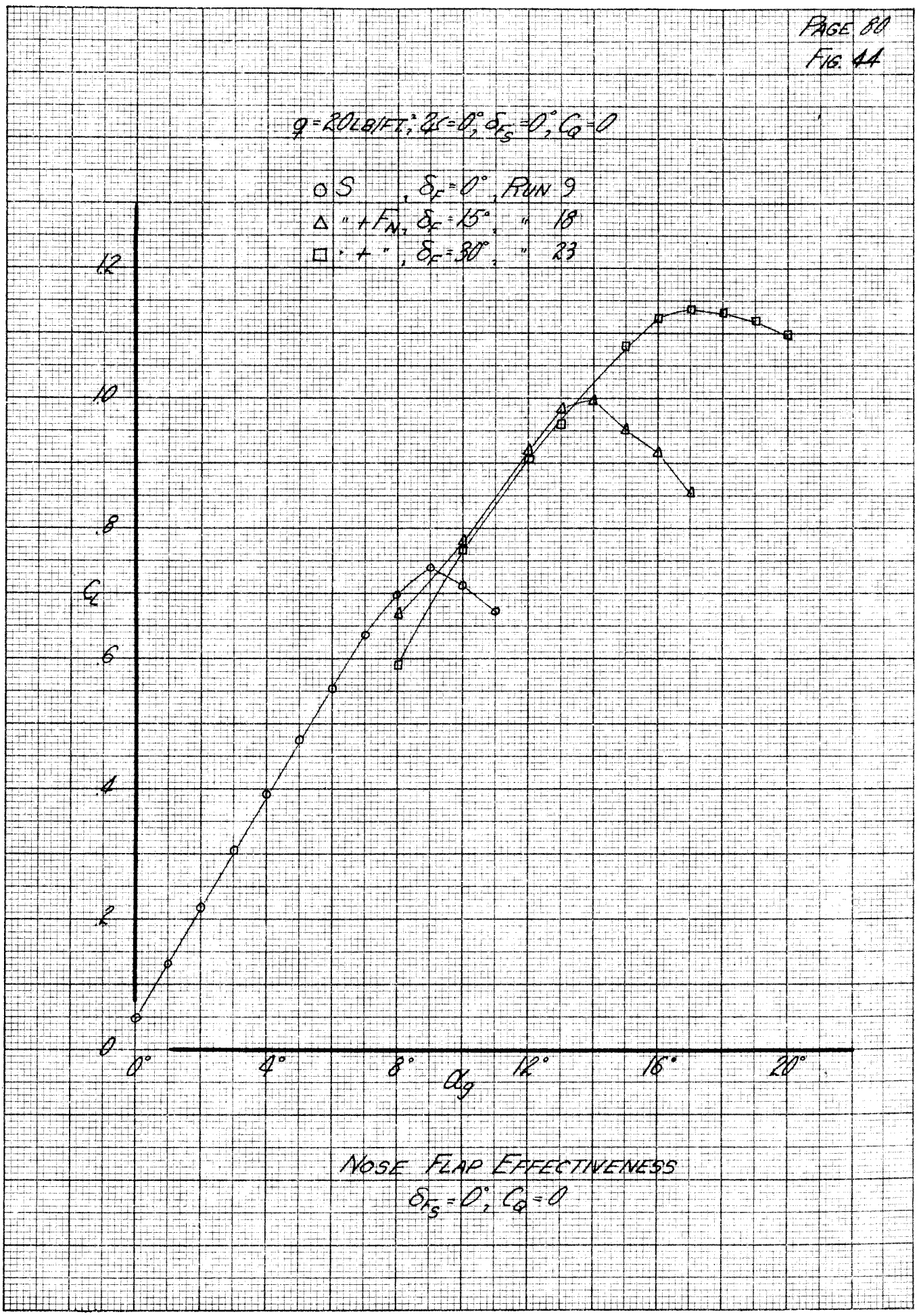

NOSE FLAP EFFECTIVENESS

$\delta_{FS} = 0°$, $C_Q = 0$

$q = 20$ LB/FT.^{2}, $\psi = 0°$, $\delta_{F_S} = 0°$, $C_Q = .0071$

○ S_{Δ_1}, $\delta_{F_N} = 0°$, RUN 13
△ " $+F_{N_1}$, $\delta_{F_N} = 15°$, " 23
□ " " " , $\delta_{F_N} = 30°$, " 31

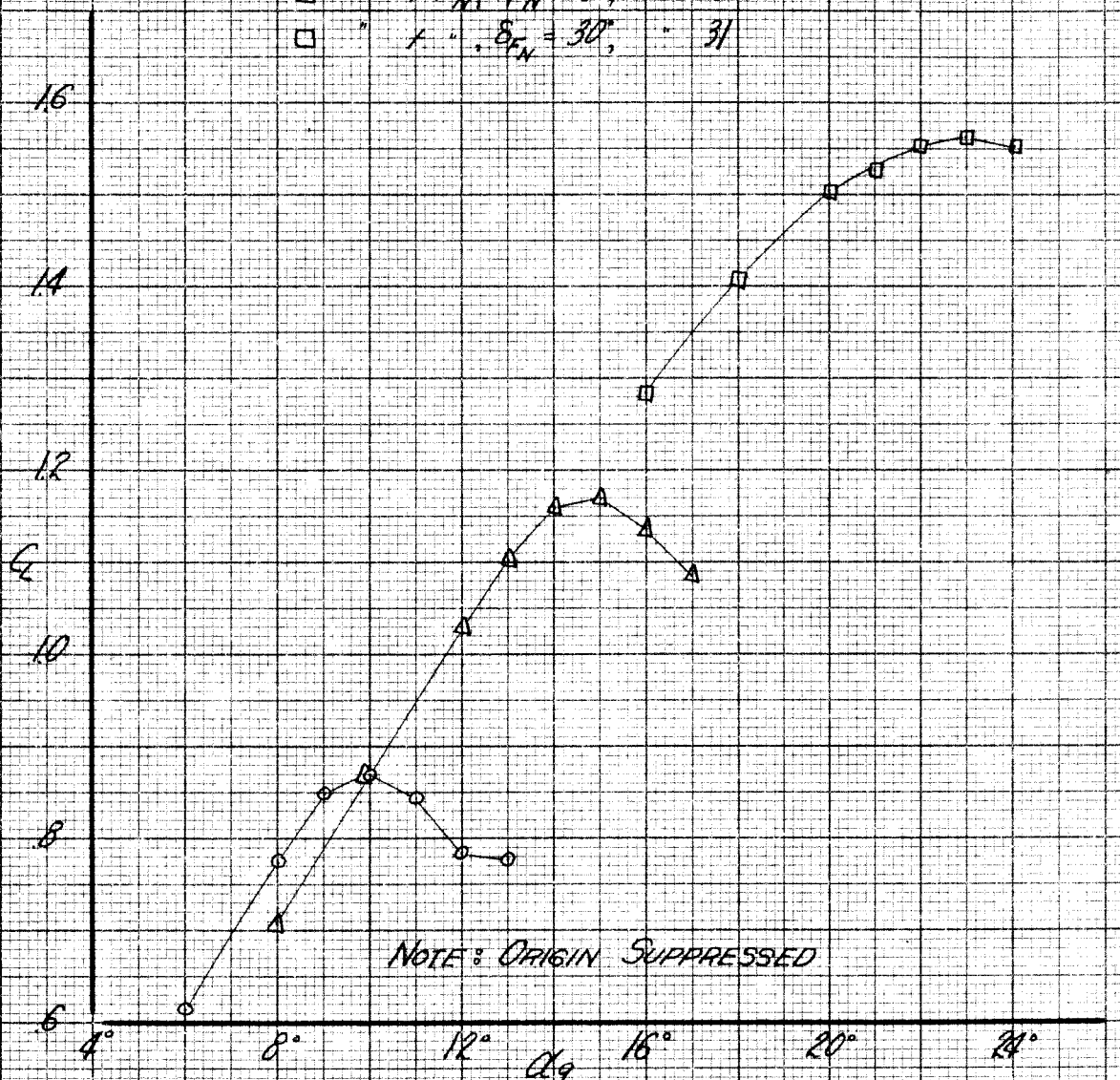

NOTE: ORIGIN SUPPRESSED

NOSE FLAP EFFECTIVENESS
$\delta_{F_S} = 0°$, $C_Q = .0071$
SLOT Δ_1

FIG. 46

$q = 20$ LB/FT.^{2}, $\beta = 0°$, $\delta_{FS} = 0°$, $C_Q = .0021$

○ Slot S_2, $\delta_{FN} = 0°$, Run 125

△ " + F_N, $\delta_{FN} = 15°$, " 118

□ " + " , $\delta_{FN} = 30°$, " 117

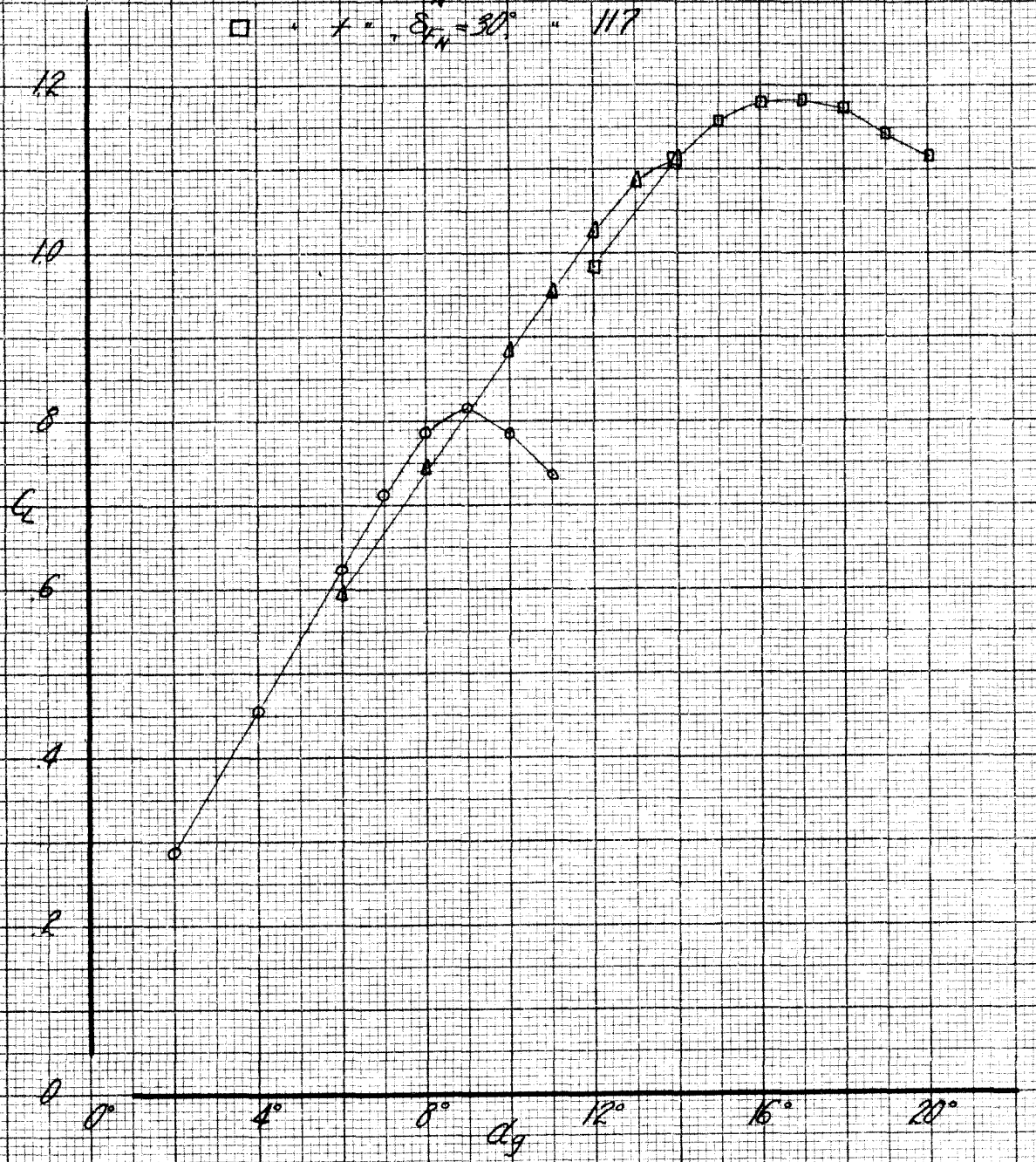

NOSE FLAP EFFECTIVENESS

$\delta_{FS} = 0°$, $C_Q = .0021$

SLOT S_2

$q = 20$ LB/FT.; $\gamma_s = 0°$; $\delta_{F_S} = 0°$; $C_Q = .0071$

○ $S\Delta_1\Delta_2$, $\delta_{F_N} = 0°$; RUN 14
△ " $+F_N$; $\delta_{F_N} = 15°$; " 22
□ " " ; $\delta_{F_N} = 30°$; " 32

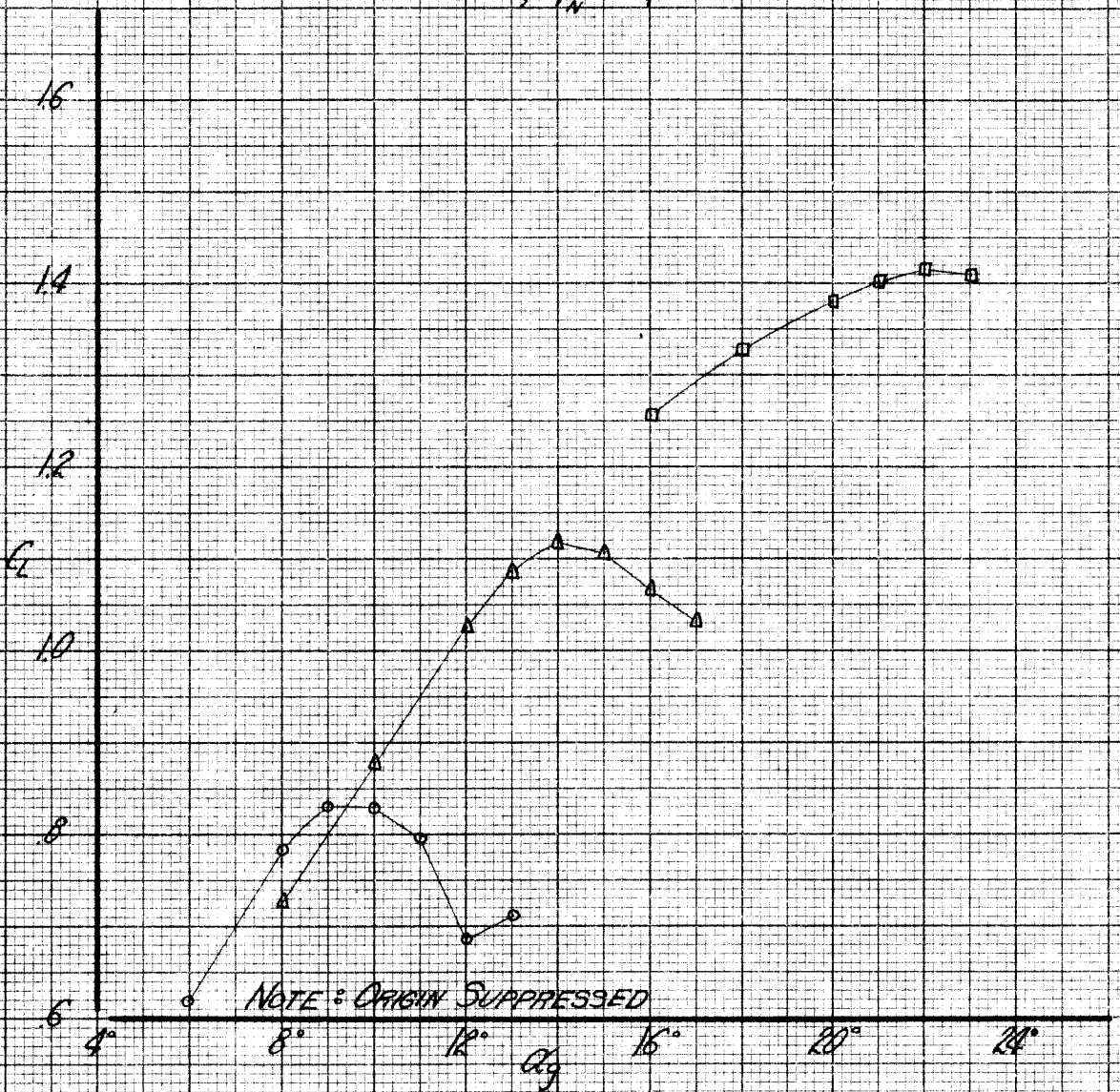

NOSE FLAP EFFECTIVENESS
$\delta_{F_S} = 0°$, $C_Q = .0071$
SLOTS $\Delta_1\Delta_2$

$q = 20$ LB/FT², $\delta_{F_S} = 0°$, $\delta_{F_N} = 0°$, $C_\phi = 0$

○ S , $\delta_{F_S} = 0°$, RUN 9
△ " + F_S, $\delta_{F_S} = 30°$, " 72
□ " + F_S, $\delta_{F_S} = 60°$, " 81

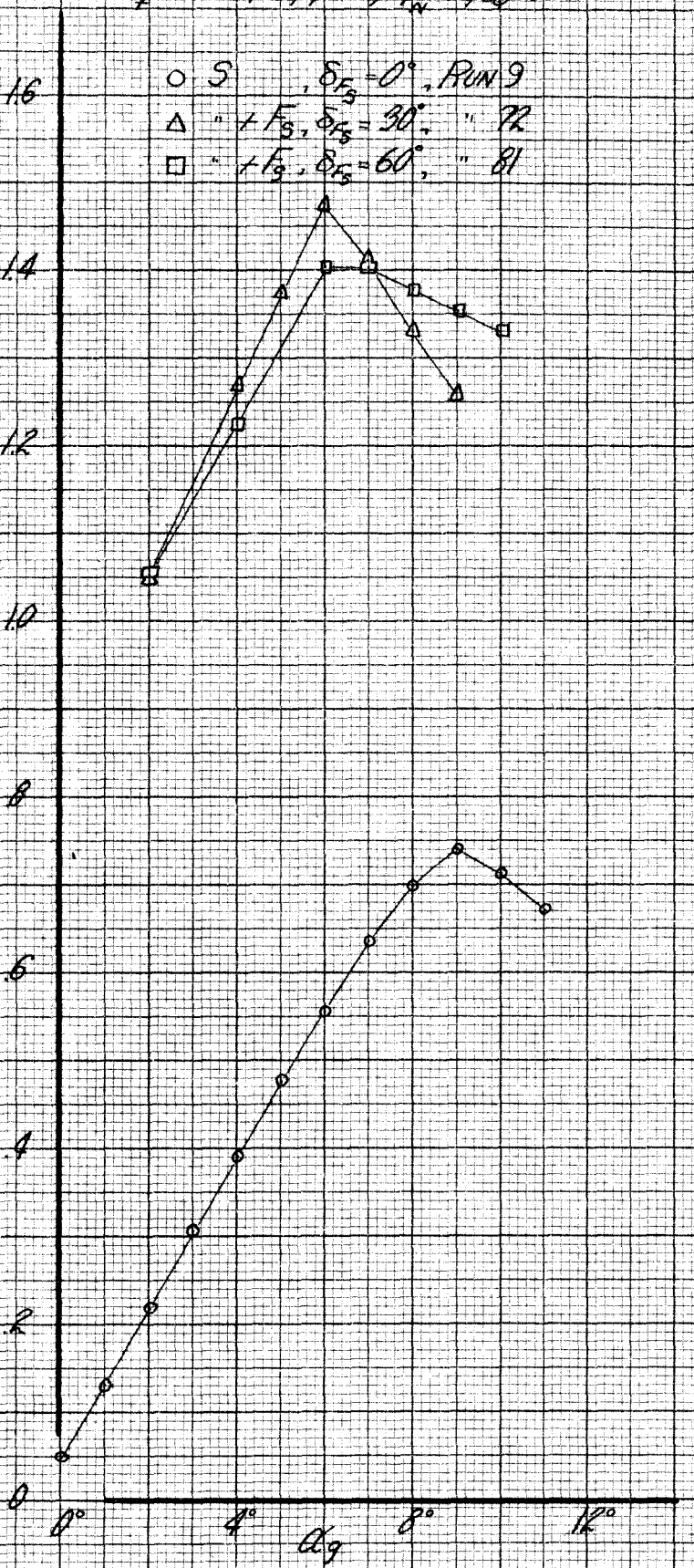

SLOTTED FLAP EFFECTIVENESS
$\delta_{F_N} = 0°$ $C_\phi = 0$

$q = 20\frac{1}{2}$ LB/FT.^{2}, $\beta = 0°$, $\delta_{F_N} = 0°$, $C_Q = .0071$

○ $S\Delta_1$, $\delta_{F_S} = 0°$, RUN 13
△ " + F_{S_1}, $\delta_{F_S} = 30°$, " 77
□ " + " , $\delta_{F_S} = 60°$, " 85

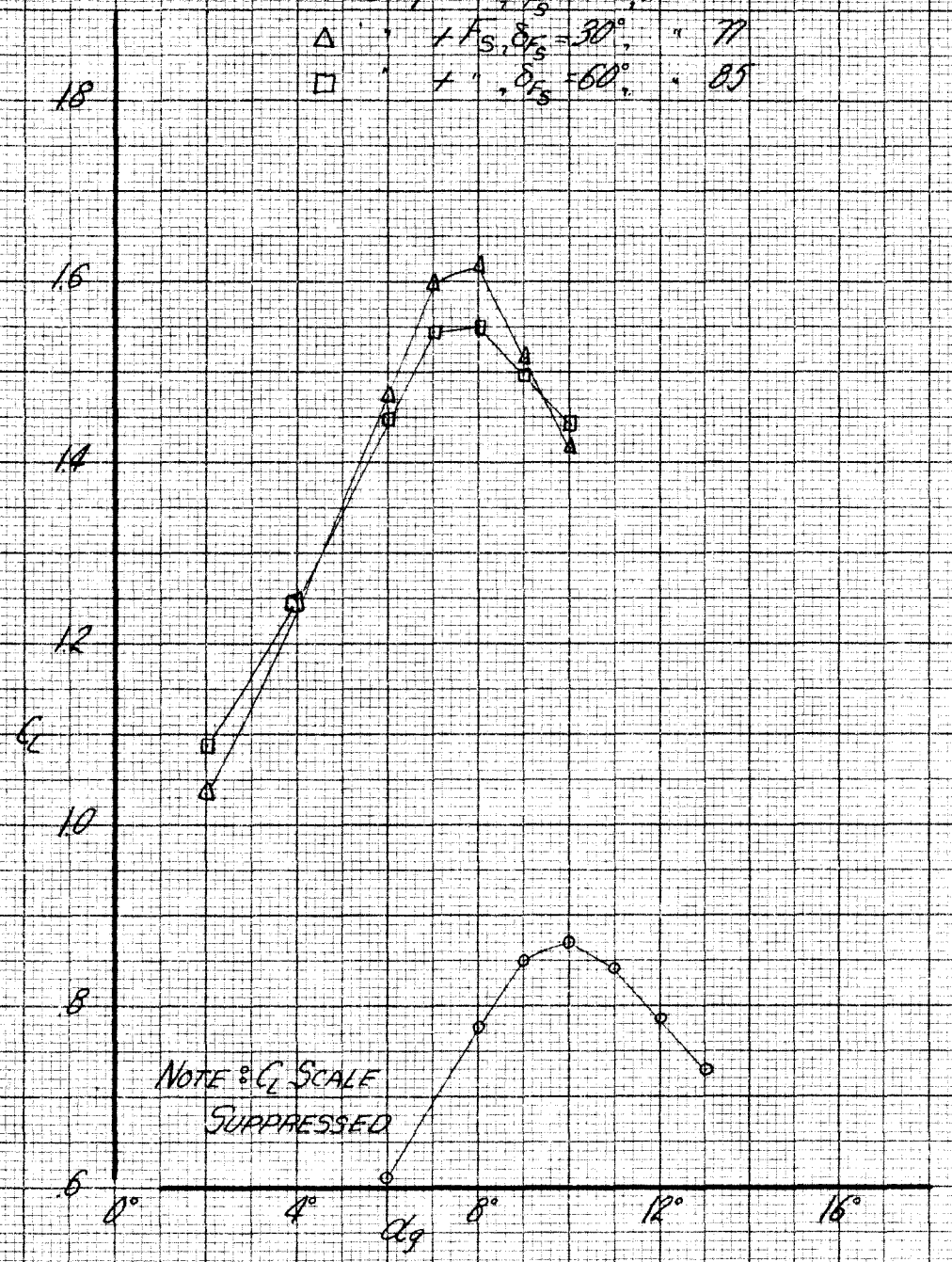

SLOTTED FLAP EFFECTIVENESS
$\delta_{F_N} = 0°$, $C_Q = .0071$
SLOT Δ_1

$q = 20$ LB/FT^2; $\psi = 0°$, $\delta_{F_N} = 0°$, $C_0 = .0071$

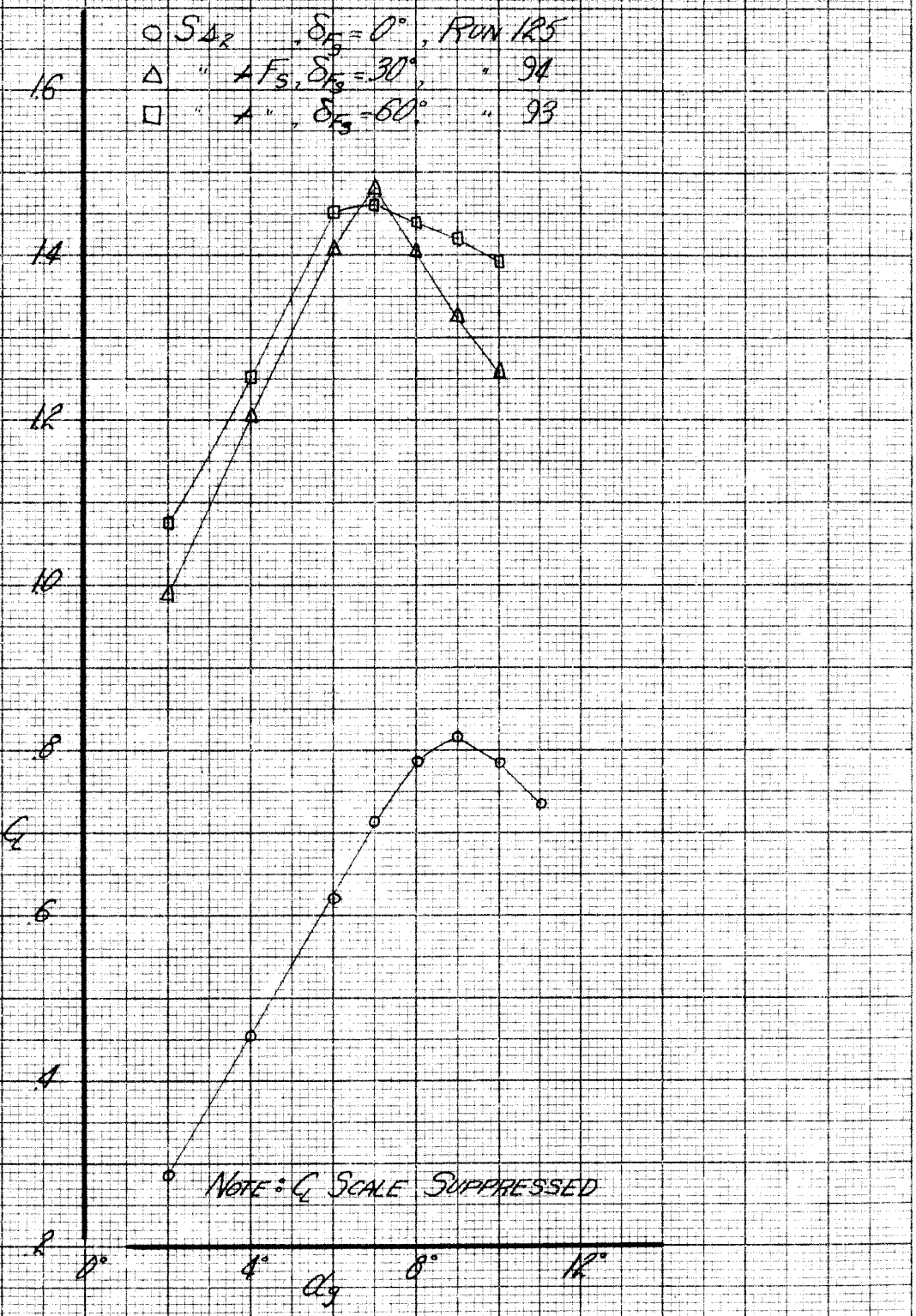

SLOTTED FLAP EFFECTIVENESS
$\delta_{F_N} = 0°$, $C_0 = .0071$
SLOT Δ_R

$q = 20$ LB/FT^2, $\delta_f = 0°$, $\delta_{F_N} = 0°$, $C_\phi = .0071$

○ $S_1 S_2$, $\delta_{F_S} = 0°$, RUN 14
△ " + F_S, $\delta_{F_S} = 30°$, " 76
□ " + " , $\delta_{F_S} = 60°$, " 86

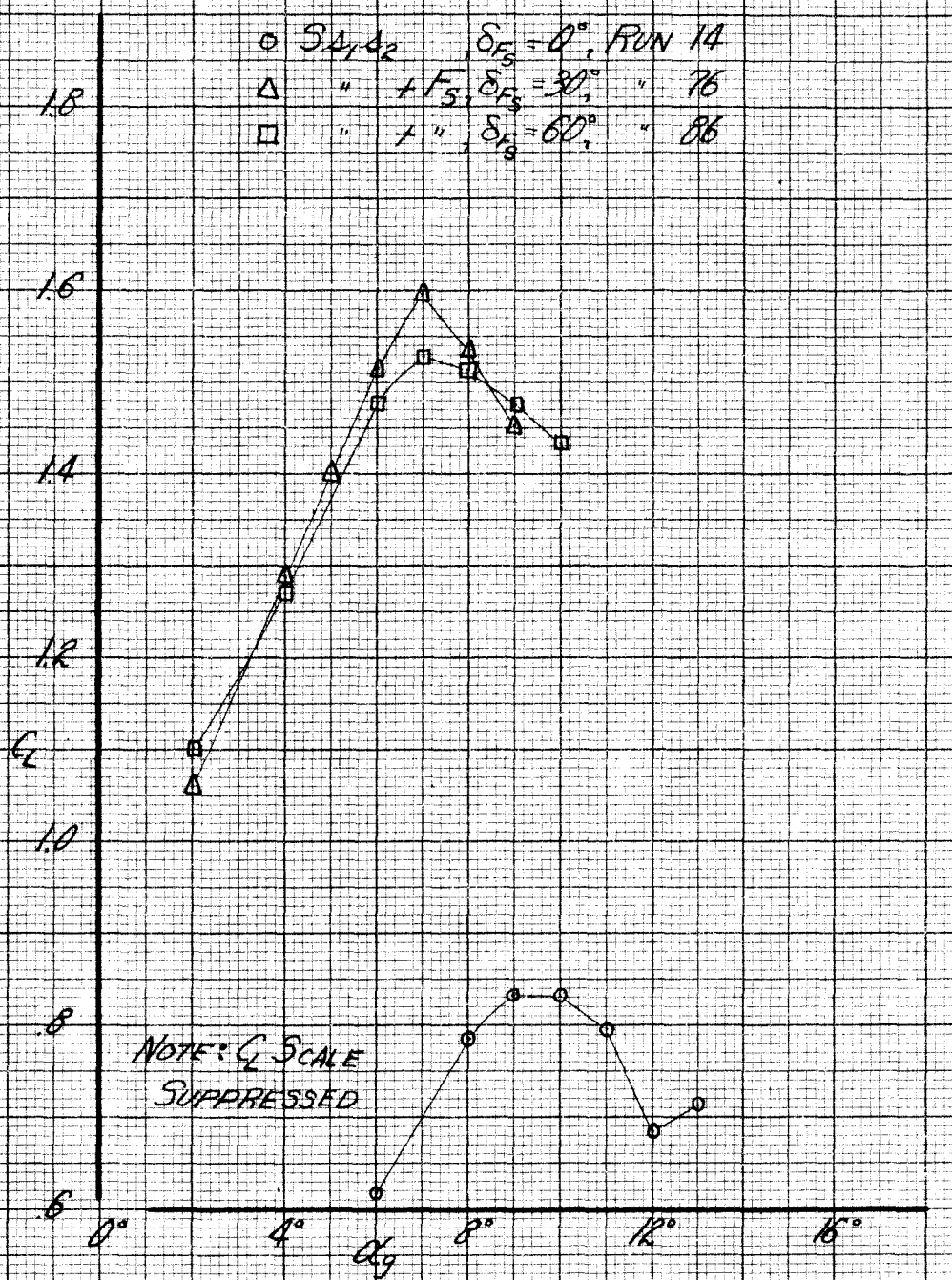

SLOTTED FLAP EFFECTIVENESS
$\delta_{F_N} = 0°$, $C_\phi = .0071$
SLOTS $S_1 S_2$

$q = 20$ LB/FT.^{2}, $\alpha_T = 0°$, $\delta_{F_N} = 15°$, $C_\phi = 0$

○ SF_N, $\delta_{F_S} = 0°$, RUN 18
△ " $+F_S$, $\delta_{F_S} = 30°$, " 63
□ " " , $\delta_{F_S} = 60°$, " 54

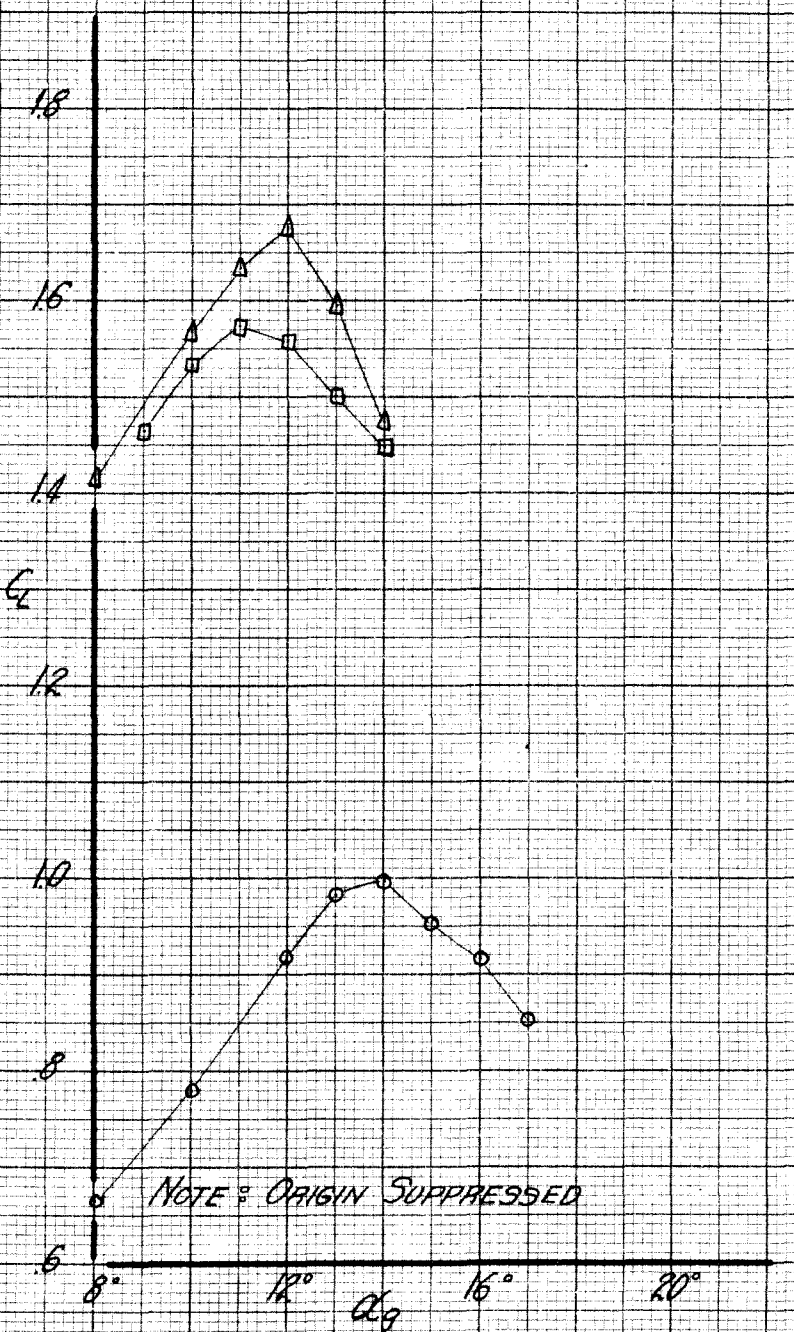

SLOTTED FLAP EFFECTIVENESS
$\delta_{F_N} = 15°$, $C_\phi = 0$

$q = 20$ LB/FT., $\alpha = 0°$, $\delta_{F_N} = 15°$, $C_Q = .0071$

○ $SF_N\Delta_1$, $\delta_{F_S} = 0°$, RUN 23
△ " $+F_S$, $\delta_{F_S} = 30°$, " 67
□ " $+F_S$, $\delta_{F_S} = 60°$, " 59

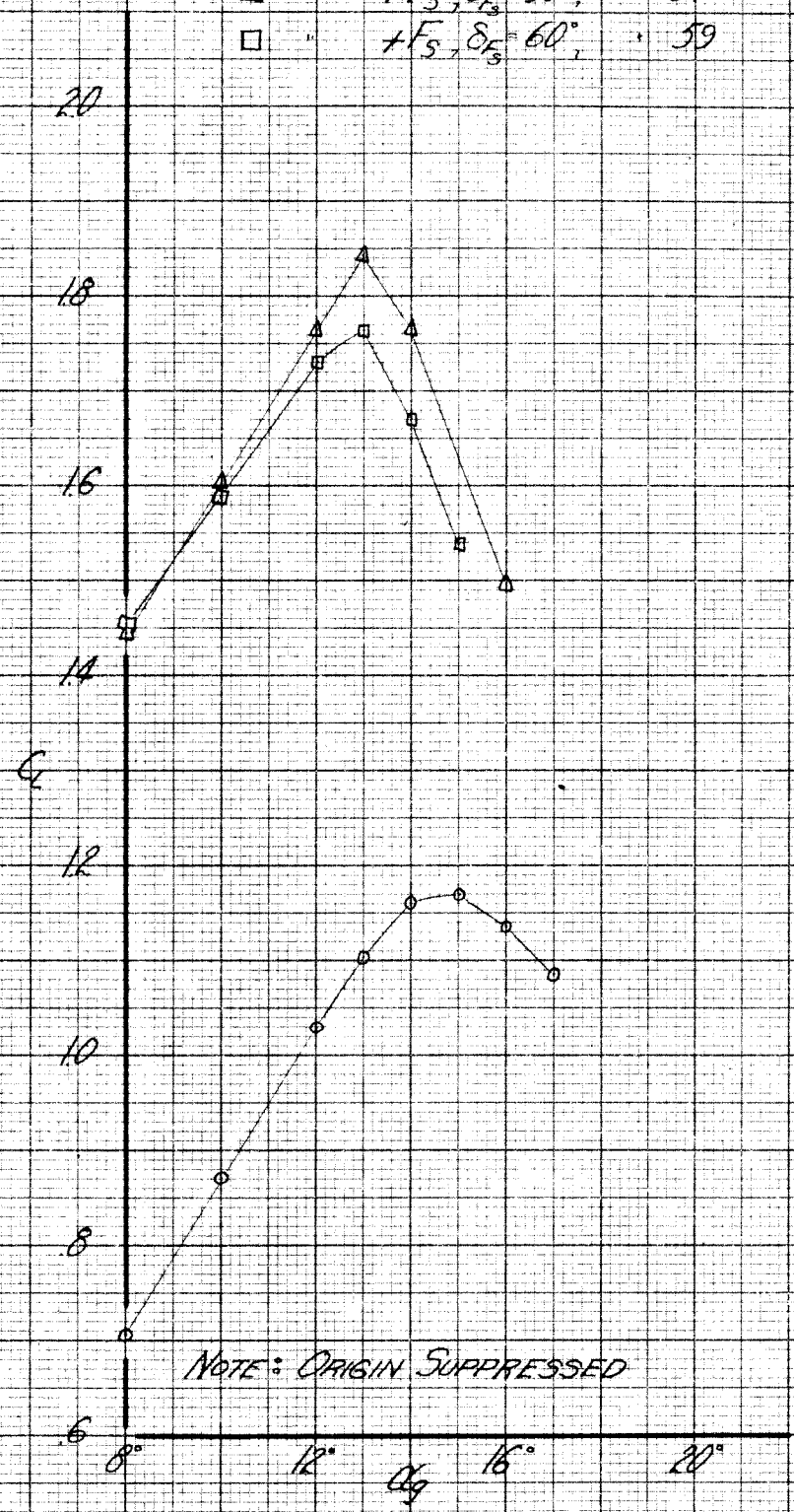

NOTE: ORIGIN SUPPRESSED

SLOTTED FLAP EFFECTIVENESS
NOSE FLAP DEFLECTED 15°
SLOT Δ_1, $C_Q = .0071$

$q = 20$ LBS/FT.^{2}, $\psi = 0°$, $\delta_{F_N} = 15°$, $C_Q = .0071$

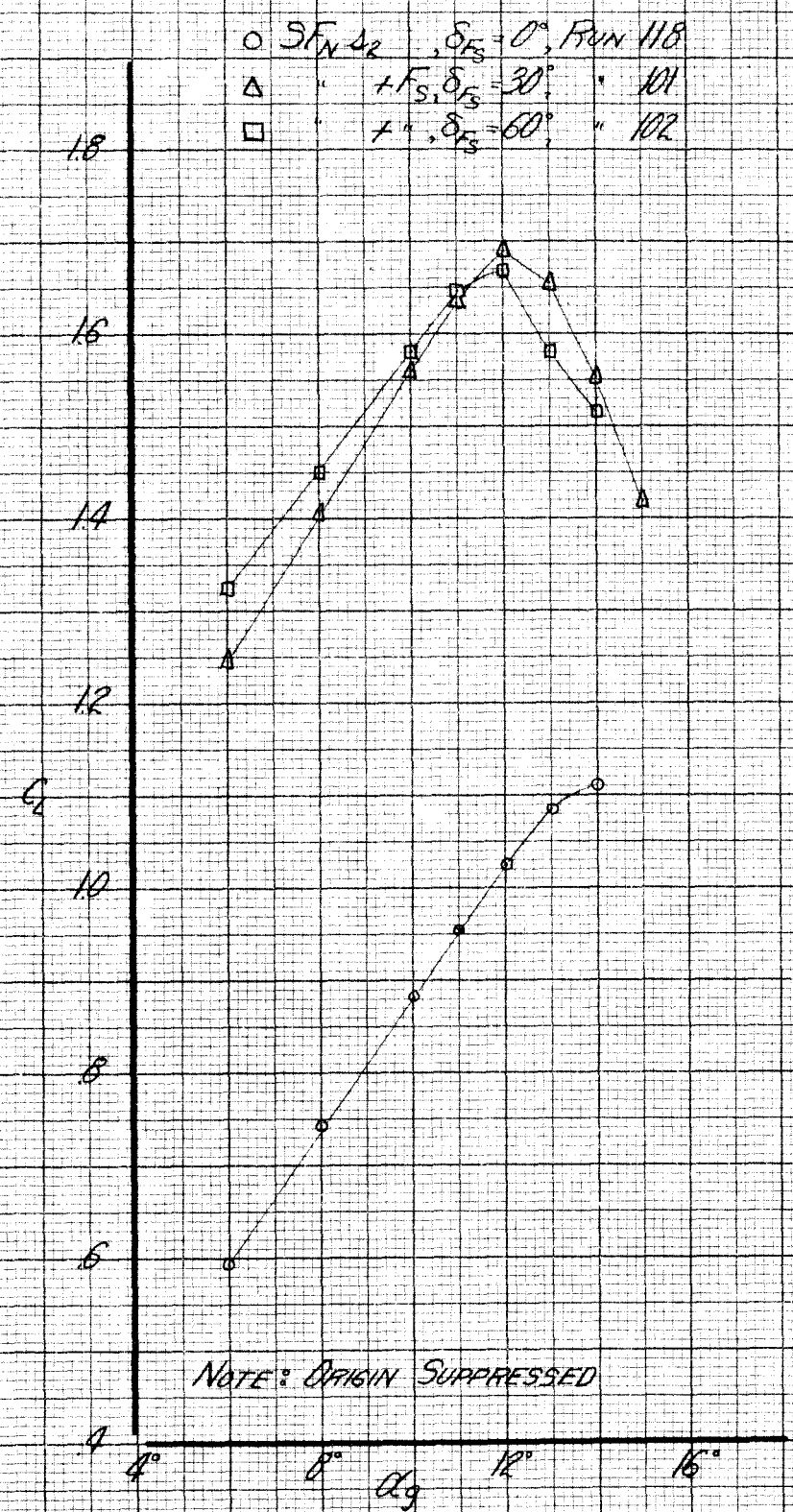

SLOTTED FLAP EFFECTIVENESS
NOSE FLAP DEFLECTED 15°
SLOT Δ_2, $C_Q = .0071$

$q = 20$ LB/FT^2, $\beta_s = 0°$, $\delta_{F_N} = 15°$, $C_Q = .0071$

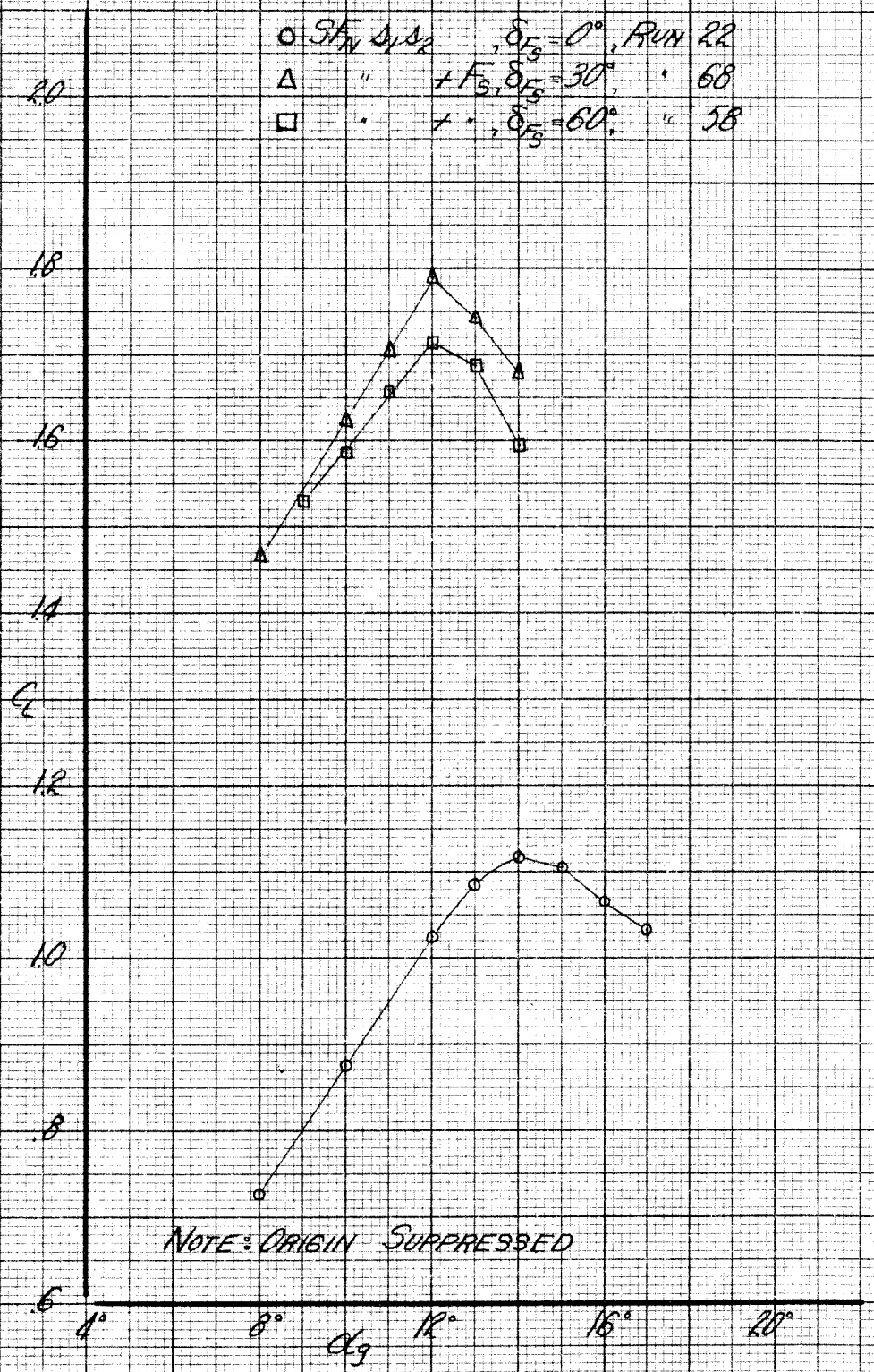

NOTE: ORIGIN SUPPRESSED

SLOTTED FLAP EFFECTIVENESS
NOSE FLAP DEFLECTED 15°
SLOTS S_1, S_2, $C_Q = .0071$

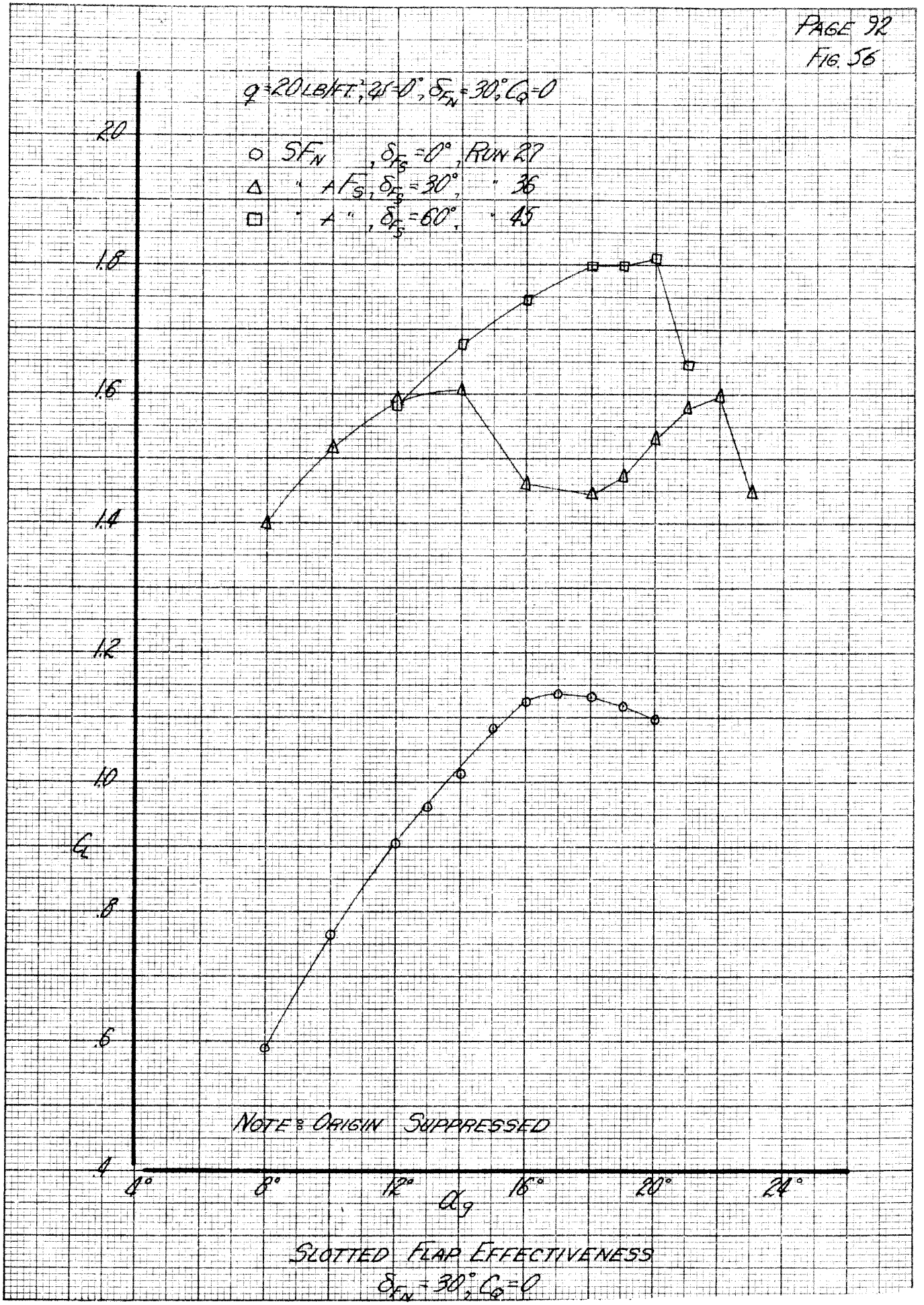

SLOTTED FLAP EFFECTIVENESS
$\delta_{FN} = 30°, C_Q = 0$

$q = 20 LB/FT^2$; $i_T = 0°$, $\delta_{F_N} = 30°$, $C_Q = .0071$

○ $SF_N \Delta_1$, $\delta_{F_S} = 0°$, RUN 31
△ " $+F_3$, $\delta_{F_S} = 30°$, " 41
□ " " , $\delta_{F_S} = 60°$, " 49

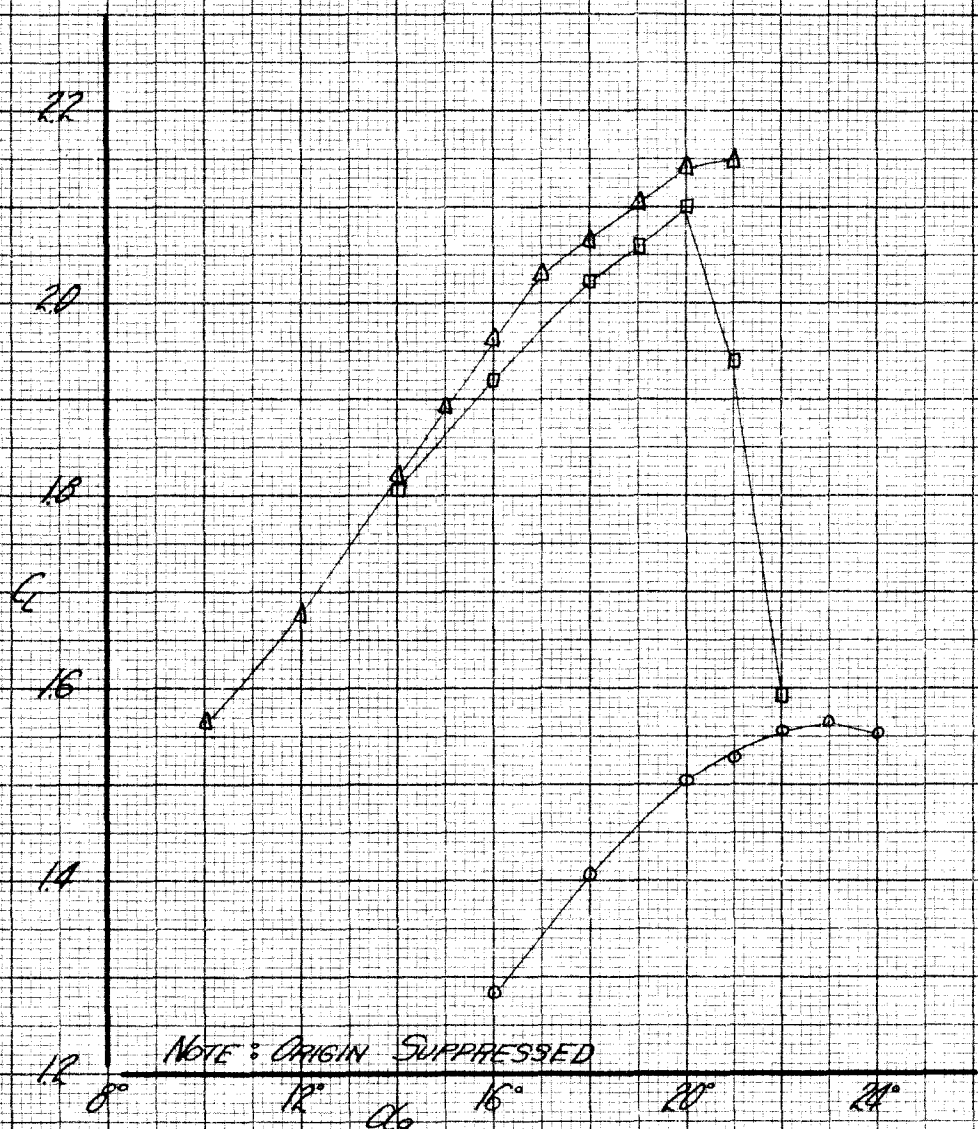

SLOTTED FLAP EFFECTIVENESS
NOSE FLAP DEFLECTED 30°
SLOT Δ_1, $C_Q = .0071$

$q = 20$ LB/FT.^{2}, $\beta = 0°$, $\delta_{F_N} = 30°$, $C_Q = .0071$

○ $SF_N \Delta_2$, $\delta_{F_S} = 0°$, RUN 117
△ " AF_S, $\delta_{F_S} = 30°$, " 110
□ " " , $\delta_{F_S} = 60°$, " 109

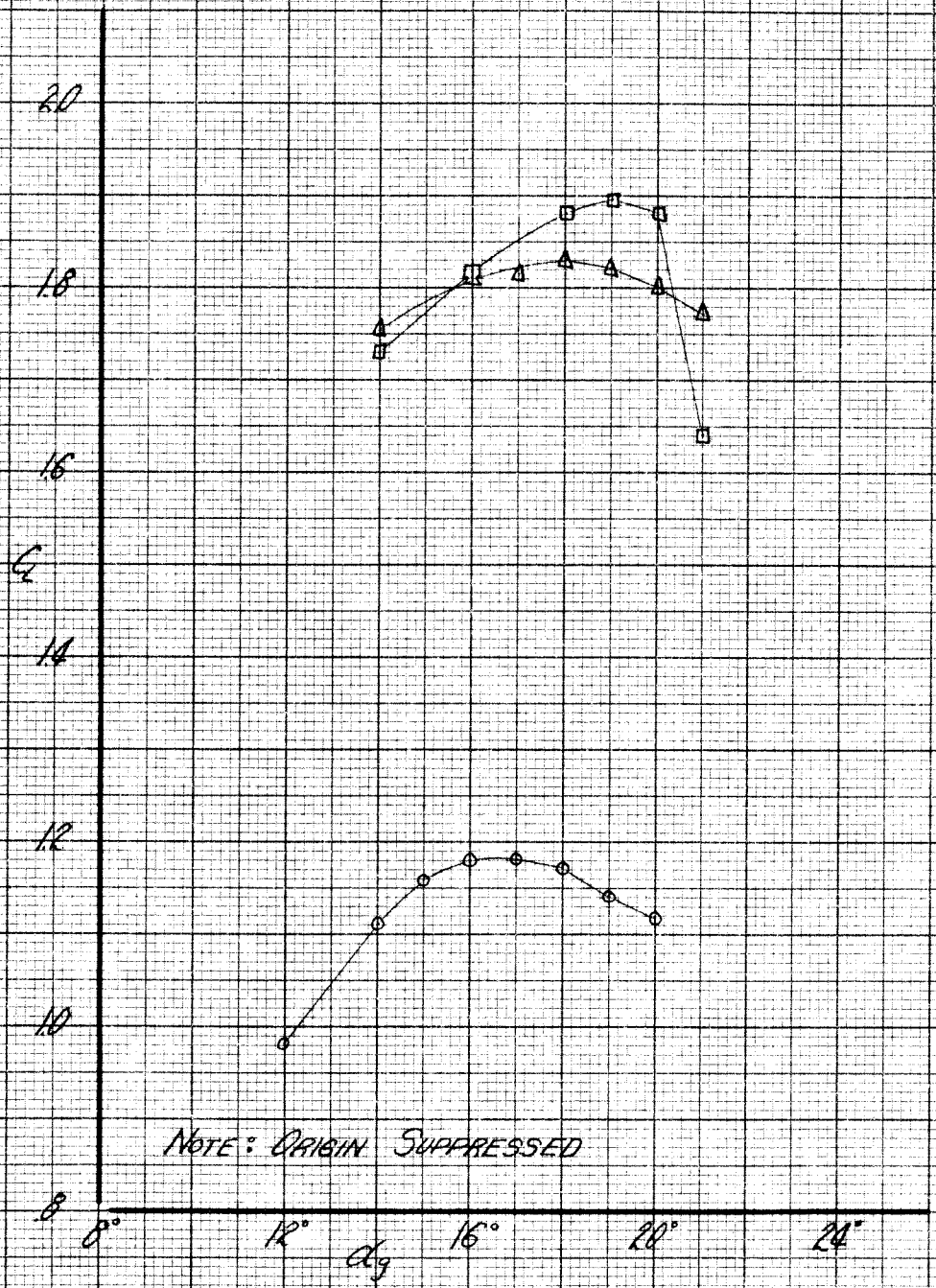

SLOTTED FLAP EFFECTIVENESS
NOSE FLAP DEFLECTED 30°
SLOT Δ_2, $C_Q = .0071$

$q = 20$ LB/FT.^{2}, $\alpha_i = 0°$, $\delta_{F_N} = 30°$, $C_Q = .0071$

○ SF_N Δ_1, Δ_2 , $\delta_{F_S} = 0°$, RUN 32
△ " $+F_S$, $\delta_{F_S} = 30°$, " 40
□ " " , $\delta_{F_S} = 60°$, " 50

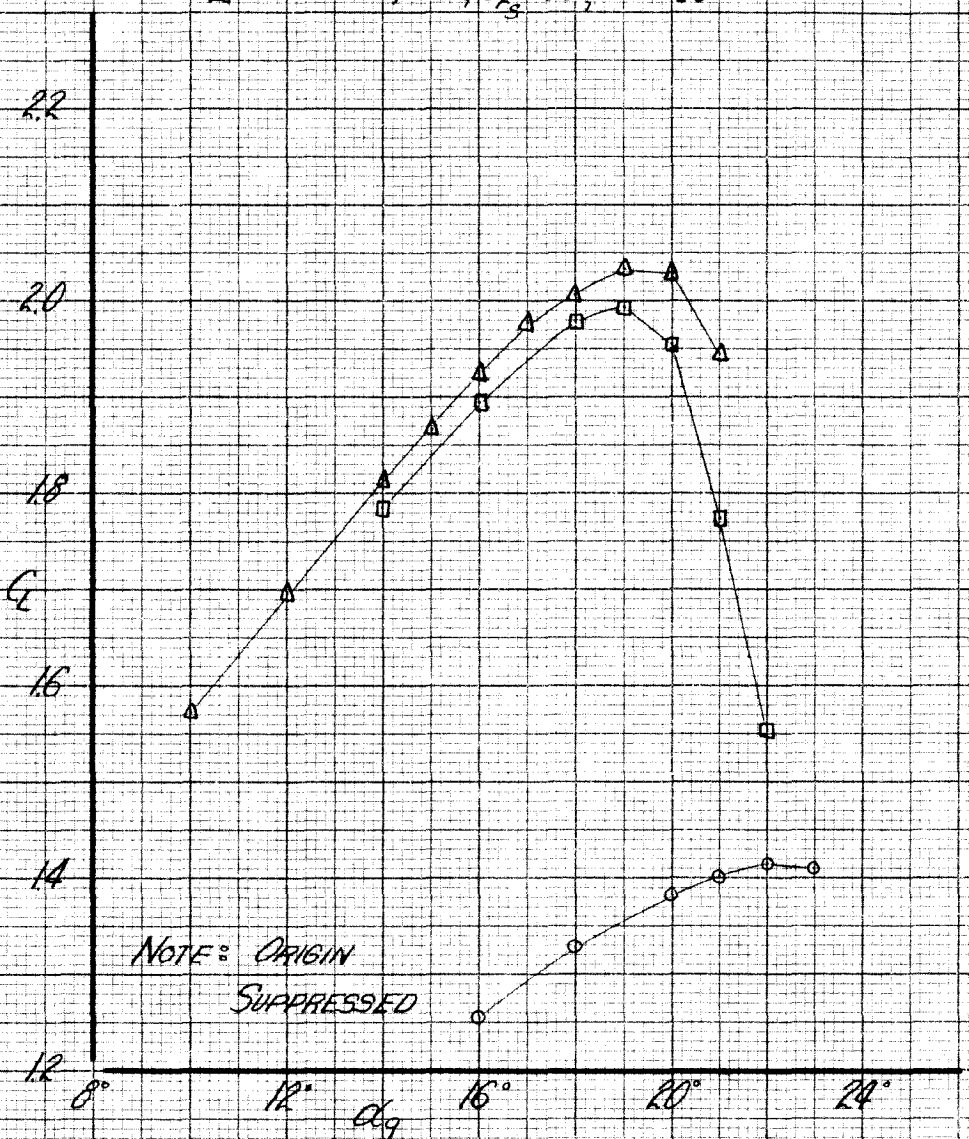

SLOTTED FLAP EFFECTIVENESS
NOSE FLAP DEFLECTED 30°
SLOTS Δ_1, Δ_2, $C_Q = .0071$

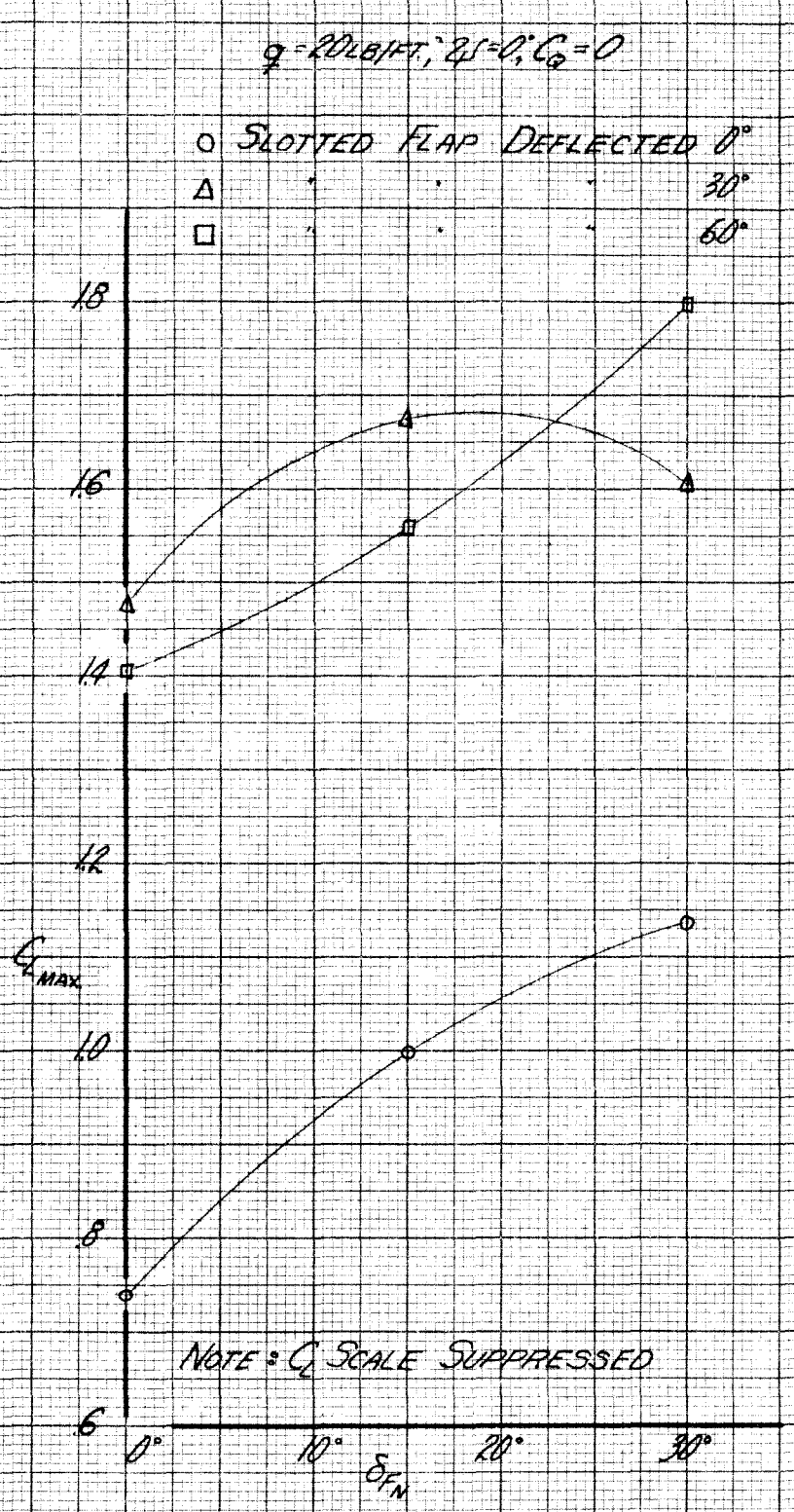

VARIATION OF MAXIMUM LIFT COEFFICIENT WITH FLAP DEFLECTION
$C_Q = 0$

FIG. 61

q = 20 LB/FT.; ψ = 0°, C_ϕ = .007, SLOT S_1

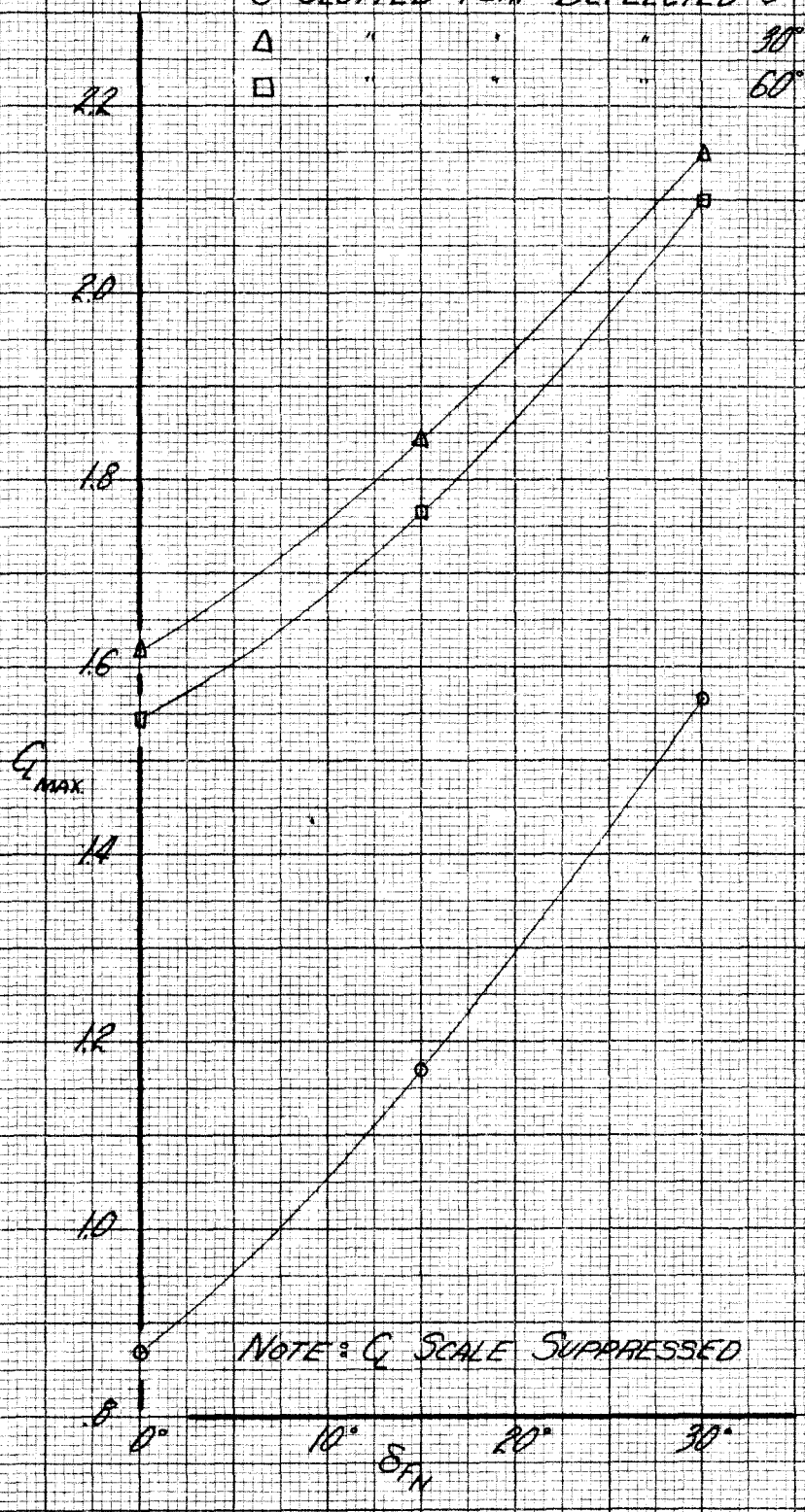

VARIATION OF MAXIMUM LIFT COEFFICIENT WITH FLAP DEFLECTION

C_ϕ = .007, SLOT S_1

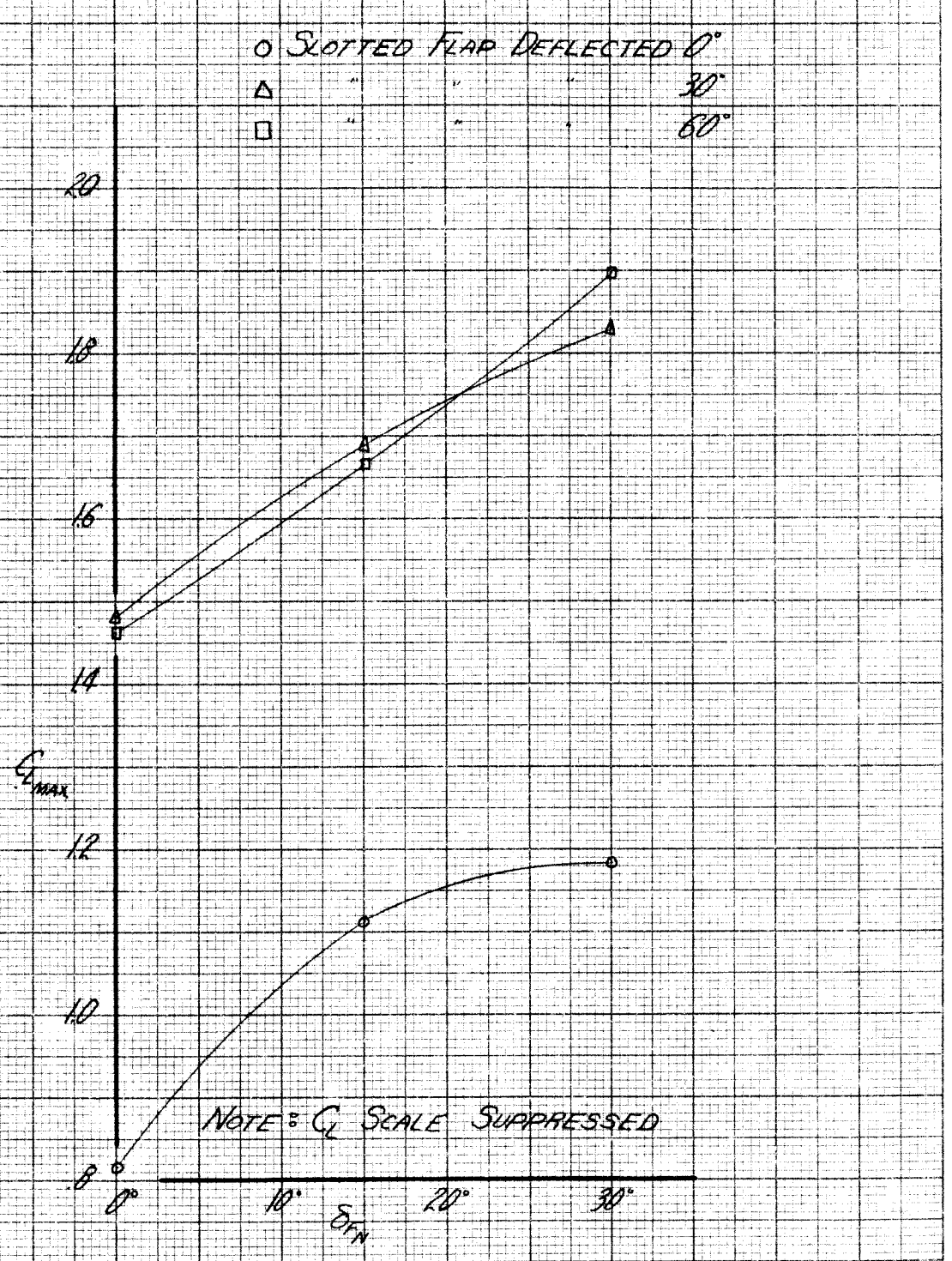

VARIATION OF MAXIMUM LIFT COEFFICIENT WITH FLAP DEFLECTION
$C_Q = .0021$, SLOT S_2

$q = 20$ LB/FT.^{2}, $\varphi = 0°$, $C_Q = .007$, SLOTS $S_1 S_2$ FIG. 63

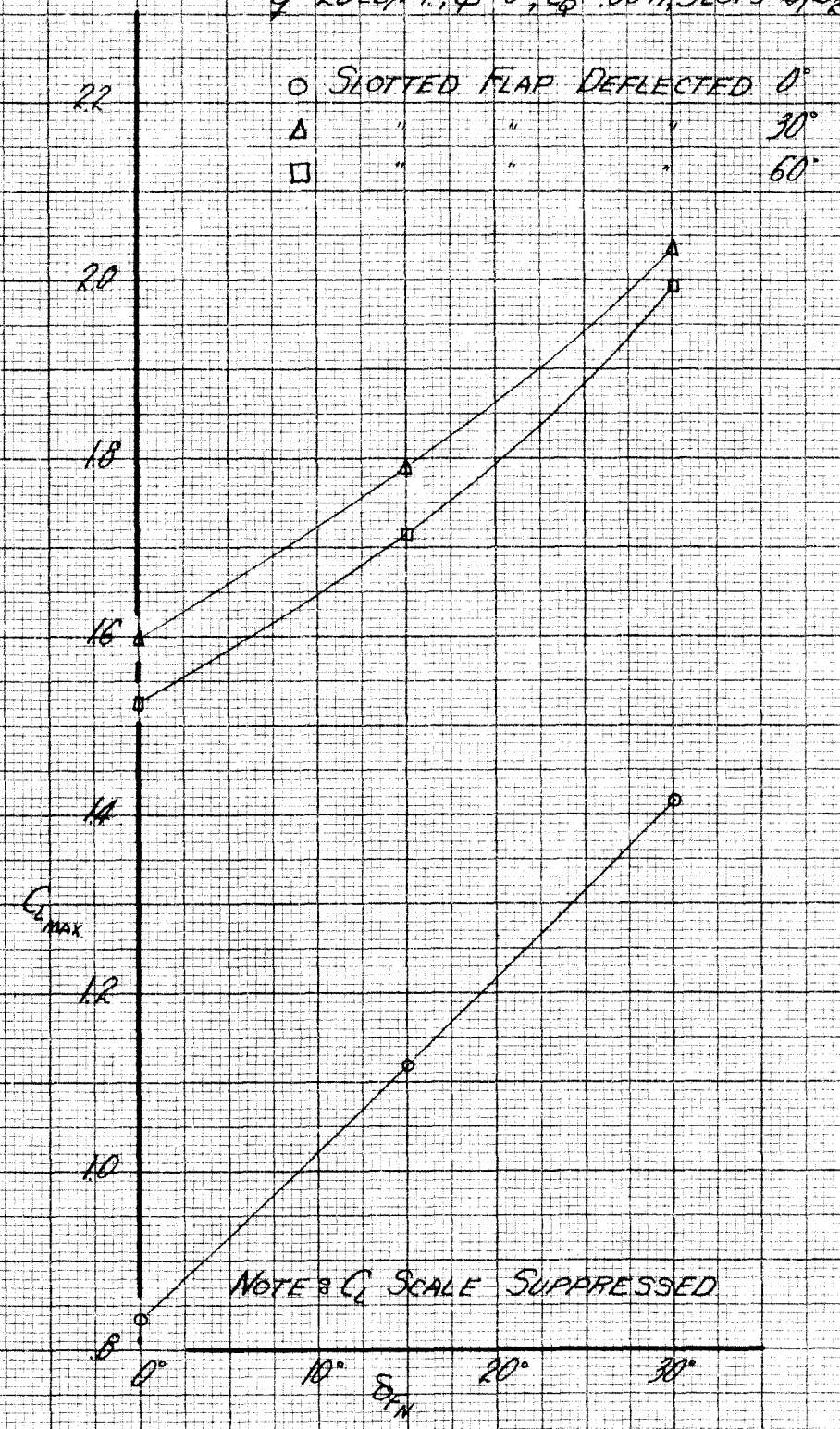

VARIATION OF MAXIMUM LIFT COEFFICIENT WITH FLAP DEFLECTION

$C_Q = .007$, SLOTS $S_1 S_2$

FIG. 64

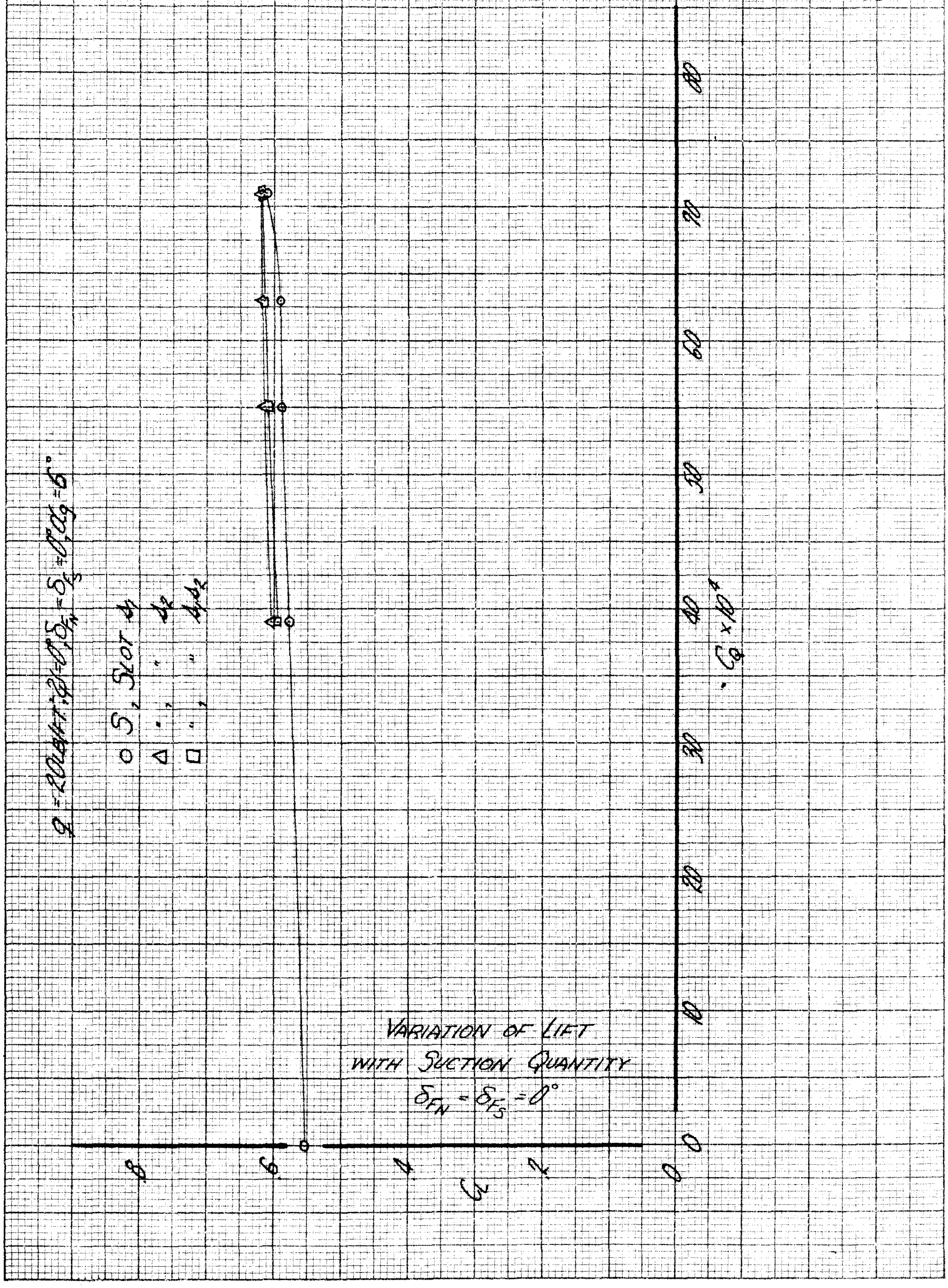
VARIATION OF LIFT
WITH SUCTION QUANTITY
δFN = δFS = 0°
q = 20 LB/FT², φ = 0°, δFN = δFS = 0°, αg = 6°
○ S, SLOT A1
△ " " A2
□ " " A1,A2
CQ × 10⁴
0
10
20
30
40
50
60
70
80
CL
0
.2
.4
.6
.8

Variation of Lift
with Suction Quantity
$\delta_{FN} = 15°, \delta_{FS} = 0°$
Note: Q Scale Suppressed
$C_Q \times 10^4$
0
10
20
30
40
50
60
80
C_L
.8
.6
.4
○ S_{FN}, Slot S_1
△ " " S_2
□ " " S_1, S_2
Q = Pounds, $\beta = 0°, \delta_{FN} = 15°, \delta_{FS} = 0°, \alpha_g = 8°$

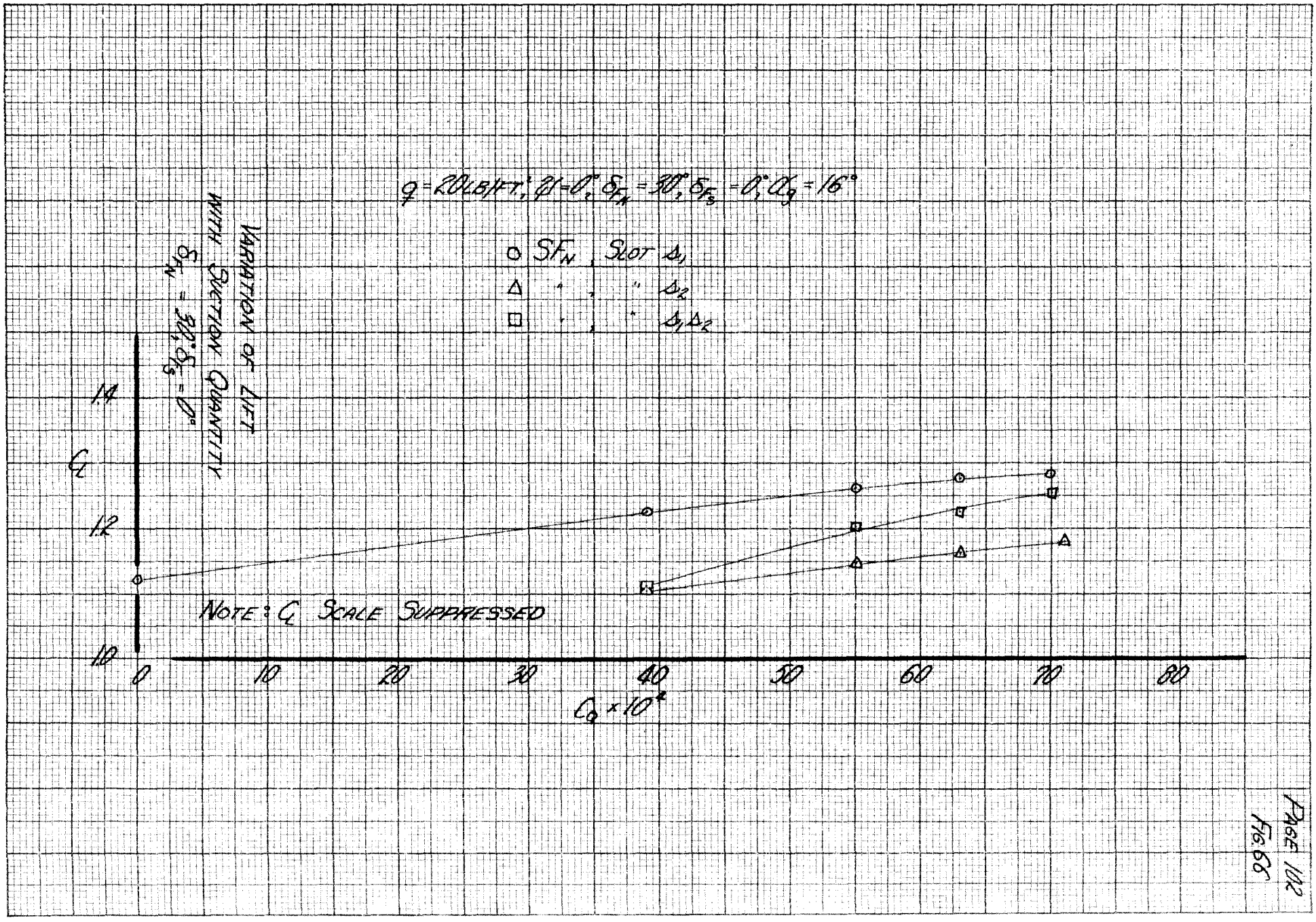

PAGE 102
FIG 66

VARIATION OF LIFT WITH SUCTION QUANTITY
$\delta_{F_N} = 0°$, $\delta_{F_S} = 30°$

FIG. 68

Q = 20 lb/ft, α = 0°, δFN = 0°, δS = 60°, αg = 2°
○ SFS, Slot Δ1
△ " " Δ2
□ " " Δ1, Δ2
Variation of Lift
with Suction Quantity
δFN = 0°, δS = 60°
Note: CL Scale Suppressed
CQ × 10³
CL
1.2
1.0
0
10
20
30
40
50
60
70
80

VARIATION OF LIFT WITH SUCTION QUANTITY
$\delta_{F_N} = 15°, \delta_{F_S} = 30°$

Q = 280 LBS/FT, β = 0°, δF = 15°, δS = 60°, Cq = 10°
○ SLOT S1
△ " S2
□ " S1+S2
NOTE: CL SCALE SUPPRESSED
Cq x 10⁶
0
20
40
60
80
100
120
CL
16
14
12
VARIATION OF
LIFT WITH
SUCTION QUANTITY
δF = 15, δS = 60°

FIG. 71

VARIATION OF LIFT WITH SUCTION QUANTITY

$\delta_{FN} = 30°, \delta_S = 60°$

VARIATION OF LIFT
WITH SUCTION QUANTITY
$\delta_{FN} = 30°, \delta_{FN} = 30°$
$q = 20$ LB/FT², $\beta = 0°, \delta_{FN} = 30°, \delta_{FS} = 30°, \alpha_0 = 14°$
○ $S_N F_S$, SLOT d_1
△ " " d_2
□ " " d_4
NOTE: C_L SCALE SUPPRESSED
$C_Q \times 10^4$
0
10
20
30
40
50
60
70
80
C_L
14
16
18
20

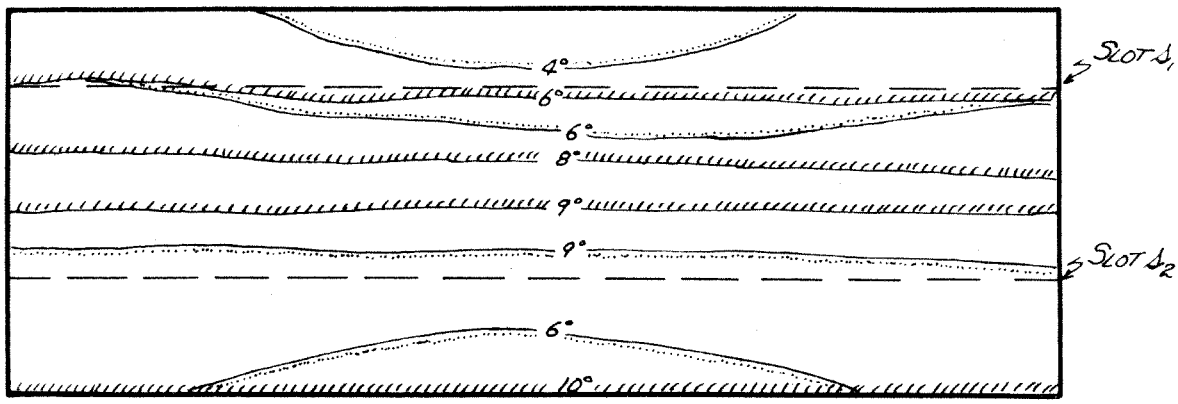

TUFT SKETCH FOR RUN 132
CONFIGURATION S
$\delta_{F_N} = \delta_{F_S} = 0°$
NO SUCTION

FIGURE 73

ROUGH AREA
STALLED AREA

V

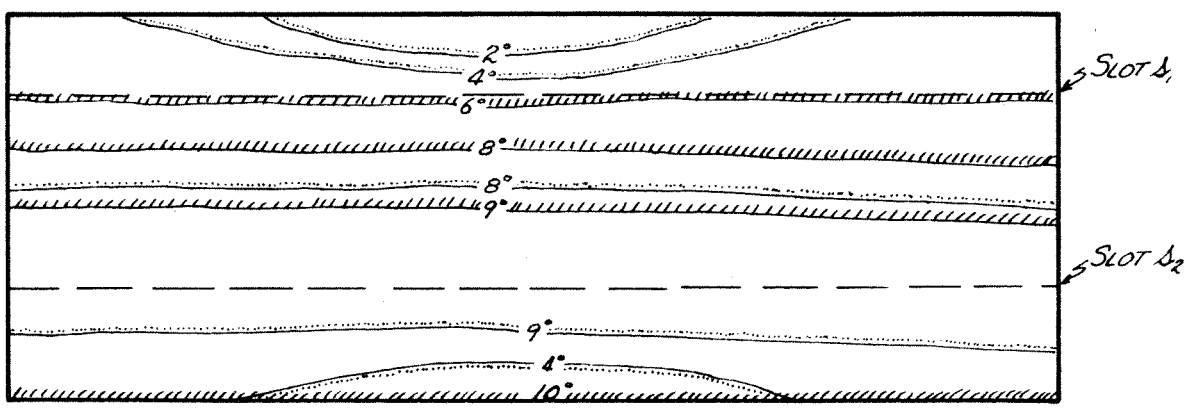

TUFT SKETCH FOR RUN 130
CONFIGURATION $S+\Delta_1$
$\delta_{F_N} = \delta_{F_S} = 0°$
$C_Q = .0071$

FIGURE 74

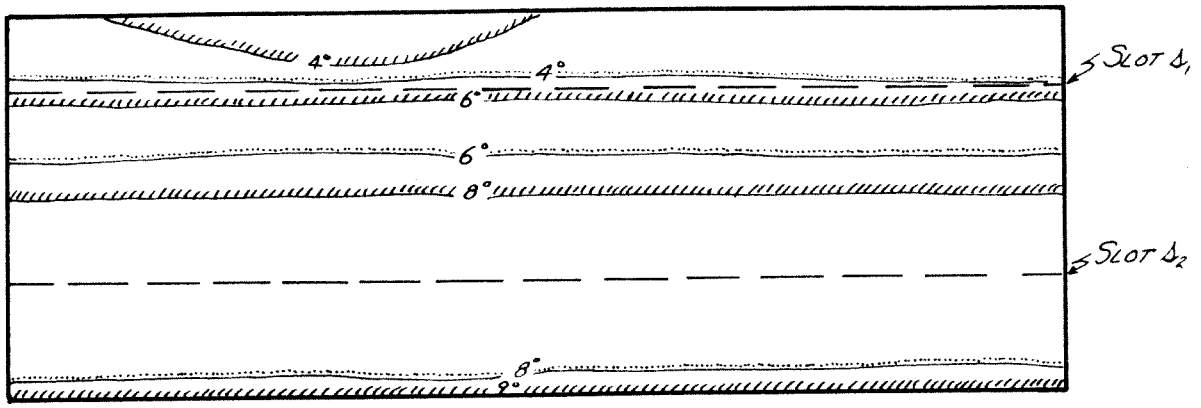

TUFT SKETCH FOR RUN 126
CONFIGURATION $S + \Delta_2$
$\delta_{F_N} = \delta_{F_S} = 0°$
$C_Q = .0071$

FIGURE 75

V

ROUGH AREA
STALLED AREA

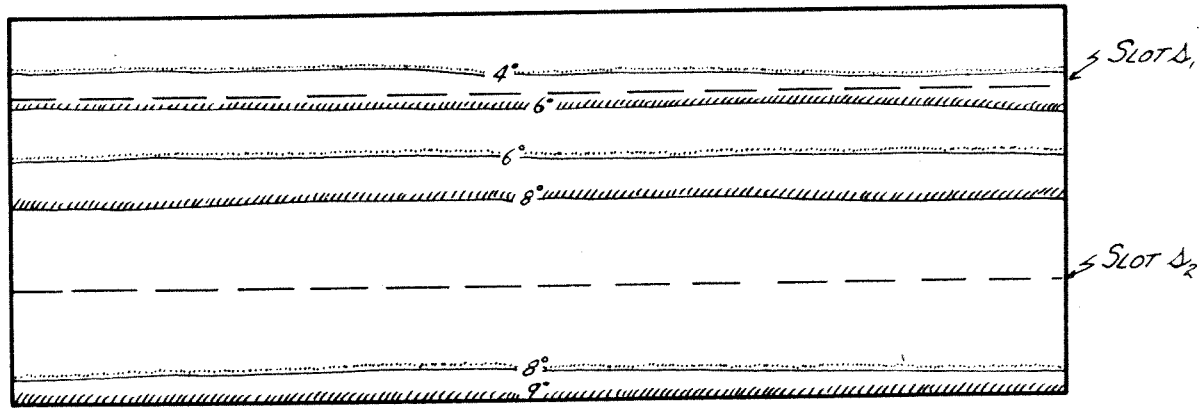

TUFT SKETCH FOR RUN 131
CONFIGURATION $S + \Delta_1, \Delta_2$
$\delta_{F_N} = \delta_{F_S} = 0°$
$C_Q = .0071$

FIGURE 76

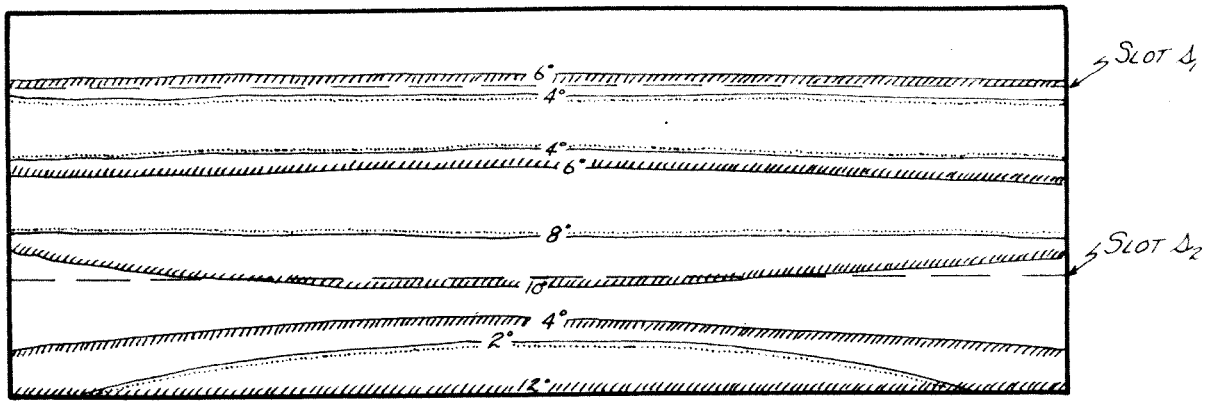

TUFT SKETCH FOR RUN 138
CONFIGURATION $SF_N F_S$
$\delta_{F_N} = \delta_{F_S} = 30°$
NO SUCTION

FIGURE 77

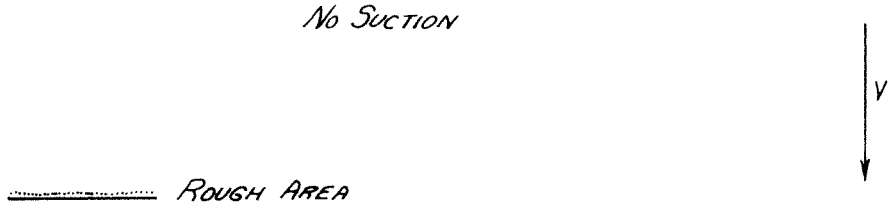

ROUGH AREA

STALLED AREA

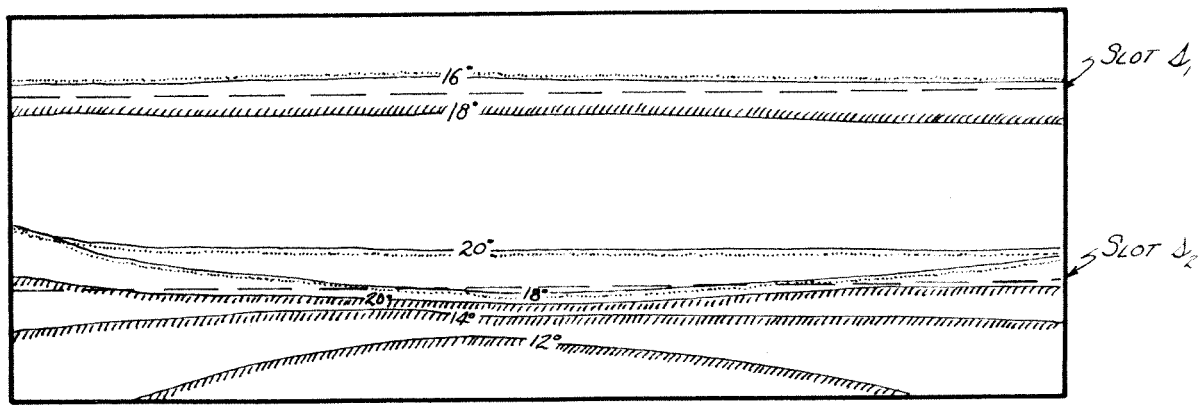

TUFT SKETCH FOR RUN 129
CONFIGURATION $SF_N F_S + \Delta_1$
$\delta_{F_N} = \delta_{F_S} = 30°$
$C_Q = .0071$

FIGURE 78

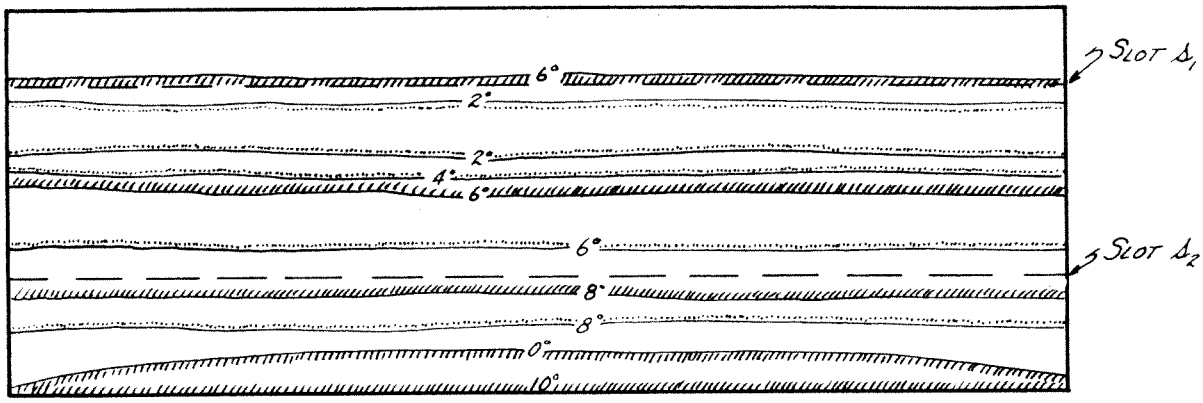

TUFT SKETCH FOR RUN 139
CONFIGURATION $3F_N F_S$
$\delta_{F_N} = 30°$, $\delta_{F_S} = 60°$
NO SUCTION

FIGURE 79

V

ROUGH AREA

STALLED AREA

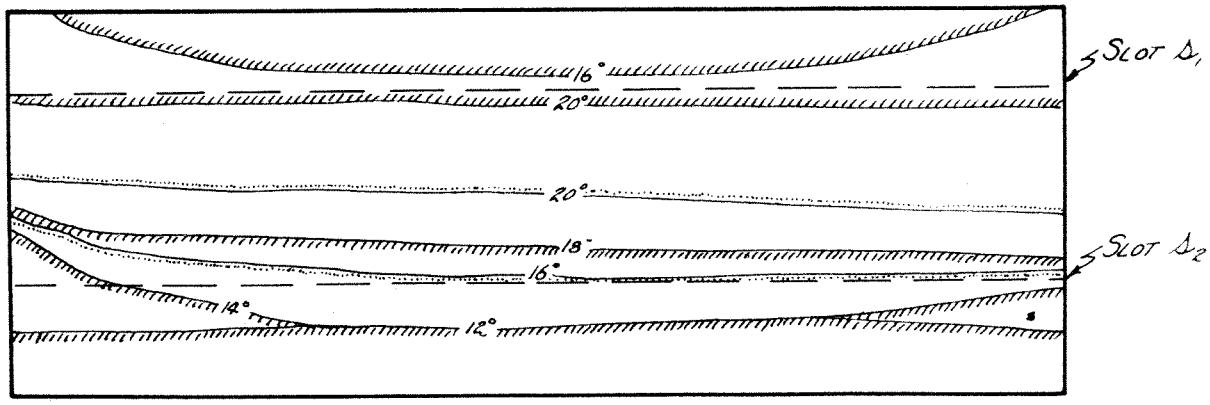

TUFT SKETCH FOR RUN 127
CONFIGURATION $5F_N F_S + \Delta_2$
$\delta_{F_N} = 30°$, $\delta_{F_S} = 60°$
$C_Q = .0071$

FIGURE 80

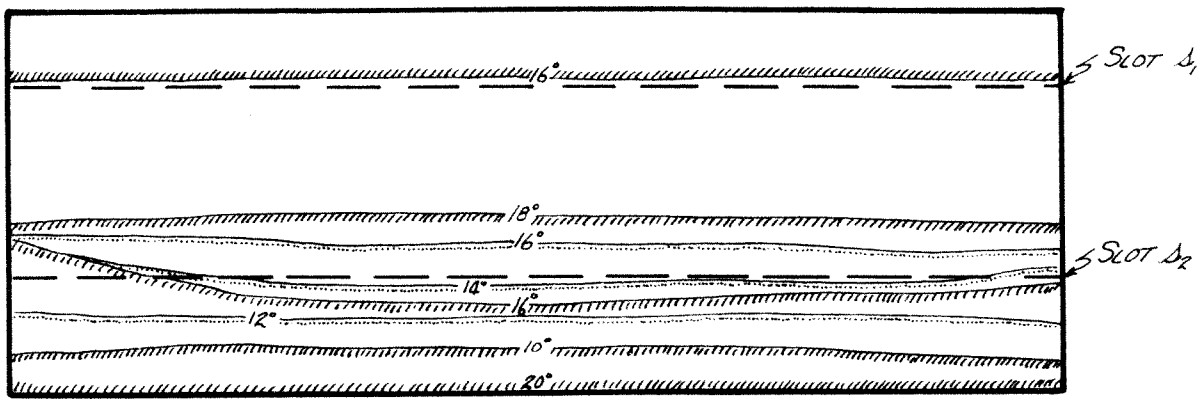

TUFT SKETCH FOR RUN 128
CONFIGURATION $SF_N F_S + \Delta_1 \Delta_2$
$\delta_{F_N} = 30°$; $\delta_{F_S} = 60°$
$C_Q = .0071$

FIGURE 81

ROUGH AREA

STALLED AREA

V

TUFT PICTURES FOR RUN 138

CONFIGURATION $SF_NF_S, \delta_{F_N} = \delta_{F_S} = 30^\circ$

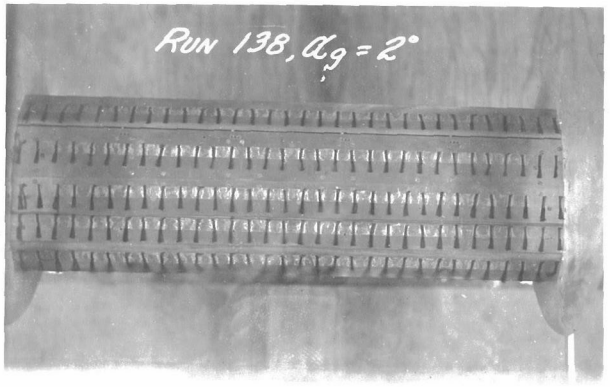

$\alpha_g = 2^\circ$

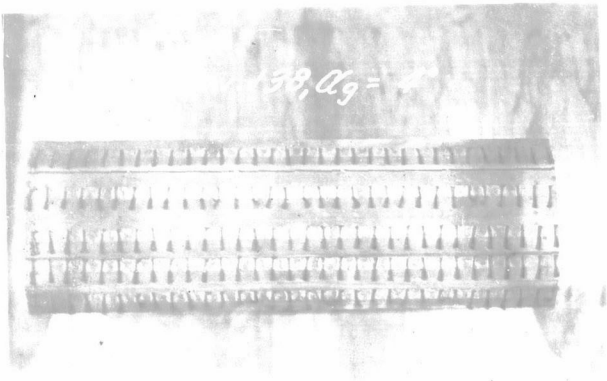

$\alpha_g = 4^\circ$

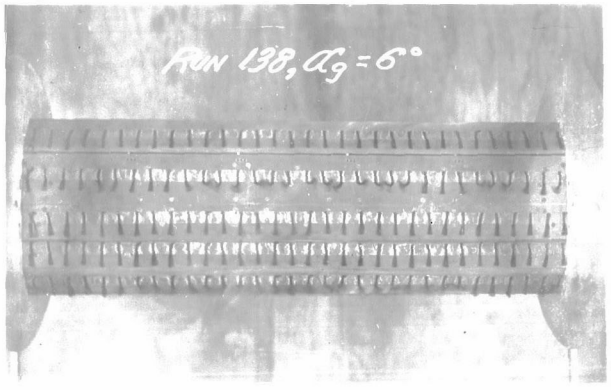

$\alpha_g = 6^\circ$

TUFT PICTURES FOR RUN 138

CONFIGURATION SF_NF_S, $\delta_{F_N} = \delta_{F_S} = 30^\circ$ (cont'd)

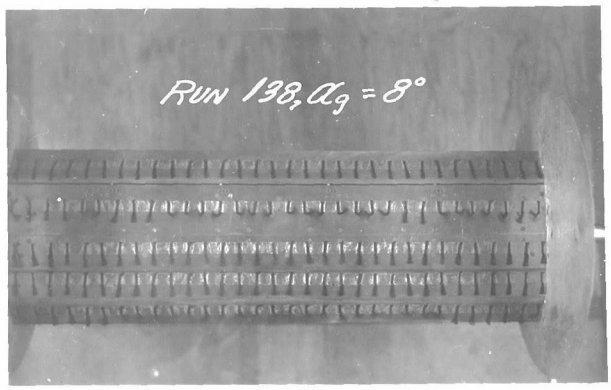

$\alpha_g = 8^\circ$

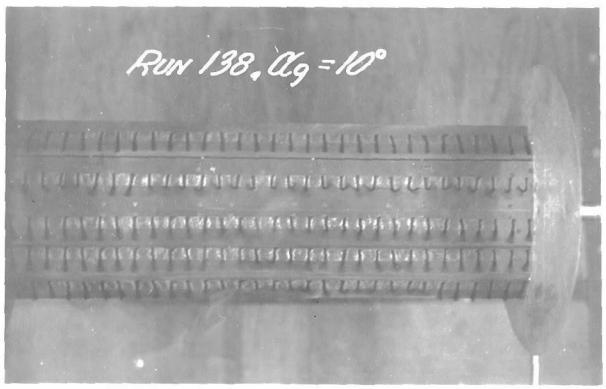

$\alpha_g = 10^\circ$

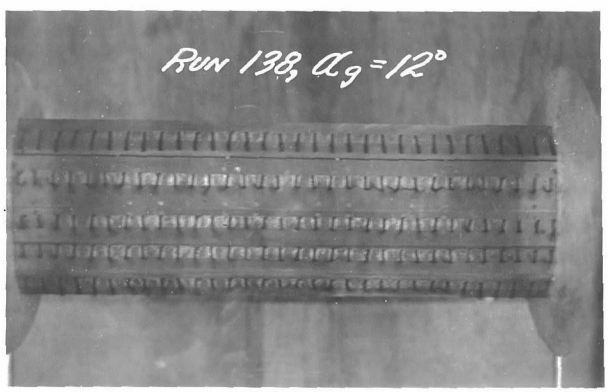

$\alpha_g = 12^\circ$

XVI. MODEL PICTURES

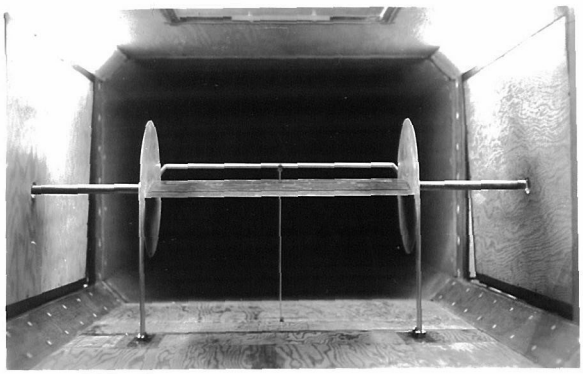

Photo 1. Front view of complete model installed in wind tunnel

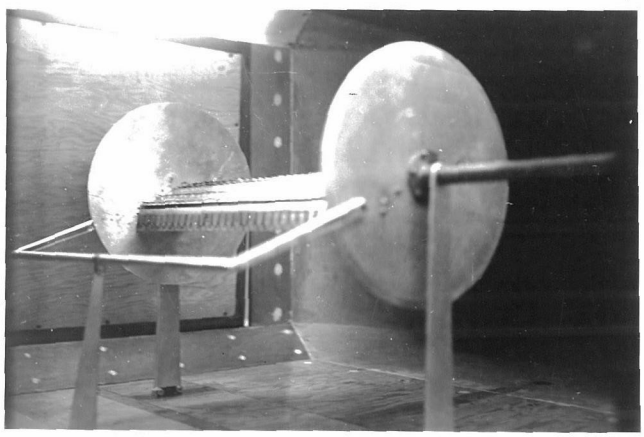

Photo 2. 3/4 rear view of model showing endplates and sting mounts

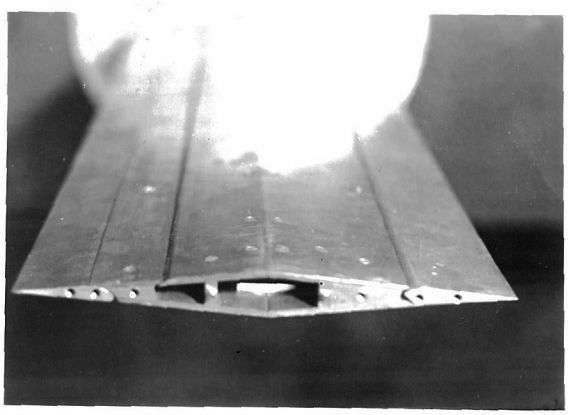

Photo 3. Side view of model showing airfoil cross-section for the "flaps up" configuration

MODEL PICTURES (cont'd)

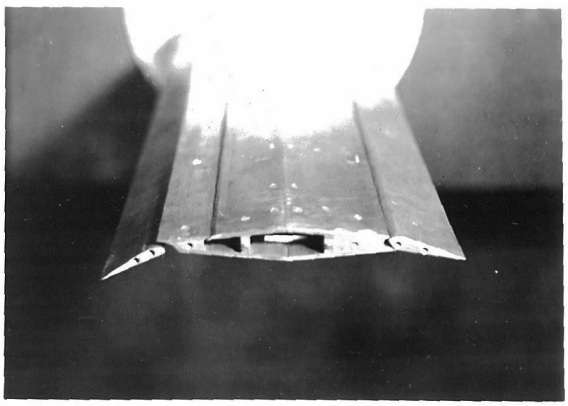

Photo 4. Side view of model showing airfoil cross-section for $\delta_{F_N} = 15^\circ$, $\delta_{F_S} = 30^\circ$

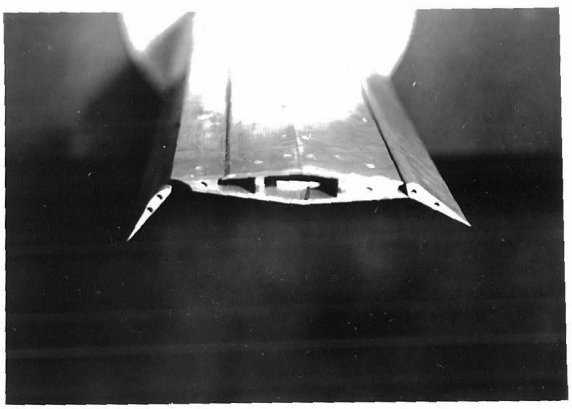

Photo 5. Side view of model showing airfoil cross-section for $\delta_{F_N} = 30^\circ$, $\delta_{F_S} = 60^\circ$

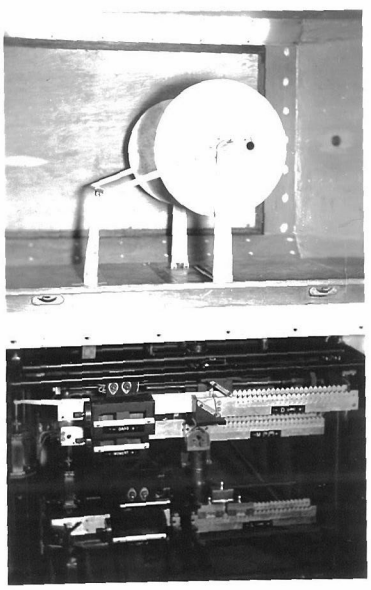

Photo 6. Side view of tunnel working section showing the model support system and balance

MODEL PICTURES (cont'd)

Photo 7. View showing suction pumps and manometer

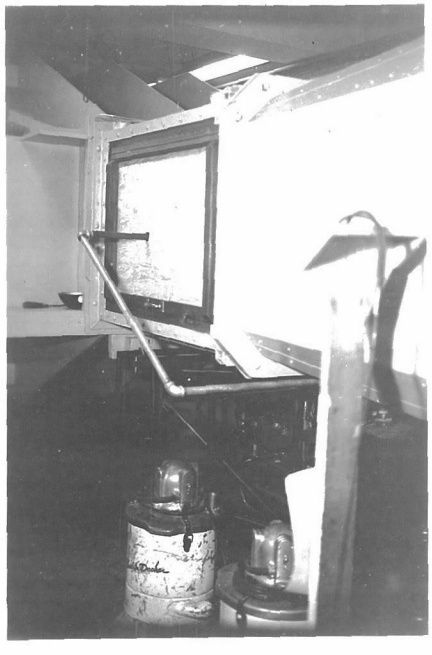

Photo 8. View showing airflow duct on north side of tunnel